Eutectic Freeze Crystallization

An experimental study into the application of the EFC process on two different aqueous waste streams.

Master Thesis Project

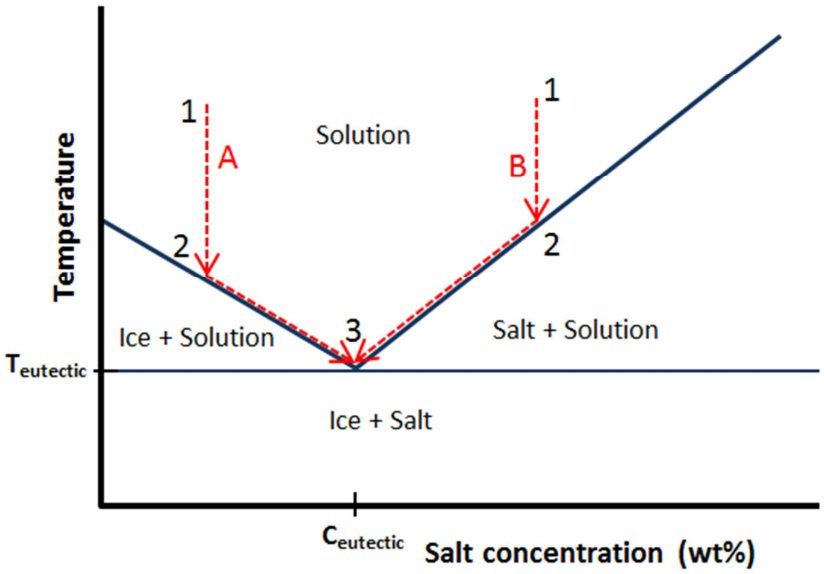

Name: Bart de Graaff
Student Number: 1302078
Program: Chemical Engineering

Supervising Professor: Prof. dr. Geert-Jan Witkamp
Research Group: Laboratory for Process Equipment, Process & Energy

2nd Reviewer: Dr. Elif Genceli
3rd Reviewer: Dr. ir. Adrie Straathof
4th Reviewer: Dr. Jaap van Spronsen

Start Date: April 4, 2011
End Date: March 7, 2012

Summary

In the past decades the prevention of water pollution and the reuse of process water are widely recognized as essential means to sustain our society and the environment. In many cases this recognition is translated into new or more stringent legislation, forcing industries to install wastewater treatment facilities and optimize their water household.

A new and very promising water treatment technology is Eutectic Freeze Crystallization or EFC. This technology is in particular suited for the treatment of aqueous streams containing a single or multiple inorganic salts. The basis of eutectic freeze crystallization is the existence of eutectic points. The eutectic point is a characteristic point in the phase diagram of a salt-water mixture. At the eutectic point an equilibrium exists between ice, salt and a solution with a specific concentration. In multi-component mixtures a range of eutectic points (lines) will exist at which one (or more) salt crystallizes simultaneously with ice. So the EFC process converts an invaluable and/or hazardous waste stream into clean water and (valuable) solid salt products. The energy consumption for the EFC process is considerably lower than for alternative evaporative processes. Moreover the low temperatures and the ambient pressures at which the process operates give relative few issues with corrosion and safety.

At this moment a TU Delft owned company called EFCseparations BV is in the business of commercializing the eutectic freeze crystallization process. Various parties from both the research and the industrial sector have already shown serious interest in the EFC process. In this thesis two different industrial aqueous waste streams are studied for their possibilities to be treated by the EFC process.
The first stream, a sodium sulfate containing wastewater stream is used as a base case for studying the scaling of the cooling surfaces at a 10 liter scale. Also the effect of added impurities on the scaling and heat transfer properties is explored. This work is described in chapter 3. In addition, extensive experimentation in a 200 liter EFC pilot set-up was done to study the crystallization behavior and product purities of both a synthetic sodium sulfate stream as well as a real industrial acidic impure sodium sulfate waste stream (Chapter 4).
A second stream that was investigated is a concentrated salt water stream originating from the production of shale gas. This stream is studied for its crystallization behavior (e.g. ion recoveries as a function of temperature) and the purities of the ice product. Also 200 L pilot scale tests were done to identify possible issues that could be encountered in an industrial EFC process treating a shale gas water stream. The results of this study are presented in Chapter 5.

The experiments done with a 8 wt% sodium sulfate solution have shown that scaling of the heat exchangers leads to a decrease of almost 50 % in heat transfer coefficient when ice crystallization starts at the eutectic point. Samples taken from the formed scale layer were mainly made of ice, however 3.4 wt% of Na_2SO_4 was also incorporated in this ice layer. The characteristics of the scale development are studied and discussed in chapter 3. Addition of NaCl and $MgCl_2$ is shown to have a significant scale reducing effect and a concentration of 3 wt% of these salts is enough to completely eliminate the problem of scaling at the cooling surfaces. Tests in the 200 L pilot set-up indicated that the addition of NaCl does not lead to decrease in product purity because no chloride ions are incorporated into either the ice or the salt product.
During the pilot scale experiments it was also found that the current method of ice removal by overflowing of the crystallizer is not suited for the production of large amounts of ice. In addition, the accumulation of solids (both salt and ice) around the upper heat exchangers is believed to have a negative influence on both the heat transfer performance as well as the ice product purity (i.e. entrainment of salt crystals in the ice product slurry).

Studying the industrial impure and acidic sodium waste water stream showed that pure water and sodium sulfate decahydrate crystals can be obtained from this stream. However severe sulfide corrosion of metal surfaces was observed during the treatment of this solution. In a chemical reaction connected to this corrosion hydrogen sulfide gas is produced in the crystallizer. The addition of NaCl, to increase the heat transfer, is unfortunately also increasing the amount of sulfide corrosion.

Shale gas water (SGW) is produced by the hydraulic fracturing process used to fracture the gas containing rock bed allowing the gas to flow into the well. The amount of water used is large (about 5-6 million gallon/well) and the supply of fresh water is often an issue at the locations where shale gas fields are being developed. The EFC process was identified as a potential treatment technology to convert the SGW into clean water and solid salts. The possibilities for this are studied at 1, 10 and 200 liter scale and the crystallization behavior of this solution is studied down to -30 °C.

The experimental results show that Ba, Na and K are crystallizing as chloride salts simultaneously with ice at a temperature of -23.4 °C. The produced ice product is washed successfully to obtain high purity water. At a temperature of -26 °C, 34 wt% of the incoming stream is converted into clean water and 61 wt% is left behind as a concentrated brine. At this temperature 81 % of the incoming barium and 47 % of the sodium is removed from the feed stream. The crystallization behavior at lower temperatures has not been studied yet, as in the batch experiments the solid content (salt and ice) became too large. In theory it is possible to reach a complete conversion into ice and salt at lower temperatures.

In chapter 5 two different process schemes for the treatment of SGW with the EFC process are given and very basic mass and energy calculations are presented. Choices on the desired amount of salt removal, the specifications for the salt and water products, etc. will be necessary to further explore the required operational conditions and unit operations.

In chapter 6 recommendations are done for further studies that are deemed useful in the development of an industrial EFC process and to improve the currently used experimental set-ups. Besides research aimed at further increasing knowledge on how to treat specific waste streams (e.g. the acidic sodium sulfate or shale gas water) more general studies on the process design are suggested. These studies include: further investigation of the scaling behavior of salt mixtures in order to obtain information on the optimal scraper design and cooling strategies that minimize cooling requirements and maximize the ice and salt production, study the crystallizer internal design to increase ice/salt separation and explore the requirements of the auxiliary equipment required for ice and salt washing and isolation.

Table of Contents

Chapter 1
Introduction

Water is of vital importance to all life on our planet. It is therefore comforting to see, when looking at a map of the world, that the amount of water seems endless. However, this apparent endlessness of the water supply is a more delicate issue than just pointing at the blue spots on a globe. The majority of all water on earth is found as salt water in the oceans or as ice in the polar regions and glaciers. Only a small portion (about 0.9%) of all water is suitable for human consumption. Moreover, an increasing human usage of water (e.g. in agriculture, chemical industry, etc.) further decreases the amount of consumable water due to water pollution.

Fortunately, in the past decades the prevention of water pollution and the reuse of water are widely recognized as essential means to sustain our society and the environment. In many cases this recognition is translated into new or more stringent legislation forcing industries to install wastewater treatment facilities and optimize their water household.

As a result the development of wastewater treatment systems is and will be an important subject for the (chemical) industry, but also for research institutes, engineering firms and universities. Thanks to all this effort many new and improved processes came available for the wide variety of waste streams found in the world. Important factors influencing the success of these processes is the energy requirement and the ability to recover valuable products from the waste stream. The latter aspect is especially interesting because the reuse (or selling) of such a recovered product might compensate for the additional costs of operating the wastewater treatment process.

One of the promising new technologies for treating aqueous waste streams is eutectic freeze crystallization, or EFC. Although the EFC process might be used to treat different types of systems, (e.g. organics in water, organics in organic solvents) its biggest potential lies in the field of removing inorganic solutes from water.

Eutectic freeze crystallization can be seen as an extension to the cooling or freeze crystallization process. Instead of one solid phase, as in cooling/freeze crystallization, EFC produces two solid phases simultaneously. This is achieved by cooling the solution down to the temperature where ice, salt and solution are in equilibrium. This point is called the eutectic point and is different for different mixtures.

In figure 1.1 a very simplified representation of the EFC separation process is given. As can be seen in this figure only ice and salt are leaving the system, hence a zero liquid discharge process. The separation of ice and salt from the crystallizing solution (or mother liquor) is done by utilizing the density difference of the three phases present. In one particular crystallizer design, called the *hybrid crystallizer*, this gravitational separation is taking place inside the crystallizer. In the hybrid crystallizer ice is leaving from the top section and a salt slurry is extracted from the bottom section of the crystallizer.

The amount of energy required to treat an aqueous waste stream with EFC is shown to be much lower than for conventional evaporative processes [Ham, 1999]. When compared to evaporative processes also less expensive construction materials can be used because corrosion is less of an issue at low temperatures. Furthermore, the nature of the EFC process (low temperature and ambient pressure, no additional chemicals needed) makes it an inherently safe process as well.

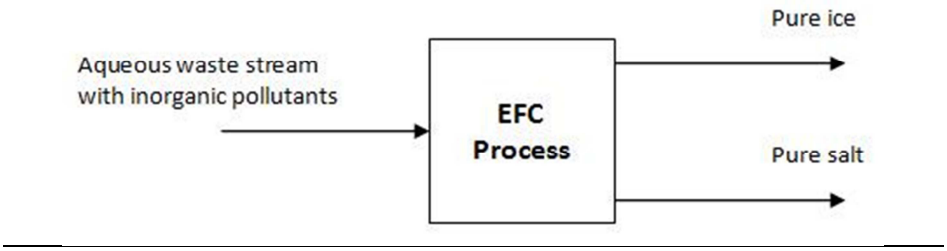

Figure 1.1. Very schematic scheme of the EFC process.

The first ideas to use EFC as a technique to treat aqueous streams dates back to the 1970's, when preliminary process designs were made for the treatment of brines from desalination plants [Stepakof, 1974; Schroeder, 1977]. Despite this early work no commercial eutectic freeze process is operated anywhere in the world yet. However, in recent years extensive research is done on this process, mainly at Delft University of Technology. At this moment the process is on the brink of being brought to the market.

In the development of EFC towards a commercial industrial scale water treatment process several different aspects of the process needs to be investigated in order to be able to design and operate such a process successfully. The list given below shows the main themes that have to be explored further:

- Products obtained from an EFC process.
  - What is the purity of the salt and ice that can be produced from multicomponent mixtures?
    - Experimental work on different industrial solutions.
  - How could a sequential EFC process be used to isolate multiple pure salt products form a waste stream?
  - How could an eventual recrystallization step be employed as an additional purification step?
  - Thermodynamic modeling of low temperature, high concentration mixed electrolyte solutions. To predict salt formation conditions.
- Scaling of ice and/or salt on the heat exchangers.
  - When and how does scaling occur?
  - What is the scaling made of?
  - What is the influence of impurities on the scaling behavior?
  - What is the ideal scraper blade design?
    - Removes all scaling
    - Increases heat transfer by good mixing
    - Low mechanical and hydrodynamic resistance (i.e. low energy consumption)
- Heat exchanger design and heat transfer design policy
  - What is the optimal arrangement for the heat exchanger elements?
    - Vertical location in the crystallizer.
    - Space between the concentric elements and between the elements and wall.
  - How to optimize total heat transfer in the crystallizer?
    - Small areas with high heat transfer rates vs. Large areas with lower transfer rates.
  - Influence of solid content on the heat exchangers performance.
- Salt/ice separation
  - A hybrid crystallizer versus crystallizer-settler combination?
  - What is the influence of internal design on the separation properties?
- Crystallizer design for a continuous operated EFC process.

    - What are issues related to feed introduction (e.g. location)?
    - How is product extraction from the crystallizer occurring and how can this be improved?
    - What are the ideal crystallizer dimensions (volume/height-ratios, etc.)?
- Controllability of the EFC process
    - What are the best process control parameters and variables?
    - The auxiliary equipment in order to design a complete treatment process.
    - How should the ice and salt products be isolated from the product slurries?
        - Belt filters, hydro cyclones, filter presses, etc.
    - How to wash the ice and salt products to enhance product purity?
        - Wash columns, spray wash, etc.
    - What type of pumps are best suited for the various streams in the process?
- How can the energy requirements of the complete process be decreased by heat integration?
- The possibilities to combine the EFC with other technologies used in the (water) industry.

Most of the issues given in this list are closely related to each other and it is not possible (neither necessary) to investigate them as strictly separated research subjects. The blue colored topics were investigated and discussed in this work in greater or lesser extent. Two different aqueous waste streams formed the basis for the work presented in this thesis. The first stream is an impure sodium sulfate stream. This stream served as a basis for the investigation into the scaling behavior on the heat exchangers (Chapter 3). Also extensive pilot scale experiments were performed on this stream to study the behavior of the current crystallizer design and the product purities (Chapter 4).
A second case study was done for a large oil and gas company to study the feasibility of the EFC process to treat a waste water stream originating from shale gas production. This study included product purity analysis, crystallization behavior, pilot scale experimentation and a preliminary description of possible process options (Chapter 5).

Chapter 2
Crystallization and EFC

This chapter is intended to give an overview of some important aspects of crystallization processes in general. In the second part of this chapter the concept of eutectic freeze crystallization is introduced.

Crystallization

Crystallization is a process in which solid particles (with a crystalline structure) are formed from a liquid solution. It is commonly used as a separation and purification technique in the chemical industry. Different types of crystallization are cooling crystallization, evaporative crystallization, melt crystallization, etcetera. This section will briefly introduce some important aspects found in any crystallization process.
Any crystallization reaction can be seen as a process that is build up of three separate steps, these are:

- *Nucleation*: This is the 'birth' of a new crystal in the mother liquor. Nucleation can be either of the *primary* or *secondary* type.
- *Mass transfer*: The transport of solute from the bulk to the crystal surface
- *Incorporation*: Uptake of a solute molecule into the crystal lattice.

The driving force for all these steps is shown to be the *supersaturation* of the solution [Seader, 2006]. The supersaturation is a measure to describe the difference between the state in which a system is and the state that it would be in if the system is in thermodynamic equilibrium. In figure 2.1 this is represented graphically in a phase diagram of a solute-solvent system.

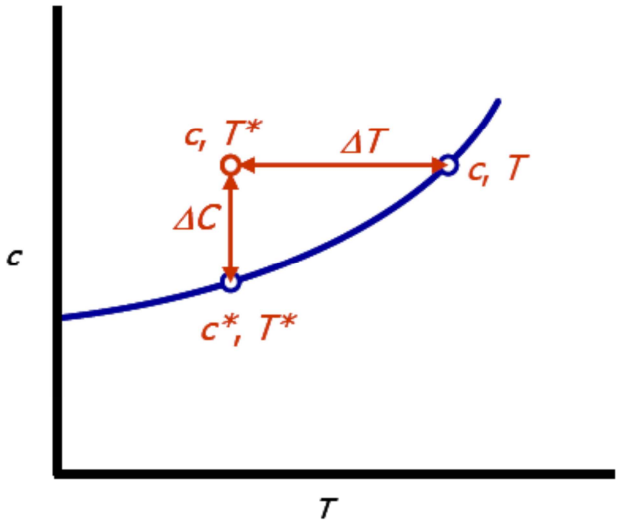

Figure 2.1. Schematic representation of the concept supersaturation and undercooling. A system with concentration c and at temperature T can be said to have a supersaturation of C-C*=ΔC or being undercooled by T-T*=ΔT. (Picture taken from Kramer, et al)

Two different properties can be used to define the deviation from equilibrium, concentration and temperature. In the former case it is called the supersaturation (ΔC), which is the difference between the actual concentration (C) and the equilibrium concentration (C*) at that temperature. The other measure is called *undercooling* (ΔT) and is defined as the difference between the actual temperature (T*) and the temperature that a system with this concentration would have had if in equilibrium (T).

Nucleation

The growth of crystals starts with nucleation. A nucleus is the starting point of a crystal and will increase in size by crystal growth. There are two different types of nucleation, primary nucleation and secondary nucleation.

Primary Nucleation

Primary nucleation can be seen as the absolute starting point of any crystallization process and can be either classified as homogeneous or heterogeneous.

In the process of *homogeneous primary nucleation* local concentration fluctuations in a supersaturated solution can result in the formation of clusters consisting of an ordered packing (crystal lattice) of solute molecules. When the cluster reaches a critical radius a stable nucleus is formed. The critical radius is determined by the trade-off between the free energy changes for volume creation ($\Delta G < 0$) and surface creation ($\Delta G > 0$).

In *heterogeneous primary nucleation* the starting point for a new nucleus is a foreign particle present in the supersaturated solution onto which solute molecules can attach and form a stable crystal lattice. Examples of heterogeneous nucleation sites are dust particles or the crystallizer wall.

The energy barrier for heterogeneous nucleation is lower compared to homogeneous nucleation due to the lower value for the free energy change associated with surface creation. Therefore at low supersaturations and industrial conditions (i.e. presence many heterogeneous nucleation sites) heterogeneous nucleation is the main source of primary nucleation.

Secondary Nucleation

When existing crystals act as nuclei for the formation of new crystals it is called secondary nucleation. Sources for secondary nucleation are amongst others collisions between crystals and the stirrer or crystallizer wall or between crystals itself. Fragments of crystals arising from these collisions act as growth centers (i.e. nuclei) for new crystals.

A special type of secondary nucleation is *seeding*. Seeding is the addition of crystals to a supersaturated solution to initiate crystallization. This is done for example to initiate crystallization when there is no time to wait for primary nucleation to occur or to control the type of crystals (i.e. the composition and morphology) to be formed in the reaction. Seeding can also be used in batch crystallization to exert some control on the crystal size distribution of the final product.

The table in figure 2.2 lists several sources of nuclei, both primary and secondary, found in industrial crystallizers.

Source of Nuclei	Type of Nucleation Process	Prevention or Remedy
Boiling zone	Primary	Reduce specific production rates, increase crystal surface area
Hot feed inlet	Primary	Enhance heat dissipation, reduce degree of superheating, carefully chosen inlet position
Inlet of direct coolant	Primary	Enhance heat dissipation, reduce temperature of coolant chosen inlet position
Heat exchangers, chillers, etc.	Primary	Reduce temperature gradients by increasing surface area, increase liquid velocities
Reaction zone	Primary	Enhance mixing and dissipation of supersaturation, increase crystal surface area
Cavitating moving parts	Primary	Adjust tip speed, suppress boiling by sufficient static head
Crystal/crystallizer contacts Collisions with moving parts (impellers, pumps etc.) Collisions with crystallizer walls	Secondary	Adjust tip speed and design configuration, coat impellers with soft materials, reduce if possible magma density and mean crystal size
Crystal/crystal contacts Crystal grinding in small clearance spaces (impeller/draft tube, pump stator/rotor)	Secondary, attrition breakage	Carefully specify all clearances and hydrodynamics of two-phase flow therein
Crystal/solution interaction Fluid shear, effect of impurities, etc.	Primary or secondary	Reduce jetting, get to know the effect of impurities for each particular system, prevent incrustation

Figure 2.2. Table showing sources of nuclei in industrial crystallizers. (Taken from Myerson, 2002)

Mass transfer and incorporation

The rate of transport of solute molecules towards the crystal surface is an important parameter in the overall rate of crystal growth. Mass transfer is a function of the diffusivity, film layer thickness and the concentration difference between the bulk and the crystal surface. The film layer thickness is mainly influenced by the motion of the fluid surrounding the crystal, high velocities decrease the thickness (thus increasing transport rates). The diffusivity is determined by the chemical and physical properties of the solute and solvent (e.g. size, polarity, charge, etc.) and by properties of the system as a whole like its temperature, viscosity and density. Especially for multi-component electrolyte solutions predicting the exact value of a diffusivity constant (and eventually the mass transfer rate) is complex, so often experimentally determined diffusivity constants needs to be found if one wants to calculate mass transfer rates.

When a solute molecule reaches the surface of a crystal it may or may not be incorporated into the crystal lattice. The process of incorporation is an important factor influencing the shape of a crystal and the purity of a product crystal. Although crystallization is a very selective process due to the highly structured nature of a crystal lattice, it may occur that impurities are incorporated into the lattice. This is more likely to happen when impurities molecules are similar (in size and charge) to the main product molecules.
Another mechanism of impurity up-take in crystals is by *inclusion*. Inclusions are a result of defects in the growing crystal surface. These defects can be due to local variations in growth rates (e.g. caused by impurities near the surface or high supersaturations) or by mechanical sources (e.g. crystal-impellor or crystal-crystal collisions). When a defect causes an overhang to form this will eventually lead to the formation of a pocket into which mother liquor gets trapped. See figure 2.3 for a schematic representation of inclusion formation. As a general rule of thumb it can be said that higher growth rates increases the chance on impurity uptake in the product [Myerson, 2002].

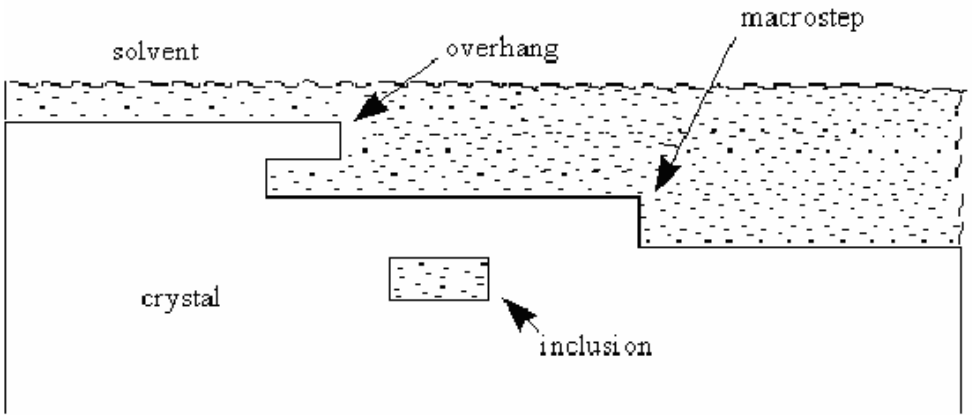

Figure 2.3. Schematic representation of impurity uptake by inclusion formation. Inclusions are formed due to defects caused by local changes in growth rate or by collisions of crystal with other crystals or crystallizer internals. [Taken from Kramer, et al]

The rates of nucleation (primary and secondary) and growth (mass transfer and incorporation) determine the eventual product properties like particle size distribution and the purity of the crystals. However these relationships are complex and extensive data collection is required to establish a good predictive model for a particular mixture and crystallizer. In *The Handbook of Industrial Crystallization* [Myerson, 2002] more detailed information on the data acquisition and growth rate modelling is given. Himawan described the development a population balance model for

the eutectic freeze crystallization process of a $MgSO_4$-solution in a scraped wall crystallizer [Himawan, 2002].

Eutectic Freeze Crystallization

The basis of eutectic freeze crystallization (EFC) is the existence of the eutectic point. The eutectic point is a characteristic point in the phase diagram of a salt-water mixture. At the eutectic point equilibrium exists between ice, salt and a solution with a specific concentration. This specific concentration is called the eutectic concentration and the temperature at which this equilibrium is found is the eutectic temperature.
Figure 2.4 shows a typical phase diagram for a binary system (salt-water). In the case that an aqueous solution has exactly the eutectic concentration cooling the solution down towards its eutectic temperature will lead to the simultaneous crystallization of both ice and salt. However, it is more common that a solution has a salt concentration that is lower or higher than the eutectic concentration. In the former case ice will crystallize first (point 2) when the temperature is decreased. Due to the formation of ice the salt concentration in the remaining liquid (the *mother liquor*) increases, which leads to a decrease in freezing point and by continuing cooling the *ice line* is followed till the eutectic point (3) is reached. This is represented by path A in figure 2.4. When the original salt concentration is higher than the eutectic concentration the opposite happens (Path B); first salt is crystallizing (2) till the salt concentration of the mother liquor decreases to the eutectic concentration, from that moment on also ice will be formed (3).

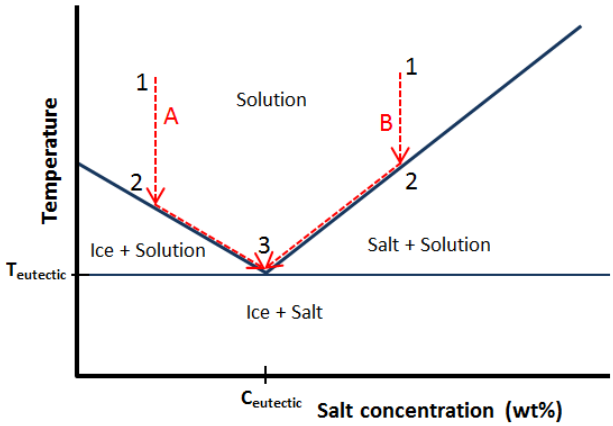

Phase diagram for a binary salt-water system. Two different paths to the eutectic point are possible. Path A is followed when the starting solution has a lower than eutectic concentration. In that case first ice is crystallizing from the solution till the eutectic concentration is reached. For a solution with a higher than eutectic concentration the opposite happens (Path B).

Figure 2.4. A typical phase diagram for binary system.

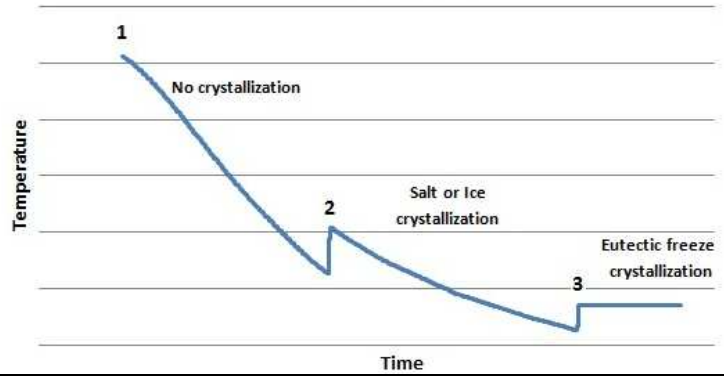

This graph shows the typical cooling profile for cooling down a solution to its eutectic point. The numbers are indicating the positions in the phase diagram in figure 2.4. For path A position 2 is the start of ice crystallization and for path B position 2 is the start of salt crystallization. Number 3 indicates the eutectic point.

Figure 2.5. Cooling profile observed when cooling down a solution to its eutectic point. The numbers correspond to the numbers in figure 2.4.

The graph in figure 2.5 is a typical cooling profile for a solution that is cooled to its eutectic point. Cooling down an unsaturated solution (1) will at a certain temperature lead to the crystallization of

either ice or salt (depending on the initial concentration). Crystallization will not initiate immediately when the equilibrium temperature is reached but the solution will become supersaturated first. When nucleation occurs the energy that is released by the crystallization process leads to a jump in the temperature (2). This first jump is called the either the salt or ice jump (depending on the crystallizing component). The second jump in temperature marks the systems arrival at the eutectic point (3). After the jump the temperature remains constant at the eutectic temperature of this specific system. These temperatures jumps are not always observed very clearly. The size of the jumps is determined by the level of undercooling the system reaches before crystallization starts. Sometimes only little undercooling is achieved and in these cases the temperature jumps may not be recognizable.
Extracting heat from a suspension at its eutectic temperature will not lead to a decrease in temperature but to the production of ice and salt crystals only. The heat that is released by this crystallization is used to maintain the constant temperature. (This property of an eutectic mixture is analogue to water at its boiling point, the water will remain at 100 °C independent of the amount of heat added). Because the salt concentration in the mother liquor remains constant the ratio of ice and salt production is fixed.
The difference in density of the three phases present at the eutectic point (ice, salt and solution) makes it possible to separate these phases by gravity methods (i.e. settling). In the ideal EFC crystallizer complete separation is realized inside the crystallizer itself.

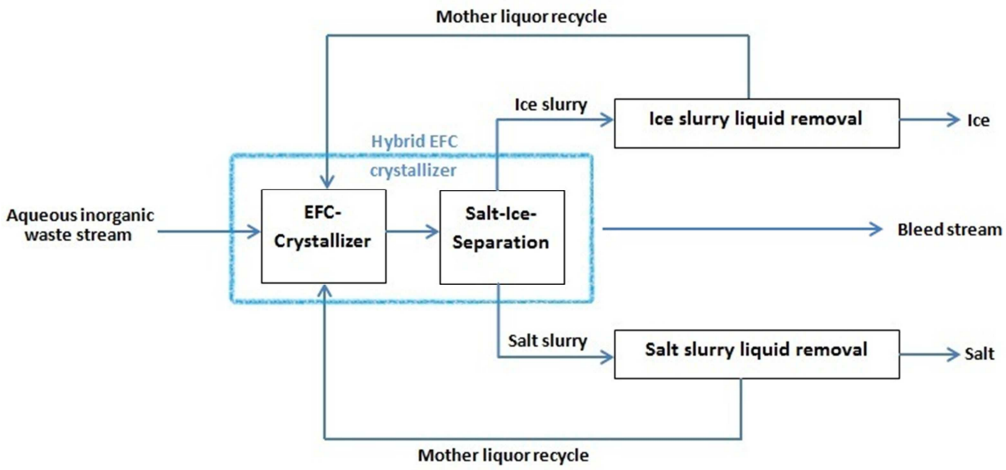

Figure 2.6. Scheme of an EFC process. In a hybrid crystallizer crystallization and solid-solid liquid separation is combined into one unit. A bleed stream is not necessarily required (its need is determined by process optimization decisions)

Such a design is called a *hybrid crystallizer* (see blue box in figure 2.6). When for some reasons separation inside the crystallizer is not sufficient an additional settling device can be installed after the crystallizer. Figure 2.6 shows a schematic process block scheme for the EFC process. Also depicted in this scheme is a purge stream to remove non-crystallizing components present in the feed solution.

In the figure (figure 2.7) on the next page eutectic concentrations and temperatures are given for several salts. The presence of additional components in a solution leads to a change in the eutectic concentration and temperature. A pseudo-eutectic point is reached when at least one salt species is crystallizing simultaneously with ice, while other components remain in solution.

Compared to evaporative processes EFC is more often producing hydrated salts (e.g. $NaCl.2H_2O$). The recrystallization of these hydrates to anhydrate salts could be used as an additional salt purification step (i.e. removal of impurities trapped in the hydrated crystals). A disadvantage of producing hydrated salts is the risk of recrystallization of the product salt after it is bagged, this may result in

caking of the salt product or a wet product. An efficient recrystallization step can prevent these problems.

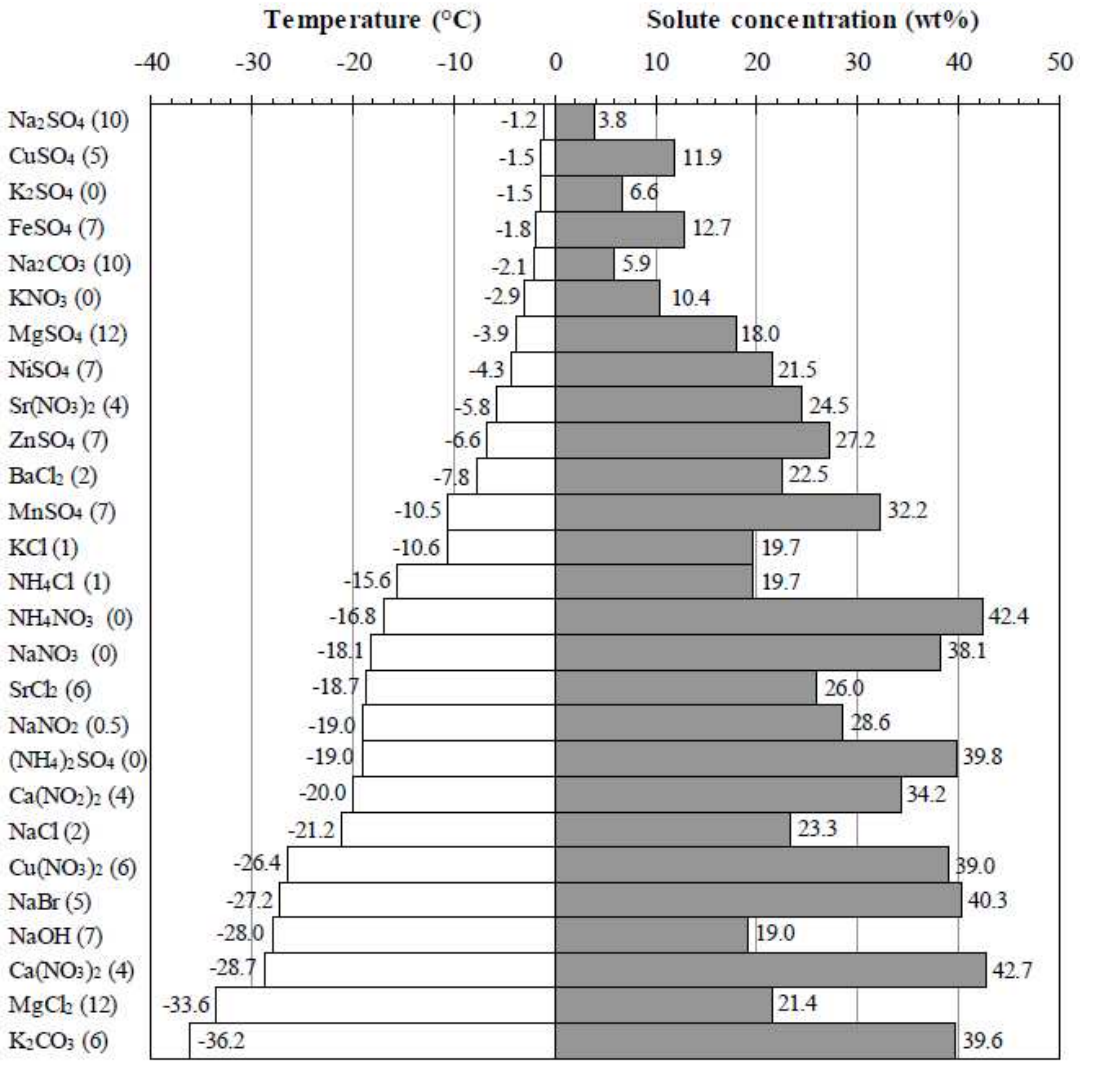

Figure 2.7. Graph showing the eutectic temperatures and concentrations of several aqueous salt solutions. The values between brackets indicate the hydrate number of the formed salt. (Taken from Pronk, 2006)

Treatment of an aqueous impure sodium sulfate waste stream with the EFC-separation process.

Chapter 3
Scale Formation during EFC of a Sodium Sulfate Solution

Introduction

A central theme in the development of the EFC-separation process is the formation of a so called scale layer on the heat exchanger surfaces. This scale layer has a negative effect on the overall heat transfer of the heat exchangers and increases the mechanical energy requirements of the process because of an increase in the scraper torque.
The scaling of the heat exchangers in the crystallizer under eutectic conditions was studied at 10 L scale. A pure 8 wt% sodium sulfate solution was used as the base case in the experiments because of its resemblance with a real industrial waste stream which is further studied in the next chapter. The experiments were aimed at three points:

- Investigate the scaling behavior and qualitatively describe the scaling phenomena.
- Study the composition of the scale layer.
- Investigate the effect of additional salts on the scaling behavior.

Scale formation

A scale layer is formed when solid particles (salt and/or ice) adhere to the cold (metal) surface of the heat exchanger. The development of a scale layer leads to a decrease in the heat transfer due to the thermal resistance of such a layer. So scaling is an important factor in the EFC process, because a decrease in heat transfer leads to a decrease in the energy efficiency of an industrial crystallization process.
To prevent the build-up of such a scale layer scrapers are used to continuously remove the crystals from the heat exchanger surface. However, in some cases the severity of the scaling is so large that the current scraper performance is not sufficient to guarantee scaling-free operation of the EFC-crystallizer. Especially pure water and purely binary systems (only one dissolved salt) show this extensive scaling behavior. The presence of non-crystallizing components in the system is believed to reduce the scale layer formation.
A theory developed by P. Pronk [Pronk, 2006], describes the effect of non-crystallizing components on the formation of scale layer. Pronk's theory was developed to describe the scaling behavior in fluidized bed ice generators, but it might also be extended to qualitatively describe the scaling behavior during EFC in a scraped wall crystallizer.

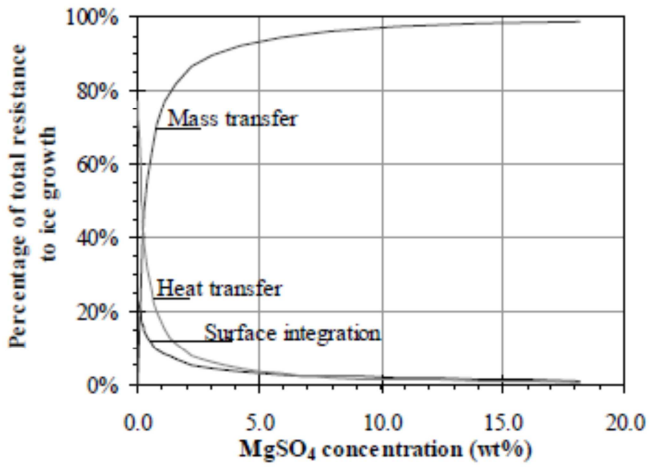

Figure 3.1. Contributions to the growth of ice crystals on a heat exchanger surface. This graph is for an aqueous $MgSO_4$-solution and a temperature difference between surface and liquid of 1K. (Taken from Pronk, 2006.)

Pronk describes three factors that together make-up the resistance to ice layer growth. The first is the heat transfer, this is because the heat of crystallization must flow away from the surface in order to remain it at its freezing temperature. The second factor is surface integration, this takes into account the rate at which (water) molecules are incorporated in the crystal lattice at the surface of a scale layer. The third contribution to the layer growth resistance is mass transfer. The mass transfer resistance determines the velocity at which molecules in the bulk can reach the cold surface. Calculations by Pronk showed that mass transfer is by far the largest

contribution to the total resistance to ice layer growth in aqueous solutions, see figure 3.1. The mass transfer resistance is caused by the accumulation of solute molecules (often ions) near the ice layer. This is because these solute molecules are, unlike water molecules, not integrated in the scale layer. This increase in local solute concentration increases the resistance that water molecules encounter on their way towards the growing ice layer.
Experiments by Pronk and Vaessen [Vaessen, 2003] also show that scaling becomes more severe when in addition to ice also salt starts to crystallize, so under EFC conditions. This is also explained using the above mentioned theory. When salt crystals are formed the accumulation of ions near the scale layer surface is decreased (solute molecules are taken away into the growing salt crystals), so also the mass transfer resistance that water molecules encounter to reach the surface is decreased. This leads to higher ice scale growth rates for EFC processes when compared to ice crystallization from an aqueous solution. Figure 3.2 schematically depicts this concept.

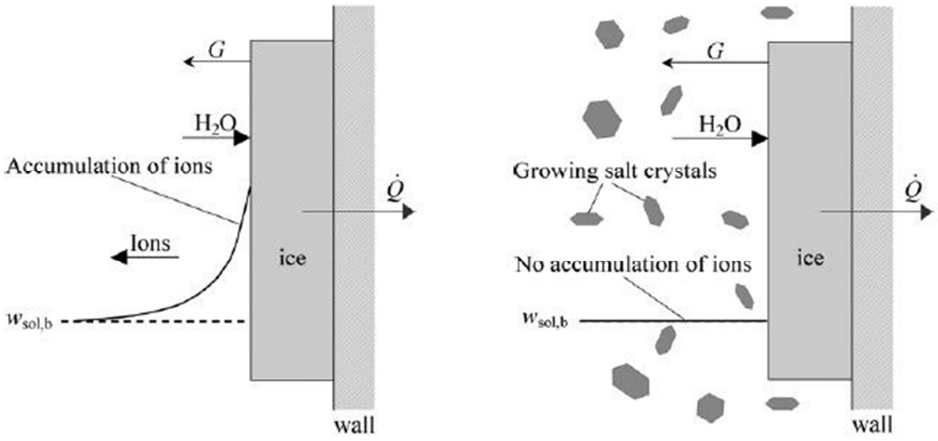

Figure 3.2. Schematic representation of the difference between non-eutectic (left) and eutectic ice scale formation (right). Accumulation of ions near the surface increase mass transfer resistance of the water molecules, thus decreasing the scale formation rate. (Picture taken from Pronk, 2006)

Experimental procedure

The experiments were performed in a 10 liter crystallizer with a scraped heat exchanger at the bottom. The scrapers are driven by an electrical motor drive set at a fixed rotational speed (120 rpm). A pressurized air device is used to push the scraper blades onto the heat exchanger surface. Figure 3.3A shows an schematic drawing of the experimental 10L set-up and figure 3.3B is a photo of the system.

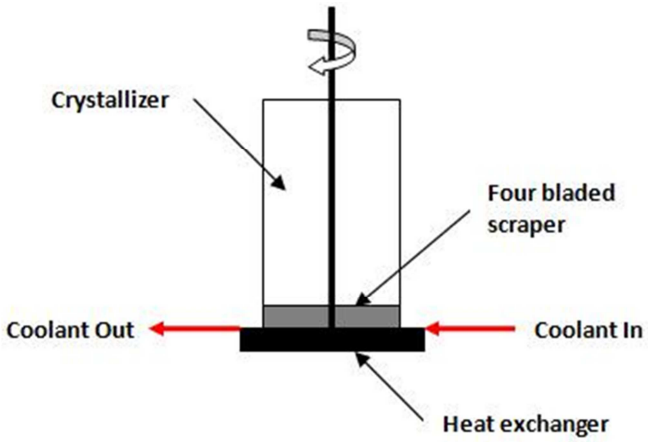

A. Schematic drawing of the 10 L crystallizer set-up.

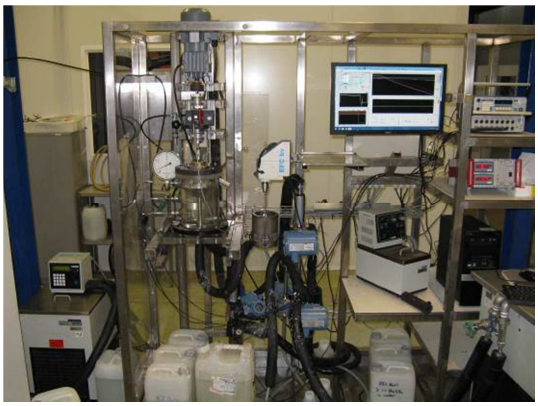

B. Photo of the 10 L crystallizer set-up.

Figure 3.3. The 10 L scraped bottom crystallizer.

The force required to move the scrapers over the cold surface is measured as a torque using a torque sensor. The flow rate of the coolant is measured with a magnetic flowmeter. Freezium™-40 is used as a coolant for all the experiments. Temperatures of the crystallizing medium and the incoming and outgoing coolant is measured with Pt-100 sensors connected to a F250 (National Instruments) temperature measurement system. Logging of the measurements is done with a dedicated Labview program, which logs all data every 5 seconds.

The amount of heat transferred from the crystallizer to the coolant is calculated with the following equation:

$$Q = \phi_V \cdot \rho_{coolant} \cdot C_P \cdot \left(T_{Coolant}^{Out} - T_{Coolant}^{In} \right)$$

Where: Q = Heat transfer [kW]
ϕ_V = Volumetric flowrate of coolant [L/s]
$P_{Coolant}$ = Density of coolant [kg/L]
C_P = Heat capacity of coolant [kJ/kg]
T^{Out} = Coolant outlet temperature [K]
T^{In} = Coolant inlet temperature [K]

From the measured heat transfer one can calculate the heat transfer coefficient (U) with:

$$U = \frac{Q}{\Delta T_{ln} \cdot A}$$

Where: U = Heat transfer coefficient [kW/(m^2.K)]
Q = Heat transfer trough the cold plate [kW]
ΔT_{ln} = Logaritmic temperature difference between coolant and mother liquor [K]
A = Area of the heat exchanger surface [m^2]

The density and heat capacity of Freezium™ is slightly temperature dependent and the values are taken from the information provided in table 3.1.

Table 3.1. Density and heat capacity of Freezium™ at different temperatures.

Temperature	Density	Heat capacity
[°C]	[kg/L]	[kJ/(kg.K)]
20	1.281	2.87
0	1.289	2.82
-10	1.293	2.79
-15	1.295	2.78
-20	1.297	2.76
-25	1.299	2.75
-30	1.301	2.74
-35	1.303	2.74

Different solutions were prepared and in all experiments the eutectic temperature was maintained for at least half an hour in order to obtain data at a constant temperature difference between heat exchanger and medium. When operating at the eutectic point the Na_2SO_4 concentration and crystallizer temperature will remain constant. However, a steady state cannot be reached in this system because the ice and salt content in the crystallizer keeps increasing in time. Also additional non-crystallizing components accumulate in the mother liquor as its volume decreases due to the removal of water and Na_2SO_4 from the solution.

Results and discussion

Scaling in a pure Na_2SO_4 solution

Cooling an 8 wt% Na2SO4 solution down leads to the crystallization of Na2SO4.10H2O crystals around 8 °C. Because no seed crystals were used a certain degree of subcooling is realized before salt or ice crystallization starts.
The torque is used as a measure for the amount of scaling on the heat exchanger surface. It can be used in a qualitatively manner only since a good relation between measured torque and layer growth is not established.
The graph in figure 3.4 shows the results of an experiment where the ΔT_{ln} was 14 °C after the eutectic temperature is reached. Although this experiment is performed with an unusual large temperature difference, it is shown here because the characteristic pattern of torque development starting at the eutectic point and after the cooling machine was turned off is very clear from this graph. The results of the experiments at different values for ΔT_{ln} all show the same pattern of torque development, only the values differ for the different conditions.

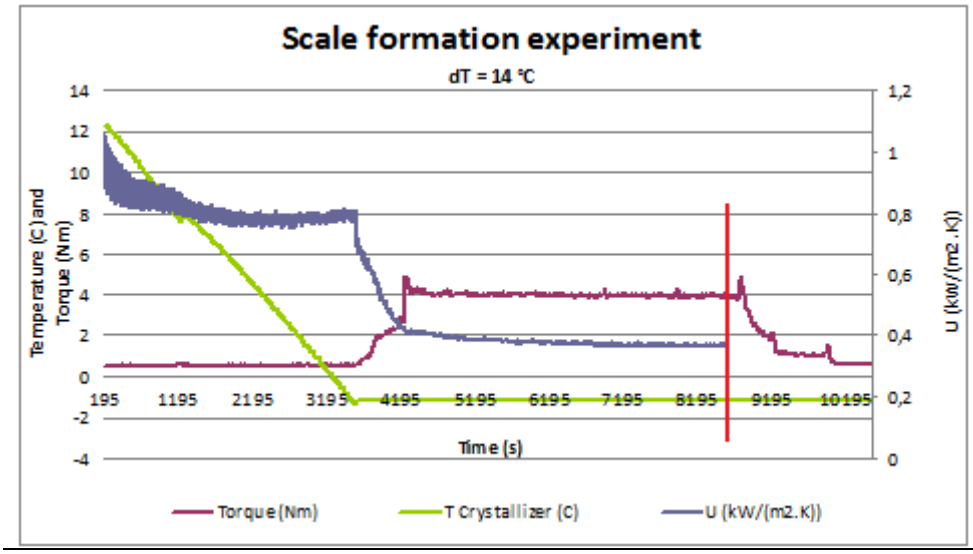

Figure 3.4. This figure shows the patterns of measured and calculated variables for a scaling experiment with a large ΔTln of 14 °C. The red line indicates the point at which the coolant flow is switched off.

A sharp decrease in the heat transfer coefficient (U) can be seen in the graph of figure 3.4 between the situation before and after the eutectic temperature was reached. The heat transfer coefficient drops from 0.8 to 0.37 kW/(m2K).
No increase in torque is observed before the mixture reaches the eutectic temperature, although salt crystallization starts already at a temperature of 7.7 °C (see figure 3.5A). This is an indication that salt crystallization alone is not responsible for the formation of a scale layer. After a certain time the torque reaches a constant value that is maintained until the cooling machine is turned off.
Another effect that can be seen in the graphs is a maximum value of the torque before it attains a constant value. The peak that is observed first (before the constant value is reached) might be due to an overshoot in the scale layer growth, the scraper blades subsequently 'polish' the solid layer. An equilibrium between crystallization and crystal removal by scraping is leads to a constant value for the torque after this point. The layer thickness is probably determined by the heat transfer resistance of the layer itself, the heat of crystallization has to leave trough the bottom plate (neglecting heat losses through the crystallizer wall). When the rate at which heat can be transported through the scale layer decreases also the rate of crystal growth at the layer surface decreases to a value which

equals the removal rate of the scraper blades. A similar explanation is given by Qin, et al [Qin, 2009] who studied the formation of an ice layer at scraped cooled surfaces from sucrose solutions.

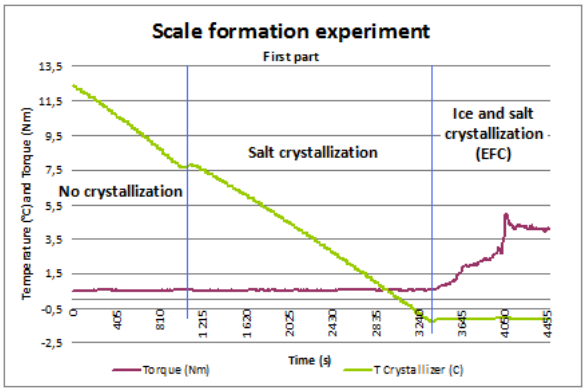

A. Close-up of the first part of the scaling experiment. The jump in the temperature curve at 7.7 °C indicates the onset of salt crystallization.

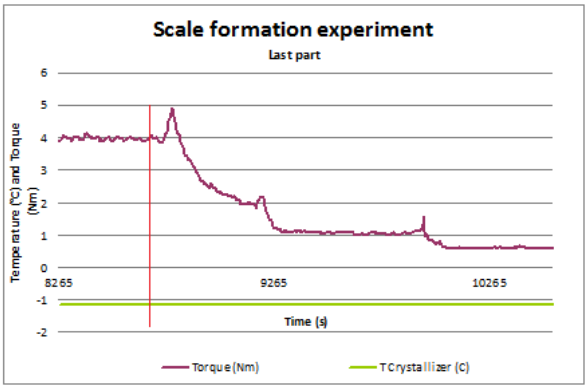

B. Close-up of the last part of the scaling experiment. The vertical line shows the moment at which the coolant flow is turned off.

Figure 3.5. Close-ups of the formation and removal of scaling for the experiment with an dTln of 14 °C after the eutectic point is reached.

The two smaller peaks after the coolant the coolant flow stopped (figure 3.5B) are associated with the breakage of the scale layer, because this was clearly heard and after these moments relatively large fragments of scaling can be seen in the crystallizer (See figure 3.6).
At the moment of the first (and largest) peak after the coolant flow is stopped no large fragments were observed to break loose yet. A possible explanation for this peak might be the softening of the upper part of the ice layer which is starting to partly melt because of the heat added by the scraper blades and the lack of heat withdrawal by the coolant. The scrapers will temporarily have to plow through the softer ice leading to a short increase in the torque.

Table 3.2. Summary of the scaling experiments results for a 8 wt% Na2SO4 solution in the 10L scraped bottom crystallizer.

ΔT	Torque	Q	U
°C	Nm	(kW/(m2))	kW/(m2.K)
7,49	2,88	3,67	0,49
7,64	2,72	3,29	0,43
8,46	2,72	3,76	0,44
9,38	3,14	3,98	0,42
10,39	3,19	3,95	0,38
11,28	3,51	4,43	0,39
12,08	3,74	4,69	0,39
12,20	3,78	4,62	0,38
13,92	3,98	5,18	0,37
15,86	4,42	5,26	0,33

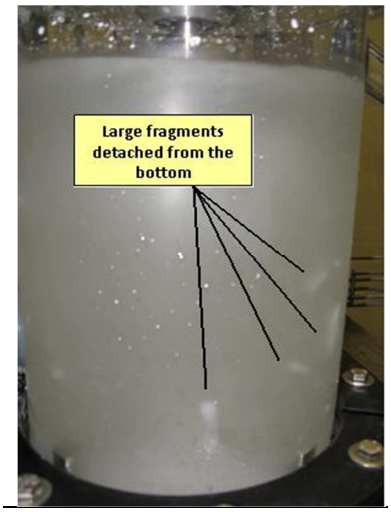

Figure 3.6. After the coolant flow is switched off for some time breakage of the scale layer is heard and large fragments become visible in the crystallizer.

The results for different temperatures differences (ΔT_{ln}) show similar patterns, only the values differ. Table 3.2 summarizes the different experimental results. The values presented in that table are averaged over a range in which the ΔT_{ln}, torque and crystallizer temperature were constant and the time of these interval is at least 45 min. The graphs in figure 3.7 visualizes the results obtained for different temperature settings.

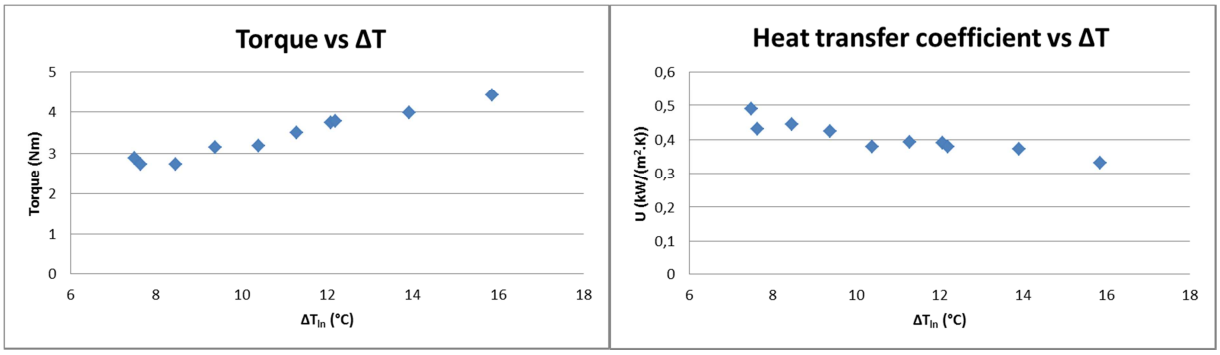

Figure 3.7. Graphs showing the results for the scaling experiments with a 8 wt% Na_2SO_4 solution.

Another experiment was done to see whether the scale layer is dynamic in nature or not. The meaning of dynamic here is that the ice layer can grow and shrink as a function of the amount of heat that is extracted from the system. To investigate this, first a layer was developed at a certain ΔT then the ΔT was decreased for some time, then the ΔT was increased again to its original value. The graph in figure 3.8 shows the results of this experiment. When the temperature set-point of the cooling liquid is increased the torque decreases and the heat transfer coefficient increases, this is very well in agreement with the other experiments. When the ΔT is increased again the torque also increases and the heat transfer decreases again.

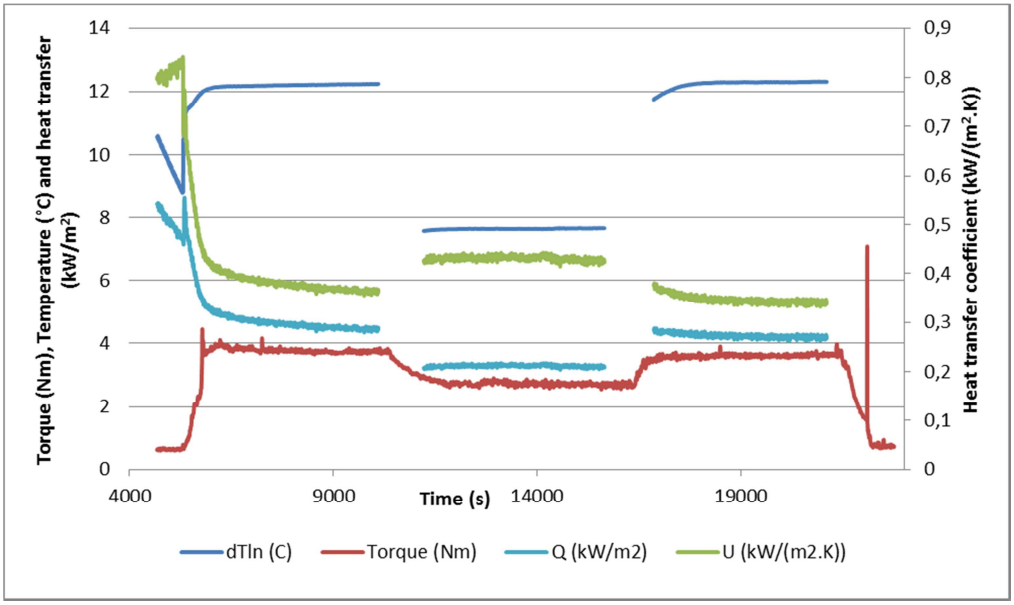

Figure 3.8. Graphs showing the effect of subsequent decrease and increase in ΔT during one experiment. The large peak in torque at the end is due to breakage of the scale layer.

<u>Comparing the EFC behavior of a 4 wt% with a 8 wt% Na_2SO_4 solution.</u>

To see the effect of the salt concentration in the start solution on the scaling and heat transfer at eutectic conditions a 4 wt% $NaSO_4$ solution was used in an experiment. The result is shown in figure 3.9, the results for an 8 wt% solution is shown also. The temperature difference between the cold plate and the solution is 7.5 °C and 7.7 °C for the 4 wt% and 8 wt% solution, respectively. Salt crystallization starts at -1.8 °C for a solution with 4 % Na_2SO_4.

The torque in the 4 wt% experiment attains a constant value of 2.6 Nm after ice crystallization is started. For the 8 wt% experiment the torque first decreases slowly until a constant value of 2.5 Nm. The heat transfer coefficient after the eutectic point is reached is 0.5 kW/(m^2.K) for the 4 wt% solution and 0.4 kW/(m^2.K) for the 8 wt% solution.

The difference in overall heat transfer coefficient cannot be explained with the scraper torque (which is higher for the 4 wt% case). A possible explanation is that a higher solid fraction in the 8 wt% case, due to the large amount of salt crystals formed before the eutectic point is reached, leads to an increase in heat transfer resistance at the scale layer/liquid interface. It is also possible that the scale layer is thicker (but smoother) for the 8 wt% case and a thicker layer leads to more heat transfer resistance. In the current set-ups it is not possible to measure the scale layer thickness.

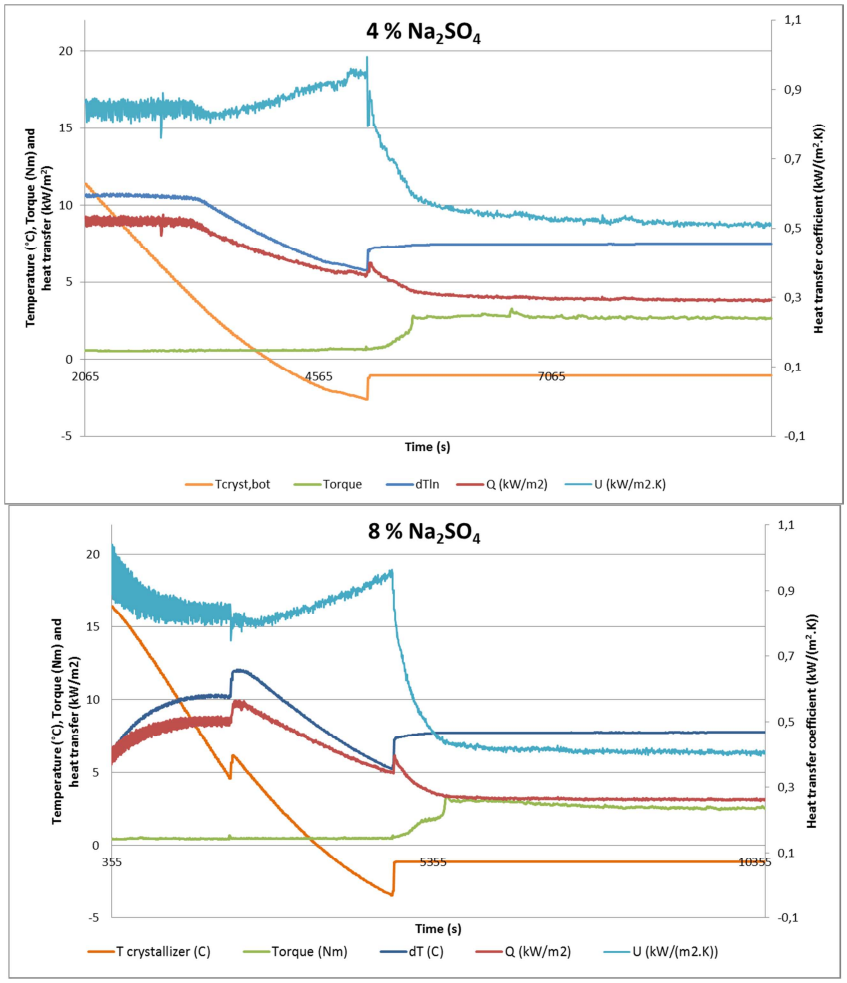

Figure 3.9. Comparing heat transfer and sraper torque in an EFC experiment with a 4 and 8 wt% Na_2SO_4 starting solution.

Starting at the 'ice-line'.

Another experiment was done to verify the observation that ice crystallization, and not salt crystallization, is causing the large increase in scraping torque and decrease in heat transfer. For this experiment a solution of 3 wt% Na_2SO_4 was used as a start solution. This concentration is lower than the eutectic concentration, so first ice is being formed.

Due to the low heat transfer rate, the time required to reach the eutectic concentration by freeze crystallization was found to be too long. Therefore, some salt was added to the solution to reach the eutectic point. After some time the temperature slightly increased and remained constant. After that point $Na_2SO_4.10H_2O$ seed crystals were added to make sure the eutectic point was indeed reached.

The results of this experiment are graphically presented in figure 3.10. A large increase in scraping torque and decrease in heat transfer is found at the onset of ice crystallization. Furthermore, no large effects were seen on the scraping torque and heat transfer after salt started to crystallize as

well. Although a minor decrease in scarping torque and heat transfer coefficient can be seen in the graphs after extra salt was added.
This result is not in agreement with the description given by Pronk and Veassen which states that scaling tends to increase when the eutectic point is reached.

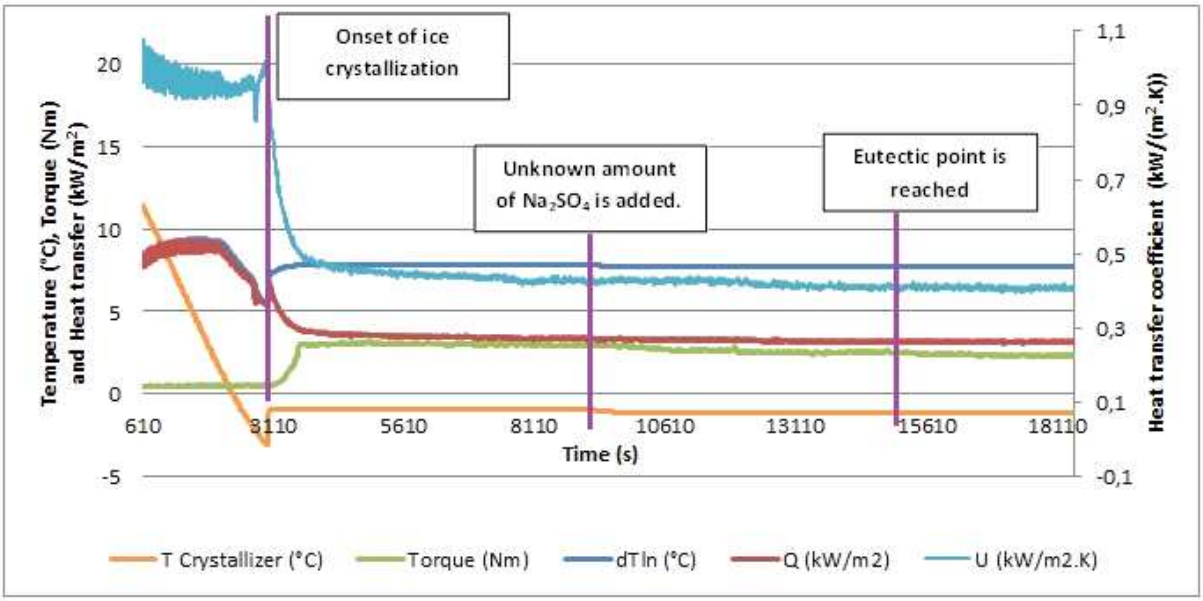

Figure 3.10. Results of the experiment in which the starting solution has a lower than eutectic concentration (3 wt% Na_2SO_4). First only ice is crystallizing leading to an increase in scraping torque and a decrease in heat transfer. After extra salt is added and dissolved the eutectic point is reached.

Composition of the scale layer

Because it is difficult to obtain samples of the scale layer from the scraped bottom crystallizer (because of its construction) a couple of experiments were done in a 10 L scraped wall crystallizer. In this set-up it was possible to grow a scale layer and remove it from the wall for visual inspection and analysis. As already shown in previous experiments also in this set-up a layer started to grow at the moment the eutectic temperature was reached. After some time the scraper is blocked by the scale formation and the cooling machine is set to a higher temperature. The temperature was increased in order to be able to detach scale fragments from the wall. At low wall temperatures (below the eutectic temperature of -1.2 °C) it was not possible to remove the layer from the wall by hand (with a metal scraper). Figure 3.11 shows the scaling in the crystallizer and figure 3.12 shows samples of the scale scraped from the wall. These samples were later placed in a stove to determine the dry weight of the scale fragments.

Figure 3.11. Scale grown on the wall of the 10 L scraped wall crystallizer. The starting solution was a pure 8 wt% Na_2SO_4 solution.

The dry weight of the samples is found be 3.4 wt% (average of three samples) for a pure 8 wt% Na_2SO_4 solution. The concentration in the liquid at eutectic conditions is 3.8 wt% [Pronk, 2006]. Although some adhering liquid was still present on the samples when they were placed in the stove, it is impossible that this will cause the salt concentration in the scale to be 3.4 wt%. So it can be

concluded that at least some Na_2SO_4 is built into the scale layer. It is not known whether this salt is incorporated into the scale layer as mother liquor inclusions within the ice or as Na2SO4.10H2O crystals (visual inspection of the samples did not clearly show the presence of salt crystals).

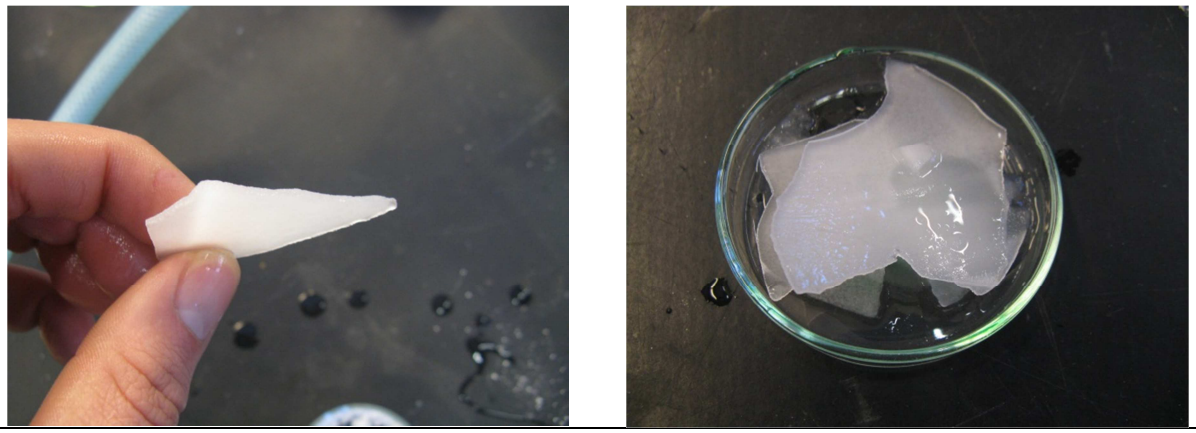

Figure 3.12. Samples of the scale scraped removed from the wall of the 10 L scraped wall crystallizer.

Based on the information about mother liquor inclusions (see Chapter 2) it is possible that these may form within the ice structures at the cooled walls of the crystallizer because the relative large temperature difference will result in high ice layer growth rates. High growth rates increases the chance on defects in the ice crystal structure, leading to the trapping of mother liquor within the ice layer.

Effect of additional salts on the scaling behavior

To investigate the effect of additional components on the scaling behavior in an EFC process a couple of experiments were performed. In the first set $MgCl_2$ was added to a 8 wt% Na_2SO_4 solution as additional salt. In the second set NaCl was added as extra non crystallizing component. Sodium chloride and magnesium chloride ware chosen because it was assumed that these salts will not crystallize at the concentrations and temperatures encountered during these experiments.

<u>Na_2SO_4 + $MgCl_2$ experiments</u>

The four graphs on the next page (Figure 3.13) show the results of the experiments in which $MgCl_2$ was added as a non-crystallizing salt. The first graph is for a pure 8 wt% Na_2SO_4 solution. The other three graphs are showing the effect of increasing $MgCl_2$ concentrations. In the first graph also the onset of salt and ice crystallization are indicated. In the other graphs these features (jumps in temperature) can also be recognized although the size and location of the jumps differ in all four experiments. Especially the size of the salt-jump decreases with increasing $MgCl_2$ concentrations.

The temperature during an experiment with extra components cannot be kept constant (with the used set-up) because during batch crystallization the non-crystallizing components accumulate in the mother liquor. This accumulation leads to a continuous depression of the eutectic temperature. However, as can be seen in the graphs the decrease in temperature after the eutectic point is reached is rather small over the time scale of the experiment.

Because the eutectic temperature is decreasing also with increasing $MgCl_2$ concentration the cooling machine setting was adjusted such that the temperature difference between the solution and the cooling plate (ΔT_{ln}) was more or less equal in all four cases.

By comparing the different graphs it becomes clear that increasing the concentration of $MgCl_2$ decreases the amount of scraping torque (from 2.7 Nm for the pure system to 1.2 Nm after adding 3% $MgCl_2$). The heat transfer coefficient shows a large decrease after the eutectic point is reached for the pure Na_2SO_4 system (from 0.94 to 0.41 kW/(m^2.K)).

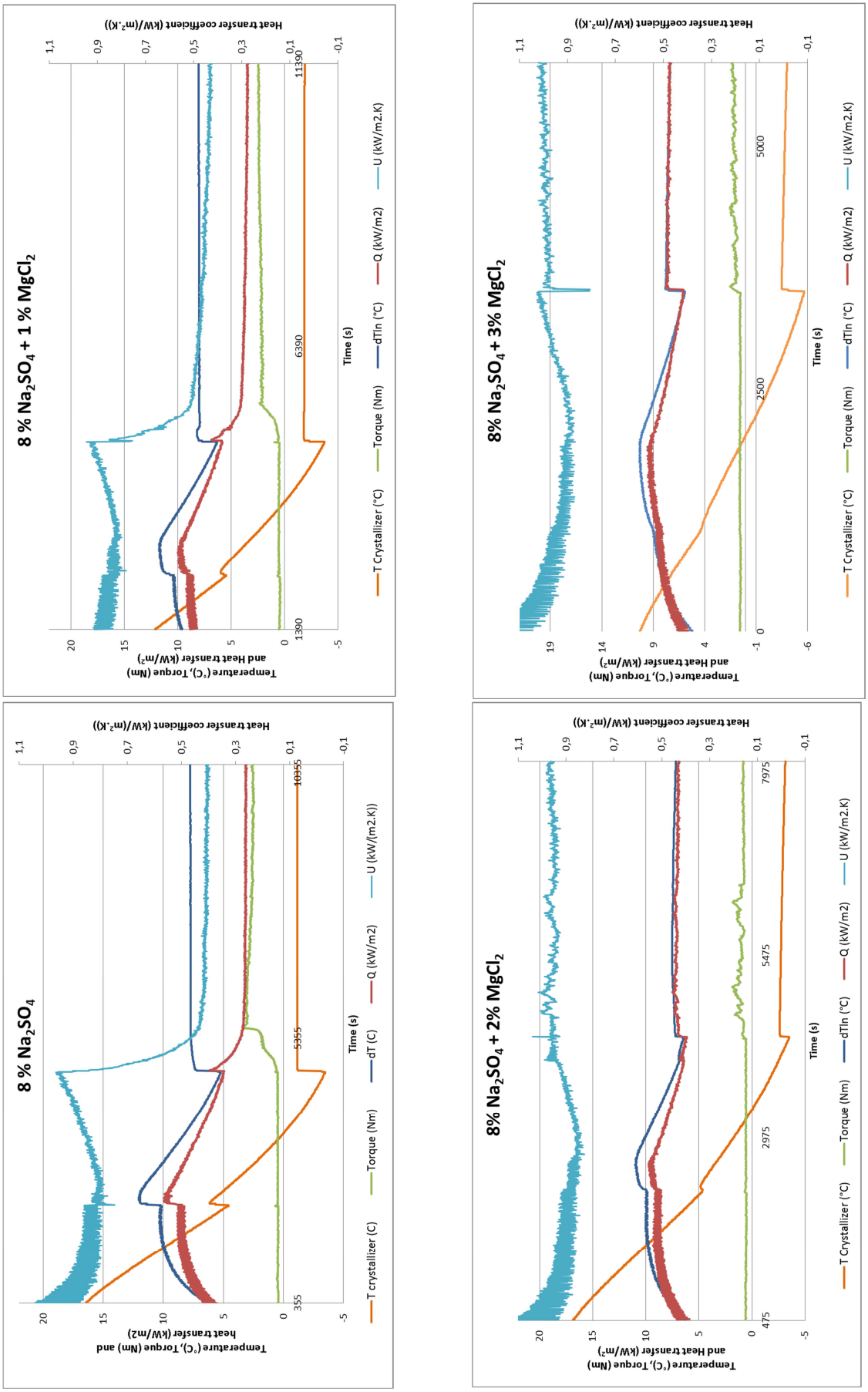

Table 3.13. Graphs showing the effect of different $MgCl_2$ concentrations on Na_2SO_4 eutectic freeze crystallization.

For the cases in which the $MgCl_2$ concentrations increases the decrease of U becomes smaller and already for 2 wt% $MgCl_2$ no decrease in heat transfer coefficient is observed at all.
Another effect that can be seen in the graphs on the previous page is that the line representing the torque becomes more irregular at higher $MgCl_2$ concentrations. In the 2% case the torque shows a very irregular behavior for about 34 minutes after which a stable value of 0.7 Nm is reached. The last experiment (3% $MgCl_2$) was stopped 40 minutes after the eutectic point was reached and over this time the torque showed an irregular behavior.

<u>Na_2SO_4 + NaCl experiments</u>
Similar experiments as described above were done with NaCl as additional component. Again 1, 2 and 3 wt% NaCl were added to a 8 wt% Na_2SO_4 solution. The trends are the same as for the $MgCl_2$ experiments and only the results after adding 1 and 3 wt% NaCl are presented here.
The graph in figure 3.14A shows the results of an experiment in which a solution of 8 wt% Na_2SO_4 + 1 wt% NaCl is crystallized under eutectic conditions and figure 3.14B the result for a comparable experiment with the 3 wt% NaCl solution.
The most remarkable result that can be seen from these graphs is that the heat transfer is increasing instead of decreasing (as is the case for the pure Na_2SO_4-systems) after the eutectic point is reached. Still there is an increase in torque due to some scaling on the heat exchanger, however the value for the torque is only around 1.8 Nm compared to a value of around 2.7 Nm for a pure Na_2SO_4 system (values taken during the first minutes of EFC). In graph B it is also seen that torque is decreasing in time.

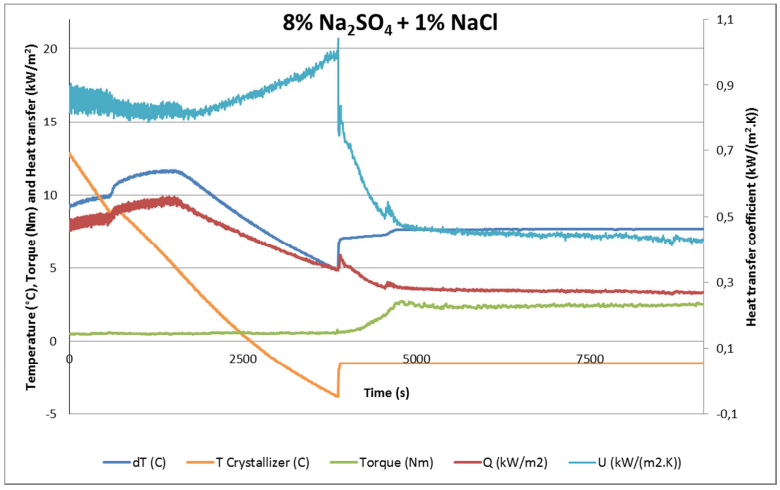

Graph A.

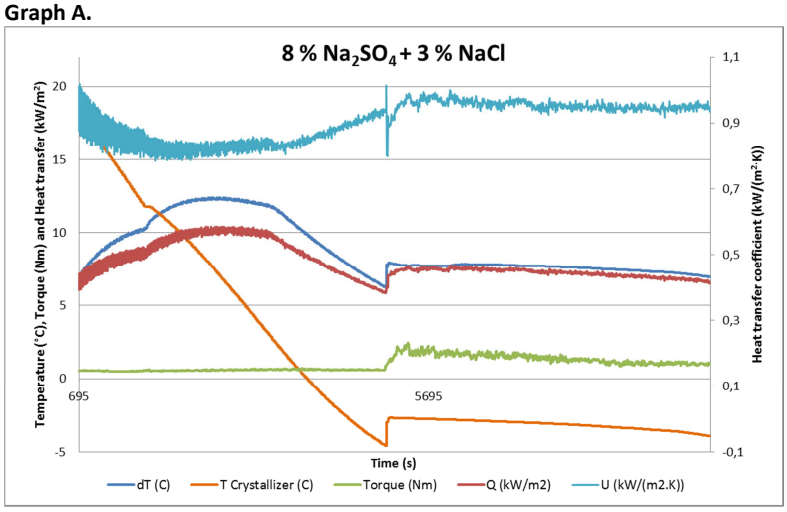

Graph B

Figure 3.14. The results for a 8 wt% Na_2SO_4 + 1 wt% NaCl (Graph A) and for a solution with 3% NaCl added (Graph B).

A comparison between the results of the $MgCl_2$ and NaCl experiments shows that the size of the effects are in the same order of magnitude for the cases of equal weight concentrations of the added salt.

The main difference between $MgCl_2$ and NaCl as additional salts is the number of non-crystallizing species near the cooling surface. In the first case both magnesium and chloride ions accumulate near the heat exchanger and in the latter case only chloride accumulates. Calculation of the molar amount of ions present in the solution (using starting concentrations) shows that in the $MgCl_2$ solutions only about 1.2% more non-crystallizing ions are present compared to a NaCl solution with the same weight concentrations.

Conclusions

From the results described above the following conclusions can be drawn:

- Crystallization of $Na_2SO_4.10H_2O$ alone does not increase scraping torque nor does it decrease the heat transfer to the coolant.
- A scale layer starts to form after ice starts to crystallize at the eutectic point.
- The scraper torque increases and heat transfer decreases after ice crystallization has started and then remain constant over time.
- In a system in which first ice is formed there is no significant effect on the scraping torque and heat transfer when also salt starts to crystallize.
- A solid scale layer is built onto the heat exchanger surface, which breaks up into large fragments after cooling of the surface is stopped.
- After the coolant flow to the heat exchanger is stopped a temporarily increase in torque is observed, this is probably caused by the plowing of the scrapers through the softening ice layer before breaking it into fragments.
- Analysis of the scale layer shows a salt content of 3.4 wt% for a scale formed from a solution with a starting concentration of 8 wt%.
- Addition of a $MgCl_2$ and NaCl leads to a significant decrease in scaling and higher heat transfer coefficients. This is in good agreement with the theory presented by Pronk.
- The magnitudes of the effect of $MgCl_2$ and NaCl on the required scraping torque and heat transfer of are similar size for equal (molar) concentrations of non-crystallizing species.
- Adding 3 wt% NaCl or $MgCl_2$ to a 8 wt% Na_2SO_4 solution roughly doubles the heat transfer coefficient under eutectic conditions.

Chapter 4
Experimental feasibility study on the EFC of an industrial sodium sulfate waste stream

Introduction

The German based chemical company Starck operates an industrial process which produces an aqueous sodium sulfate solution as a by-product. In order to reduce the costs associated with the disposal of this waste stream eutectic freeze crystallization was identified as a potential treatment technology. By treating the stream with the EFC-separation process, clean water and a high purity sodium sulfate product could be obtained.
In this chapter the possibilities to treat the aqueous sodium sulfate waste stream with eutectic freeze crystallization are studied. Therefore the purity of the salt and ice products obtained from impure Na_2SO_4 solutions is determined. Also 200L experiments were performed to study the behavior of this process at a larger scale. More information on the small scale EFC of sodium sulfate solutions is already available from several publications (e.g. Reddy, 2010) and the previous chapter of this thesis.

Experimental procedures

The experiments to investigate the obtainable purity of the sodium sulfate decahydrate and ice crystals were performed in a 1 liter crystallizer. Several solutions were prepared to observe the up-take of impurities into the $Na_2SO_4.10H_2O$ crystals. Also a real waste stream sample (provided by Starck) was treated with EFC and the products were analyzed. The procedure for a 1 liter purity experiment is described below.
Two different solutions are prepared (both 1L): a start solution and a saturated salt solution to wash the salt samples. The wash solution and 1 L of ultra-pure water (to wash the ice samples) are stored in the cold room set at -2 °C. The start solution is put in a beaker which is placed into the crystallization set-up and covered with insulation material (See figure 4.1).

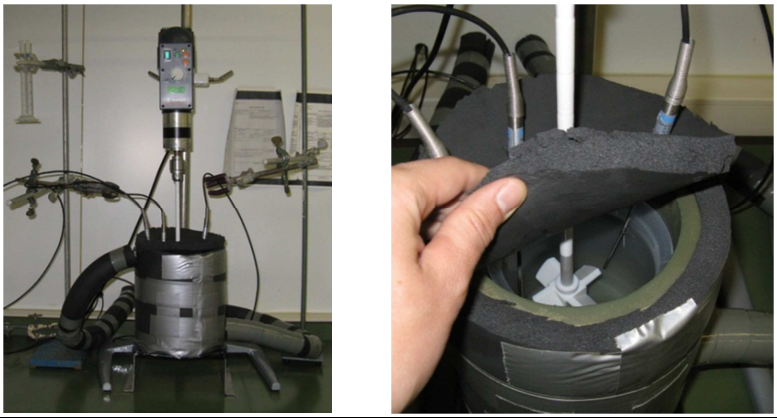

Figure 4.1. The 1 liter set-up. Left an overview and at the right a close-up of the crystallizer beaker with stirrer. This set-up is placed in a cold-room which was set at -2 °C to reduce the loss of ice product during washing and sample taking.

A Teflon coated overhead stirrer is used to stir the solution. A Lauda RK-8 cooling machine is used to cool the solution and Kryo 51 is used as coolant in the cooling jacket. Between the cooling jacket and the plastic beaker Freezium is used to ensure good thermal contact between the two. Calibrated Pt-

100 sensors, connected to a F-250 temperature measurement set-up, are used to measure the temperature. The temperatures are logged with a Labview program. A metal spoon is used to manually remove the scaling of ice from the plastic beaker's wall. When enough ice and salt has been formed the stirrer is removed and the solids are allowed to settle (ice to the top and salt to the bottom). Then the ice is removed from the top of the beaker and placed onto a glassfilter. A vacuum pump is used to remove the liquid from the ice crystals. This liquid is collected in a Buchner flask from which a sample is taken for analysis. A sample from the filtered ice is also saved for analysis. Then cold ultra-pure water is poured over the remaining ice and again the vacuum pump is used to remove the wash water. Again samples are taken. After the desired number of washing steps is reached (generally three or more) the glassfilter is cleaned with water. Now the salt is washed according to the same procedure as the ice (except that saturated Na_2SO_4-solution is used as wash solution).
All samples are analyzed by an Inductively Coupled Plasma analyzer using a spectrophotometer as a detector (ICP-AES).

A 200 liters eutectic freeze crystallization unit is located at the Process & Energy department of the TU Delft. This pilot scale set-up is used to study the behavior of the process at larger scale and (semi)-continuous conditions. A manual to operate this unit was written by the author of this thesis and can be found as Appendix B. Figure 4.2 shows a picture of the 200L pilot plant.
A schematic flow diagram of this set-up is shown in figure 4.3. A larger version of this PFD is available in Appendix A.

Figure 4.2. An overview of the 200 liter pilot plant. The insulated crystallizer is shown at the left. Samples can be drawn from the top middle and bottom section of the crystallizer vessel.

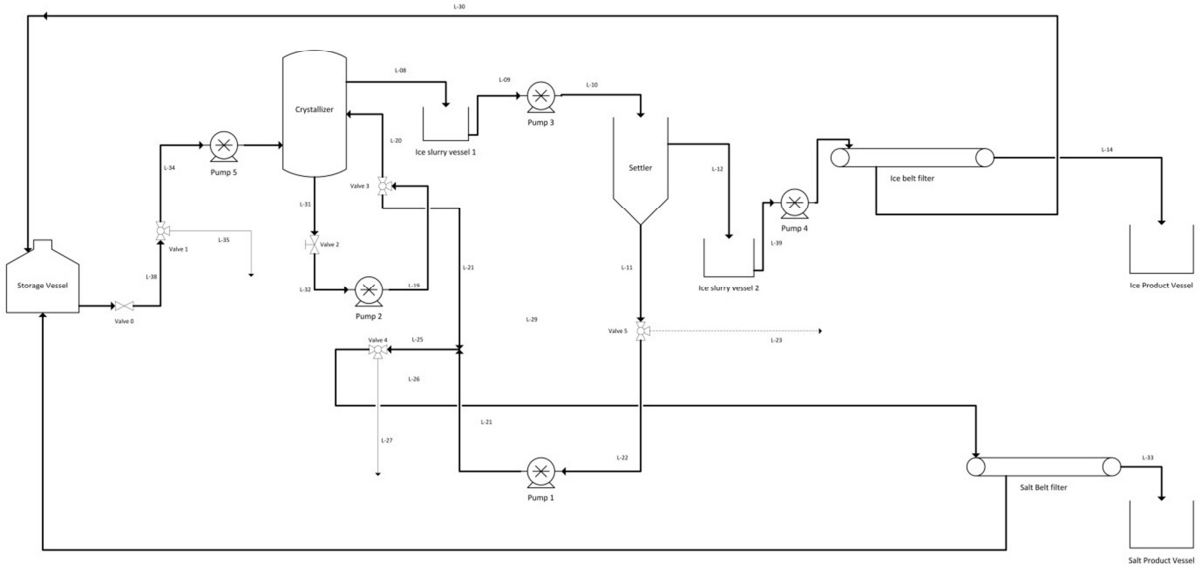

Figure 4.3. A schematic flow diagram of the experimental 200 L EFC set-up. (Appendix A shows a larger version of this scheme)

Results and Discussion

1 liter experiments with pure and impure Na_2SO_4 solutions.

The crystallization of a pure Na_2SO_4 solution provided an accurate value for the eutectic temperature of a Na_2SO_4-solution and pictures of the formed salt crystals. The eutectic temperature is found to be -1.22 °C. This is in agreement with temperatures reported in literature [Ullmann's, 2000]. Photos of the formed salt crystals show two different crystal shapes. The needle like crystals are by far the most abundant. These are verified to be $Na_2SO_4.10H_2O$ crystals. The hexagonal crystals in figure 4.4C and D are of unknown identity. Literature search seems to exclude it to be one of the other known sodium sulfate crystal shapes; $Na_2SO_4.7H_2O$ [Hamilton, 2008] or Na_2SO_4 [Garett, 2001 and *Webmineral*]. No additional experiments were done to study the identity of this hexagonal crystal. Because it occurs only very rarely compared to the decahydrate crystals it is believed that the influence on the eventual products of an industrial EFC process is small, especially when a recrystallization step is to be included in the complete process design.

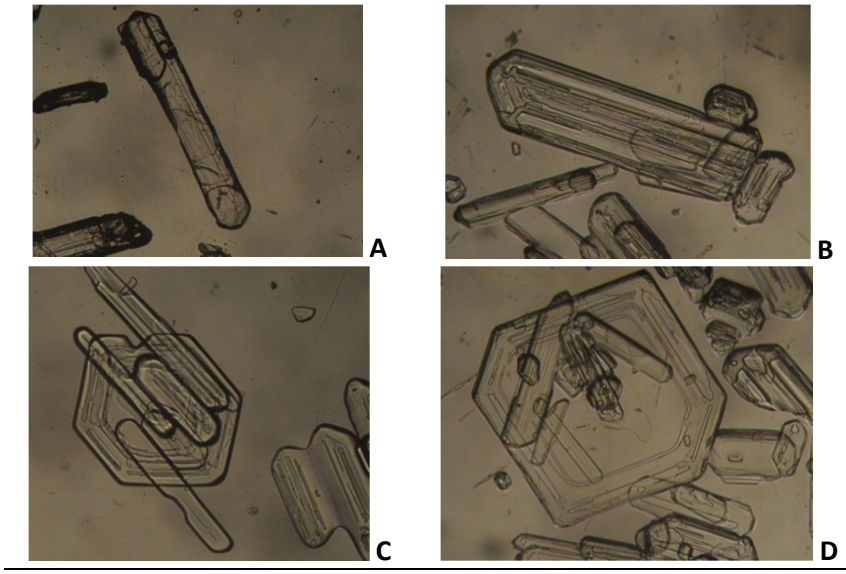

Figure 4.4. Photographs of the salt crystals formed during the 1 liter EFC of a pure Na_2SO_4-solution. The crystals in A and B are $Na_2SO_4.10H_2O$ crystals. The identity of the hexagonal crystals in C and D is not known to the author. (The width of all photos is about 2mm)

The purity of the salt and ice products made from an impure starting solution is presented in figure 4.5. In this experiment impurities were added to a 9 wt% Na_2SO_4 solution.

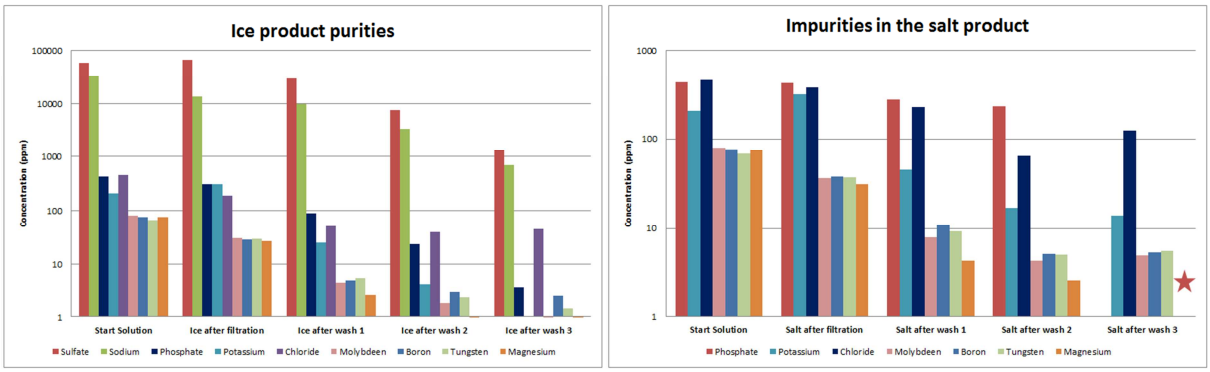

Figure 4.5. Purity of the ice products and the amount of impurities present in the salt product ($Na_2SO_4.10H_2O$). The phosphate concentration in the last salt sample showed an error. The scale is logarithmic.

Borate (B_4O_7) was added because this is also present in the waste stream of Starck, although at a much lower concentration (28 ppm). The other impurities were added arbitrarily. Tungsten was added in the form of WO_4 ions.
Both the ice and salt samples were washed three times with ultra-pure water and saturated sodium sulfate solution, respectively. After three washings the ice contained 0.2 wt% Na_2SO_4, this means a decrease of 97 % compared to the original concentration of the starting solution. In the salt samples mainly phosphate and chloride ions remain in the sodium sulfate product as impurities. The analysis of the salt sample after three washings showed an error in the phosphate figure, therefore its final concentration is not known.

200 liter experimentation with a pure 8wt% Na2SO4-solution.

A couple of 200 L batch experiments were performed to qualitatively study the EFC of a pure 8 wt% Na_2SO_4 solution at a larger scale. As was already found at 10 L scale (see Chapter 3) scraping torque is not influenced by salt crystallization alone. Torque increases only after the onset of ice crystallization. The graph in figure 4.6, shows the typical pattern for the torque increase when the eutectic point is reached during a 200 L batch experiment.

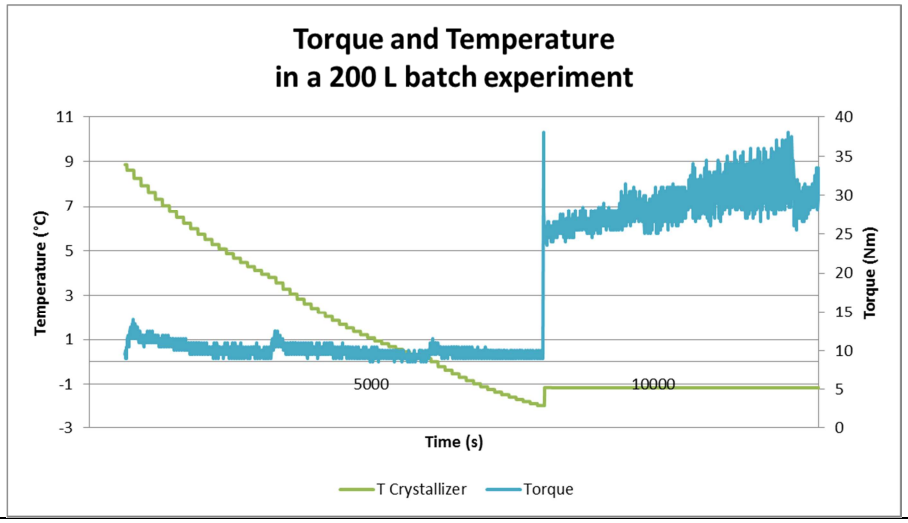

Figure 4.6. Graph showing the temperature and torque during a 200 L batch experiment with a 8 wt% Na_2SO_4 solution. Torque starts to increase fast when the eutectic point is reached. Only the outer heat exchangers were used in this experiment.

During these tests it was found that the simultaneous crystallization of salt and ice has a surprising and negative effect on the scraper construction. The springs which are used to press the plastic scrapers onto the heat exchanger surfaces came loose and eventually were removed from the scraper. When this happened the crystallizer had to be stopped and the scrapers should be repaired to prevent more severe damage to the heat exchangers and the crystallizer wall. The pictures in figure 4.7 show photos of the affected scrapers. On photo A the spring is completely removed from one scraper blade at the outside surface of the outer heat exchanger. The scraper above this one is still intact. Also at the inside surface the scraper blades are affected as can be seen on Photo B in figure 4.7. Here the spring is out of position causing the blade to not touch the heat exchanger surface.
The mechanism that is responsible for causing the scraper damage is not clear. The torque on the scrapers is not excessive and well below the torque that is encountered during tests with other solutions (e.g. NaCl solution). An observation that is related to this phenomenon is a ticking sound that is heard when the coolant flowrate to the heat exchangers is increased or the coolant temperature is decreased. Reducing the flowrate or increasing the coolant temperature causes the ticking to disappear. Both the upper and lower heat exchangers show this behavior. The value for the

flow rate at which the ticking starts and stops is not fixed and seems to be determined by different (still unknown) factors.


A


B

Figure 4.7. Photos of the damaged scrapers. On photo A the spring of one scraper blade at the outer surface is completely removed. Photo B shows a scraper blade at the inner surface of which the spring is out of position so the blade cannot scraping the heat exchanger surface.

Another observation is that the torque on the scrapers is fluctuating very fast, the range of fluctuation is in the order of plus and minus 12% around an average torque. Experiments with another waste stream containing a mixture of salts (see next section and chapter 5), shows much higher values (about five times higher) for the torque but the fluctuation is not large. An example of the torque fluctuation can be seen at the right side of the graph in figure 4.6.

During the experiments with a pure Na_2SO_4 solution it was found that the separation between ice and salt inside the crystallizer is hindered by the heat exchangers. This can be seen clearly in figure 4.8 which shows a picture of the crystallizer after the stirrer was switched off. A large accumulation of salt is found atop and around the upper heat exchanger. The salt that is trapped there is likely to leave with the ice product flow from the top of the crystallizer, instead of being pumped from the bottom section. Most probably it will also influence the heat transfer capabilities of the upper exchangers by increasing the solid fraction of the solution.

Figure 4.8. Salt accumulates atop and around the upper heat exchanger.

Continuous 200 liter experimentation with a 5 wt% Na_2SO_4 + 5 wt% NaCl solution.

In an effort to avoid the above mentioned problems with the scrapers a new solution was prepared. In this solution a non-crystallizing component was added (NaCl), also the amount of Na_2SO_4 was decreased from 8 to 5 wt% to reduce the amount of solids present in the crystallizer.
During this experiment no ticking was heard over the range of coolant flowrates at which in the pure Na_2SO_4 system the scrapers were damaged. It was even possible to continue this experiment towards continuous operation (i.e. both ice and salt were extracted from the crystallizer and isolated on belt filters).
At some point however the amount of ice present in the crystallizer became too large, this had two negative effects on the process. First, large amounts of ice crystals were trapped in the salt product pumped from the bottom section of the crystallizer, this causes blockage of the lines at the entrance

of the peristaltic pumps. Secondly, after some time the amount of ice was so large that whole crystallizer content started to rotate as one solid block. A that point the experiment was stopped. Increasing the feed flowrate was not an option to dilute the solid content in the crystallizer since this resulted in the overflow of ice trough an additional opening at the top of the crystallizer. Apparently the current way of ice extraction by overflowing is not working properly at high ice production rates. Therefore the maximum ice production rate is limited by the ice removal process instead of the heat transfer.

Pumping of the ice product slurry with the peristaltic pumps (mainly pump 3 and 4, see figure 4.3) is found to be difficult because of the blockage of the tubing at the suction side of these pumps. Using high speed stirrers in the ice slurry vessels to minimize the agglomeration of ice crystals was reducing (it takes longer before the blockage occurs) but not preventing this problem.

200 liter experimentation with an industrial sodium sulfate waste stream.

The chemical company Starck provided a 1000 L sample of their industrial sodium sulfate waste stream for experimental purposes. The composition of this stream is shown in figure 4.9. A 200 L batch experiment was done to study the heat transfer properties and the purity of the ice and salt products of the EFC process.

Compound	Concentration (ppm)
Na	21800
SO4	61900
K	380
Mg	150
B	20
Ca	10
pH	2.4

Figure 4.9. Composition of the industrial sodium sulfate waste stream.

Similar to the tests done with a pure 8 wt% sodium sulfate solution the ticking sound was clearly heard after the eutectic point was reached. Decreasing the flowrate and thus the heat transfer to the heat exchangers caused the ticking to stop. To avoid the risk of scraper damage a maximum heat transfer rate of 1.7 kW was achieved without the ticking to be heard. This was achieved with three of the four heat exchangers open, the top outer, the bottom outer and the bottom inner exchangers. The temperature difference was 2.5 °C for the bottom outer heat exchanger and 3.2 °C for both the bottom inner and top outer heat exchanger elements. In figure 4.10 a graph shows the total heat transfer rate and the torque development during the eutectic crystallization phase. When the bottom inner heat exchanger was opened too far the scraping process became noisy (ticking), so during this experiment the total heat transfer was thus limited to 1.7 kW.

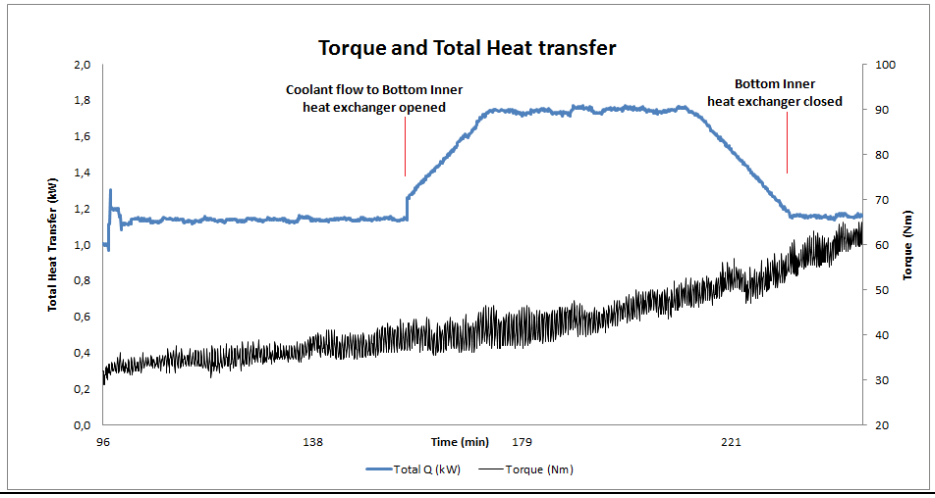

Figure 4.10. Torque and Total heat transfer during the eutectic freeze crystallization phase.

The torque just before ice crystallization started was around 15 Nm and increased fast (within 45 seconds) to a value of 30 Nm. During the eutectic freeze crystallization phase the torque continued

to increase gradually to 60 Nm over a period of 2.5 hour. This increase in torque is most likely caused by the increasing solid content in the crystallizer. Opening the coolant flow to the bottom inner heat exchanger did not have any significant effect on the total torque.

The graph in figure 4.11 shows the relative distribution of heat transfer over the three heat exchangers. It is presented to show that the lower heat exchanger is clearly responsible for the largest part of the total achieved heat transfer even though the coolant flow rate and coolant inlet temperature is equal for both heat exchanger elements. This behavior was previously observed and described for EFC of NaCl solutions [Verbeek, 2011].

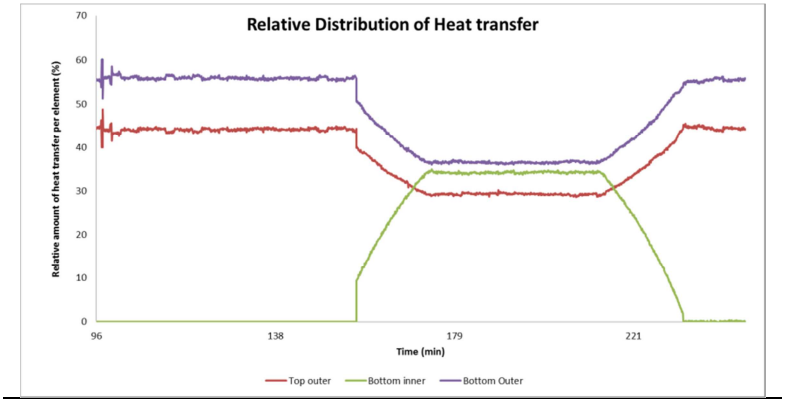

Figure 4.11. Relative distribution of the heat transfer over the separate heat exchangers during the EFC phase.

After the eutectic point was reached (at -1.2 °C) and sufficient ice and salt was present a sample was withdrawn from the crystallizer. The purities of the ice and salt product as a function of experimental washing steps was determined and photos of the crystals were made. The graph in figure 4.12 shows the concentrations in the starting solution, the mother liquor at the eutectic temperature and the ice product after filtration and washings with ultra-pure water. The concentration of Na_2SO_4 in the mother liquor at the eutectic point is 4.0 wt%, this is close to the value found in literature of 3.8 wt% [Pronk, 2006].

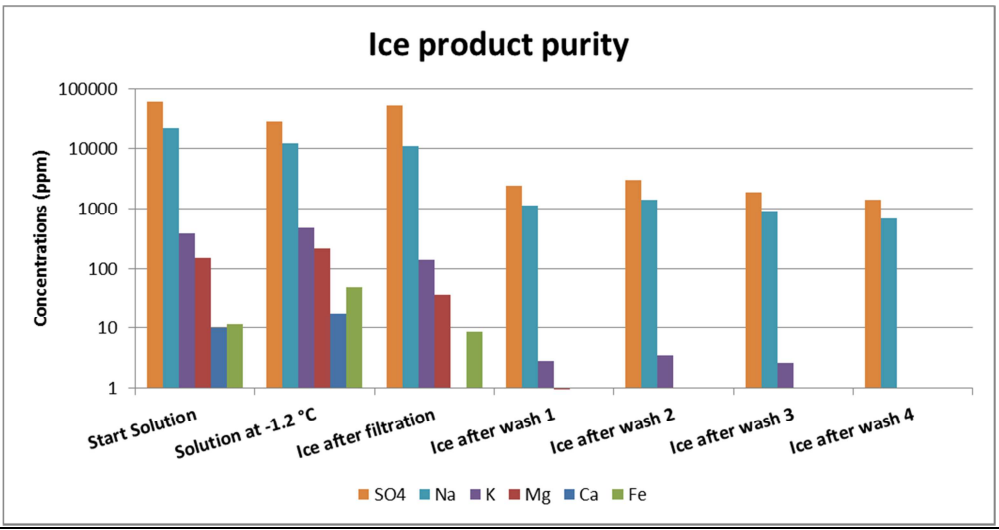

Figure 4.12. Concentrations in the starting solution, the mother liquor at -1.2 °C and in the ice product.

From the results in figure 4.12 it is clear that all ions except Na and SO_4 are removed from the ice after 4 washings. The fact that Na and SO_4 concentrations do not decrease much in the last washing seems to suggest that the ions are not present as dissolved ions in the adhering mother liquor. Rather it is likely that the relative high sodium sulfate concentrations in the final ice product is

caused by solid salt crystals because these particles will only dissolve very slowly in the cold wash water.

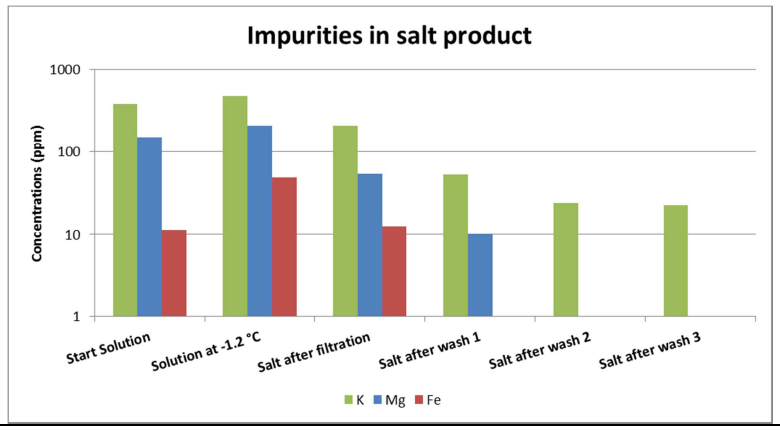

Figure 4.13. Concentrations in the starting solution, the mother liquor at -1.2 °C and in the ice product. Logarithmic scale.

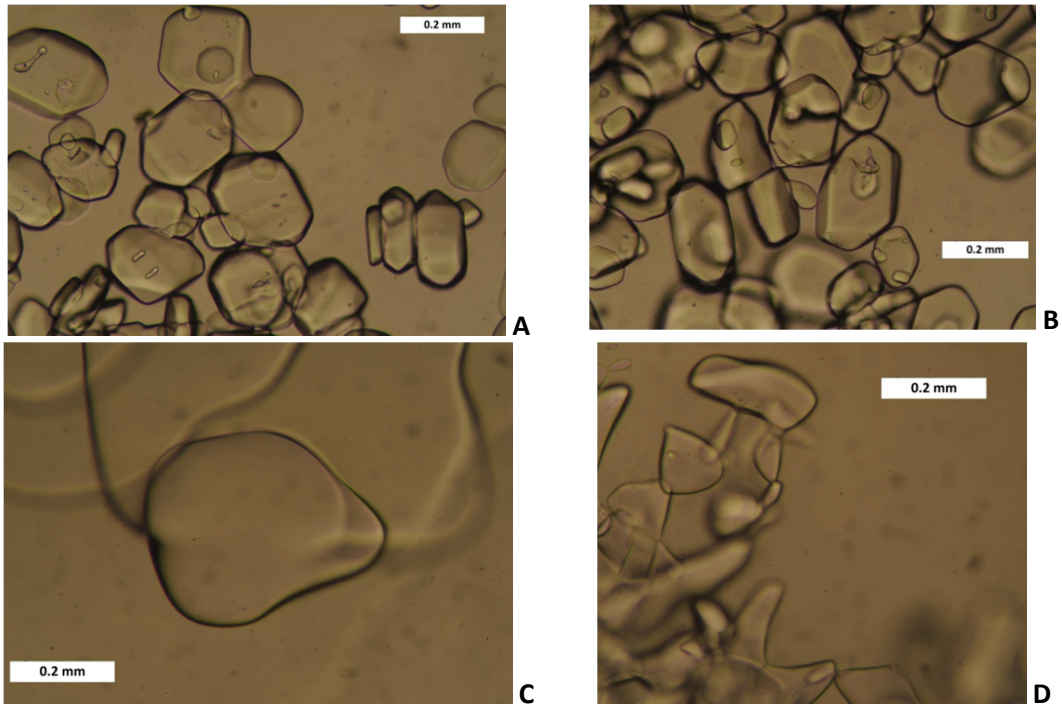

Figure 4.14. Photos of salt crystals (A and B) and ice crystals (C and D). These crystals were produced from the industrial sodium sulfate waste stream.

Figure 4.13 shows the concentrations of the impurities (all ions except Na and SO_4) in the starting solution, the mother liquor at -1.2 °C and the salt samples after washing with a saturated Na_2SO_4-solution. The results in this graph show that only potassium is present in the salt product as an impurity after three washings. Based on the almost constant value for the concentration of K it is concluded that it is present in either the $Na_2SO_4.2H_2O$ crystal lattice, replacing some sodium ions or it is forming co-crystals with the SO_4 ions. The potassium level in the final salt product however is quite low (20 ppm) and recrystallization of the decahydrate crystals into anhydrate salt crystals might be able to completely remove the K from the final anhydrate product. (This recrystallization step is not studied further in this work).

In figure 4.14 photos of the produced salt (A and B) and ice (C and D) crystals are shown. By comparing these crystals with the crystals in figure 4.4, shows that the salt crystals from the 200 L are

much more rounded around the corners and edges. This is probably caused by the high attrition rates around the fast rotating scraper blades in the 200 L crystallizer.

Another surprising observation was the formation of dark colored precipitates which became visible in the samples after a couple of hours of eutectic freeze crystallization. At the same time hydrogen sulfide (H_2S) gas was smelled and measured with a gas detector (up to 20 ppm close to the samples).

Figure 4.15. The color of the industrial Na_2SO4- solution after the crystallization experiment. Black solid particles are suspended in the liquid. H_2S gas is detected near the liquid surface.

The black precipitates were found to be formed on the metal surfaces of various equipment (e.g. spoons left in a beaker glass containing solution). The deposition or degradation on/of the metal parts in the crystallizer is indicated by the particles present in the solution after the experiments were finished (see figure 4.15). During these experiments no blackening of metal surfaces in the crystallizer was observed from the outside. However in a later experiment in which NaCl was added to this solution blackening of the heat exchanger surfaces and the stirrers used to prepare the solution was observed (see next section).
Literature provides information on the reactions occurring at the steel surface in (acidic) sulfate solutions. Smith, et al. [Smith, 2011] describes a series of redox reactions between Fe and SO_4 ions leading to the formation of FeS at metal surfaces. FeS forms a gray/blackish corrosion layer. In the presence of H^+-ions the formed FeS will react to form H_2S and Fe^{2+} ions, [Tewari, 1976]. Because the industrial sodium sulfate solution is quite acidic (pH 2.4), this reaction mechanism seems to be a plausible explanation for both the black corrosion that is observed and the H_2S coming out of the solution.

200 liter experimentation with an industrial sodium sulfate waste stream with added NaCl.

An experiment was done to investigate the previous found positive effect of NaCl, on the heat transfer and torque development during the EFC of a sodium sulfate waste stream, at a larger scale. Also the ice and salt product purities were measured to further study the feasibility of improving the EFC process by adding NaCl without contaminating the ice and salt products.
Eutectic freeze crystallization started at -2.5 °C for this system (2.4 wt% NaCl was added). The concentrations of the major components at this temperature were 1.96, 1.40 and 1.66 wt% for Cl, SO_4 and Na, respectively.
The purities of the ice and salt products are shown in the graphs in figure 4.16. In the ice sample after filtration (before washing) the sodium, sulfate and chlorine measurements were unreliable because the measured concentrations were too high and therefore outside the calibration range of the ICP analysis. In the ice sample after the second wash the same was the case for the sodium and sulfate measurements.
In the ice after five washings only 23 ppm Na and 48 ppm SO_4 is present in the product. This is much lower than in the results for the EFC without NaCl (see figure 4.12), the reason for this however is the washing procedure. The procedure in the NaCl-experiment was as follows; the ice sample is placed in a glassfilter, ultra-pure water is added and then the ice and water are mixed (with a spatula) before the vacuum pump is switched on for the filtration. Mixing of the ice and wash water was not done in the other experiments in described this thesis. It was done here to see whether complete salt removal was possible with this procedure because solid salt particles in the ice product will not dissolve fast enough to be removed by the washing step without stirring. The resulting low values for the Na and SO_4 concentrations in the final ice product clearly shows that this washing procedure is a much better way to investigate the potential uptake of ions in the ice product compared to washing without stirring.

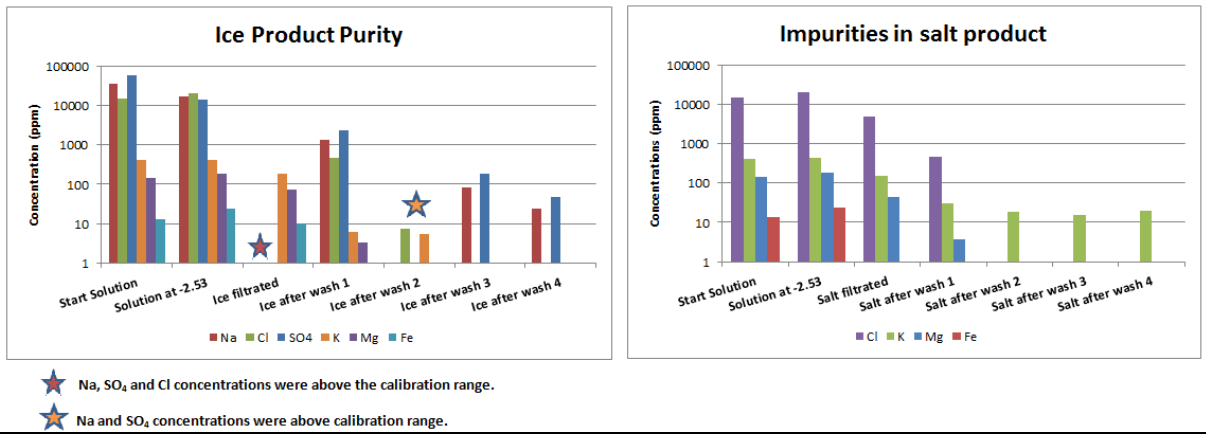

Figure 4.16. Purities of the ice and salt products produced during the EFC of an industrial sodium sulfate waste stream with additional NaCl. The stars indicate that some measured values were outside the calibration range of the ICP analyzer. Scales are logarithmic.

In the salt samples after two washings only K is present as an impurity at a concentration of less than 20 ppm, similar to the experiment without added NaCl.

The torque and the total heat transfer during of the experiments with added NaCl are shown in figure 4.17. The temperature set-point of the coolant was decreased to increase the temperature difference between the coolant and the crystallizer in order to increase the heat transfer. The coolant flow rates were not changed during the experiments. Only the outer heat exchangers were used because in earlier experiments it was established that this gave the lowest risk of scraper damage (see previous sections). The experiments were continued until a too large solid fraction in the crystallizer prevented further effective mixing.

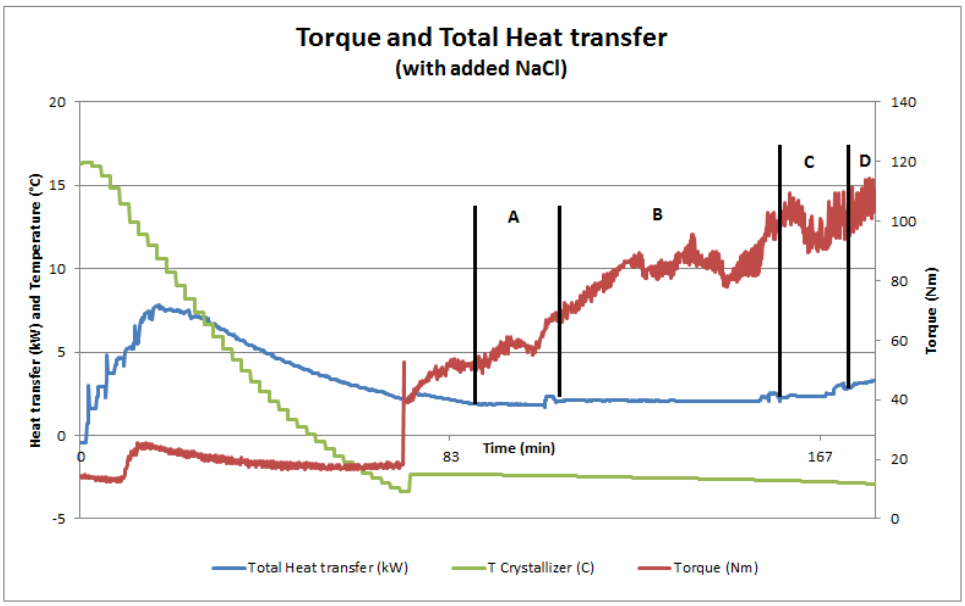

Figure 4.17. The torque and heat transfer during a 200L batch experiment with an industrial sodium sulfate solution with added NaCl (2.4 wt%). The temperature difference between the coolant and crystallizer contents is increased for the different intervals (A to D). The table in figure 4.18 shows the values for the temperature differences and total heat transfer during this experiment.

The temperature differences between the coolant and the crystallizer contents are different for the top and bottom heat exchanger although the entering coolant temperature is equal for both elements (See the table in figure 4.18). The difference between the temperature differences increases over time, this effect is most likely caused by the increasing amount of ice and salt

surrounding the top heat exchanger (see figure 4.8) and thereby decreasing the heat transfer of that element. Also the presence of large amounts of ice floating in the upper section of the crystallizer (not necessarily trapped) are believed to negatively influence the heat transfer performance of the upper heat exchanger. To avoid the heat transfer to decrease due to this latter phenomenon two different strategies can be used. First the heat exchanger should be placed further below the suspension surface (i.e. more space must be available in the section above the heat exchanger for ice to accumulate). A second solution could be to remove the ice product at higher rates by forced extraction (e.g. use an Archimedes' screw principle) to lower the ice content around the heat exchanger elements.

The total heat transfer that is achieved without the ticking sound (assumed to be an early sign of scrapers damage) for the system with NaCl added is significantly higher than for the original sodium sulfate waste stream, i.e. 3.1 versus 1.7 kW. In fact the upper limit for the heat transfer was not reached in this experiment. The test was terminated because of to the large amount of solids present in the crystallizer vessel. Any follow-up experiments at higher heat transfer rates were not done because of the severe corrosion observed on the heat exchanger (see text below).

Interval	A	B	C	D
ΔTln (°C)				
Top Outer Element	4.6	5.0	5.7	6.5
Bottom Outer Element	4.1	4.5	5.0	5.7
Total Heat transfer (kW)	1.9	2.1	2.4	3.1

Figure 4.18. Table showing the temperature differences and the total heat transfer for the intervals A to D in figure 4.17.

The torque on the scrapers is eventually much higher in this system compared to the original solution (see figure 4.10) without any negative effects on the scrapers are observed, this confirms that high torque values are not responsible for the damage as shown in figure 4.7.

During the preparation of the new solution (i.e. dissolving the NaCl) a black layer of iron sulfide was developing on the stirrers. In the crystallizer itself the heat exchanger surface were affected and turned black (see figure 4.19). It is most likely that this iron sulfide layer is developed after the crystallization experiment was stopped because during the crystallization process itself a scale layer is present on the heat exchangers and thereby preventing direct contact between the steel surface and the corrosive solution. The FeS layer on the heat exchanger surface also increases the torque on the scrapers at non-crystallizing conditions significantly. Before the corrosion layer was present the torque required for rotating the scrapers over the surface was in the order of 20 Nm after the black layer was found to be present the torque required was 40 Nm.

Figure 4.19. After the experiment with the industrial sodium sulfate solution to which NaCl was added the heat exchanger surfaces were found to be covered with a black corrosion layer.

In the article of Smith, et al. [Smith, 2011] it is stated that the presence of Cl^- ions in solution increases the sulfide corrosion rates, this explains the more severe FeS and H_2S formation observed for the industrial sodium sulfate waste stream with added NaCl.

Conclusions

Based on the experimental results presented in this chapter the following conclusions can be made.

- During the eutectic freeze crystallization of a pure sodium sulfate solution two different crystal structures are observed under the microscope. The most abundant species (by far) is verified to be $Na_2SO_4.10H_2O$, the other crystal form is not identified.

- The eutectic freeze crystallization process is able to produce a water product with low sodium and sulfate concentrations (maximum <23 ppm and 48 ppm for Na and SO_4, respectively) from an impure acidic sodium sulfate waste stream.
- In the salt product obtained from the industrial sodium sulfate waste stream only potassium is present as an impurity (< 20 ppm).
- During the EFC of a Na_2SO_4 solution with low levels of impurities (< 600 ppm) present the current scrapers construction is not able to sustain total heat transfer rates higher than 1.7 kW.
- Addition of 2.4 wt% NaCl to a Na_2SO_4 solution has a significant and positive effect on the heat transfer rates that could be achieved, >3.1 kW.
- Addition of NaCl does not influence the product purities, it is therefore considered as an attractive measure to increase heat transfer in an industrial EFC process without decreasing the value of the products. *It should be noted however that adding Cl does increase the corrosion tendency of the solution.*
- The observed separation of ice and salt being produced in the crystallizer is not efficient for a Na_2SO_4 solution in the currently used crystallizer design. Large amounts of solids are trapped around the top heat exchanger causing salt contamination of the ice slurry product and a decrease of the heat transfer performance of the upper heat exchanger.
- The method of ice extraction by overflowing is limiting the ice production rate in the crystallizer during continuous operation. Also the performance of the upper heat exchanger is decreased by a large ice solid fraction in the top section of the crystallizer.
- Severe corrosion of metal surfaces (e.g. heat exchanger surface) is observed during the treatment of an acidic sodium sulfate solution. Iron sulfide is being formed at metal parts in the crystallizer and H_2S gas is being produced in significant amounts.

Using the Eutectic Freeze Crystallization Process to treat Shale Gas Water.

This part was originally written as a final report to Shell about the experimental work done by EFC BV and it is presented in this thesis in a slightly modified form. The 1 and 10 L experiments were executed by X. Lu (Jessica), a PhD student working on EFC and Michiel Scheepers, a student from the Hogeschool Rotterdam and doing his internship at the TU Delft. The analysis and discussion of all data in this report (as well as the 200L experiments themselves) were done by the author of this thesis.

Chapter 5
Experimental Feasibility study on the treatment of Shale Gas Water with EFC

Introduction

The production of shale gas gives rise to large amounts of waste water polluted with solids, organics and salts. In finding ways to treat this stream eutectic freeze crystallization (EFC) is considered by Shell as a potential technology.

EFC as a treatment technique for shale gas water

Shale gas water is produced by the hydraulic fracturing process used to fracture the gas containing rock bed allowing the gas to flow into the well. The amount of water used is large (about 5-6 million gallon/well) and the supply of fresh water is often an issue at the locations where shale gas fields are being developed (e.g. the dry areas of Texas, USA). So to minimize the amount of fresh water that is withdrawn from public sources and to prevent the discharge of polluted water after the wells are developed, a suitable technique is required to remove the pollutants from the re-surfacing water.
The block scheme in figure 5.1 shows the shale gas water cycle. In this figure the potential location of an EFC process is indicated by the red box. Eutectic freeze crystallization is not intended to remove entrained solids, organic compounds (e.g. polymer residues and oil), but only treats the aqueous waste stream containing dissolved inorganics after the former mentioned components are removed by other techniques.

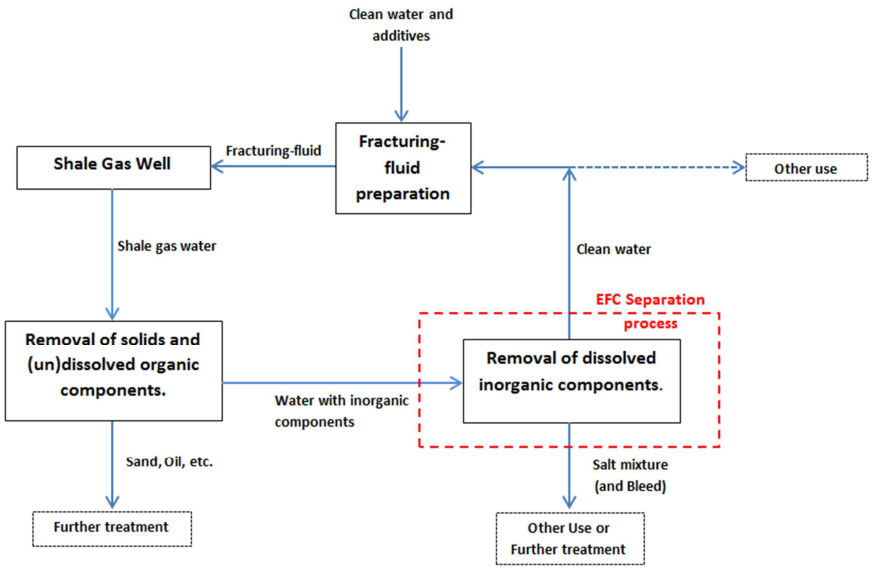

Figure 5.1. Place of the Eutectic freeze crystallization process within the shale gas water cycle. A bleed stream (i.e. a concentrated brine) is not necessarily required but it is a design parameter.

If some solids or organic material is entrained in the effluent of treatment step before the EFC process, these materials will be removed from the EFC crystallizer with the product crystals and/or the bleed stream (if present). Whether a bleed stream (i.e. a concentrated brine) is required and its size is determined by process optimization and choices on the desired product purities.

Aim of the project.

The project executed by EFC separation BV (currently a TU owned company) in collaboration with Delft University of Technology is aimed at determining the feasibility of treating the shale gas water with an eutectic freeze crystallization separation process. More specific this project is an experimental study into the crystallization behavior of shale gas water upon cooling. In addition a 200 L batch experiment is performed in the EFC pilot plant located in Delft to get a first idea of issues related to the practical application (e.g. scaling on the heat exchangers and the heat transfer rate).
Because a real shale gas water sample was not available for the experiments a synthetic composition was proposed and agreed upon with Shell. The composition used in the experiments is given in table 5.1 (1 ppm equals 1 mg/kg).

During the progress meeting (21/10/2011) it was mentioned that the iron, that was measured in the samples collected at the site, was most probably originating from corrosion of the equipment. It was therefore decided to leave out this element in further experiments because it was causing undesired precipitates in the starting solutions. These iron precipitates will end up in the salt product although they were not formed during the EFC process but in making the solution. In a real process the iron is not expected to cause any problems and will leave with the salt product. If this is undesired (e.g. because of the wish to produce iron-free salts) the iron might be removed before the EFC process.

Table 5.1. Composition of Synthetic Shale Gas Water.

Compound	Concentration (ppm)
Calcium	23000
Magnesium	1800
Manganese	10
Potassium	300
Strontium	7000
Barium	15000
Sodium	50000
All salts are added as chloride salts	

The experiments were performed at 1, 10 and 200 liter scale, each aimed at the collection of information on different parts of the EFC process. The experiments and their aims are listed in table 5.2.

Table 5.2. Overview of set-ups and experimental aims.

Set-Up	Aims
1 Liter	- Identify the eutectic point of the system. - Determine ice and salt product purities after washing. - Take photos of the produced crystals.
10 Liter (ECN)	- Determine the crystallization sequence of the different components. - Take photos of the produced crystals.
200 Liter	- Investigate the scaling behavior. - Determine the heat transfer between the cooling elements and the solution. - Look for unexpected phenomena at large scale.

Experimental procedures

The experiments were performed at 1, 10 and 200L scale the procedures for these experiments and photos of the different set-ups are presented in this section.

1 and 10 liter set-ups and experimental procedure.

Photos of the 1 and 10 liter set-ups are shown in figure 5.2 and 5.3, respectively.

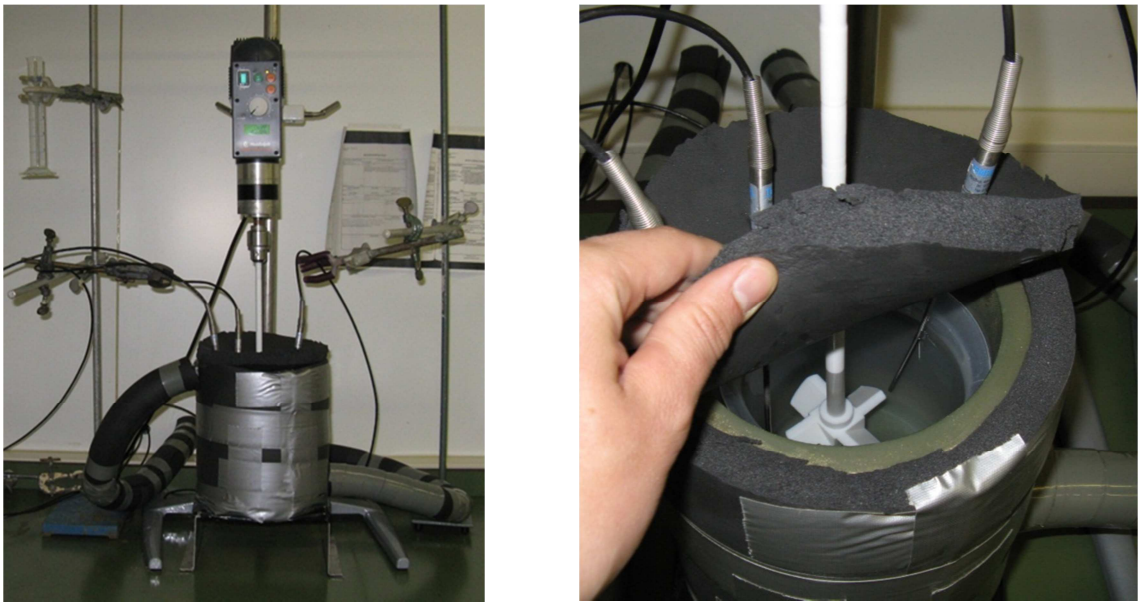

Figure 5.2. The 1 liter set-up. Left an overview and at the right a close-up of the crystallizer beaker with stirrer. This set-up is placed in a cold-room which was set at -5 °C to reduce the loss of ice product during washing and sample taking.

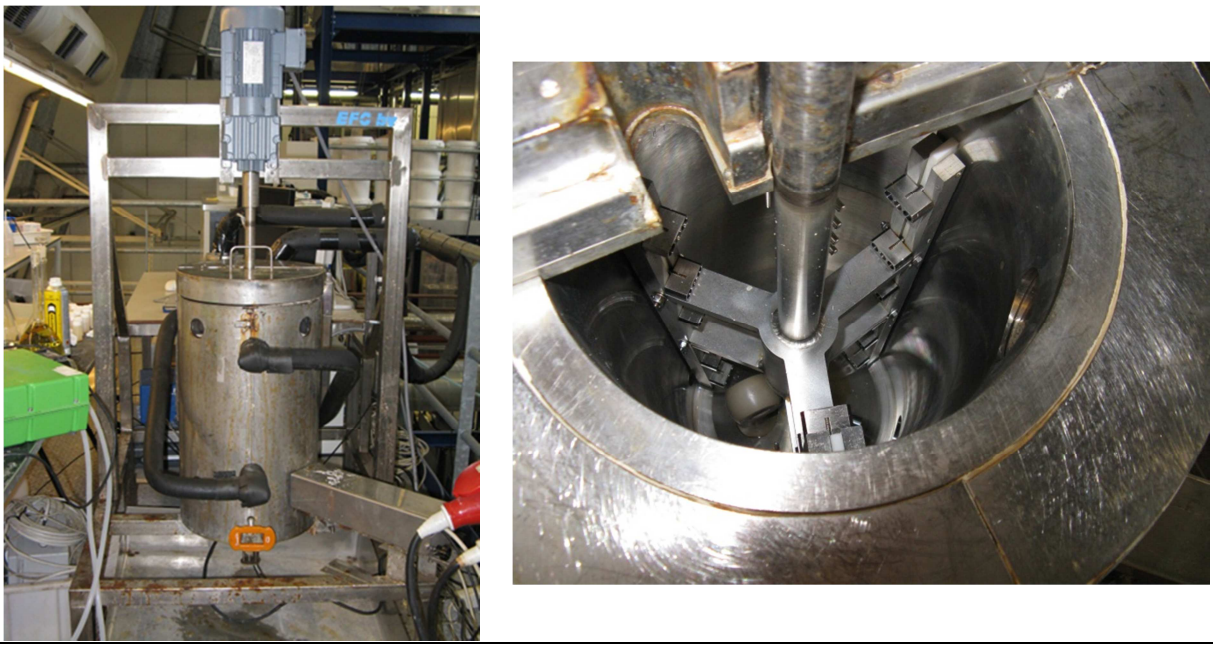

Figure 5.3. The 10 liter set-up. At the left an overview, salt slurry samples can be extracted from the bottom of the crystallizer, ice is taken from the top and solution samples are withdrawn using a tube connected to a pump. At the right a picture of the internals. The walls of the crystallizer are scraped to prevent scaling.

The experimental procedures for the 1 liter and the 10 liter set-up are similar so first a general description of a 1L experiment is given below.

- Prepare synthetic shale gas water (SSGW)
- Prepare saturated wash-solution (This was a NaCl solution in the first experiments, later there were also washings with saturated BaCl solution.)
- Fill an Erlenmeyer with ultra-pure water and leave this in an ice-bath to cool.
- Fill a 1 L plastic beaker (the crystallizer) with +/- 900 mL SSGW and place the stirrer.
- Cover the top-side with insulation material.
- Put the Pt-100 temperature sensors in place
- Switch on the stirrer and the start the temperature measurement via the computer
- Switch on the cooling machine and start cooling until eutectic temperature is reached.
- Wait until the eutectic point is reached and reset the temperature setting at the cooling machine close to the eutectic temperature to prevent excessive ice-growth at the walls. Regularly scrape the walls of the beaker with a spatula to remove the ice layer.
- When sufficient ice and salt have formed remove the stirrer and Pt-100 sensors to enable the suspension to separate by gravity.
- Remove the ice from the top layer and collect this in a glassbeaker placed in a basket with ice.
- Use the vacuum filtration set-up to remove the liquid, take samples of the remaining ice and the filtrate.
- Now pour ice water onto the ice and filtrate again. Take samples of the ice and the filtrate. *(This is the first washing).*
- Repeat the above step till desired amount of wash steps is reached.
- Now collect part of the salt slurry from the bottom of the crystallization beaker.
- Use the vacuum set-up to remove the liquid, take samples of the remaining salt crystals and the filtrate.
- Now pour saturated NaCl-solution onto the salt and filtrate again. Take samples of the salt and the filtrate. *(This is the first salt-washing).*
- Repeat the above step till desired amount of wash steps is reached.
- Take small amount of salt slurry to make photographs using the microscope-photography set-up.
- Analyze the collected samples with ICP.

The procedure that was followed in the 10L set-up differs mainly in the way samples were drawn from the crystallizer. Also additional in-line samples were extracted during crystallization by pumping solution through a glassfilter into a sample flask, these were also analyzed by ICP.

The 200 liter set-up and experimental procedure.

Figure 5.4 shows the 200L pilot-plant that was used for this project. This set-up is designed for both batch and continuous tests, however only a batch test was in the scope of this project. A process flow diagram and a manual for the 200L pilot plant is attached to this report in Appendix A and B.
For the batch tests 220 kg of solution was prepared. The composition of the starting solution is determined by ICP analysis and is given in table 5.3. This composition differs unintended from the composition shown in table 1, because of some errors (e.g. weighing errors) made during the solution preparations.

Table 5.3. Composition of the solution used for the 200 L batch tests.

Compound	Concentration (ppm)
Calcium	24000
Magnesium	1900
Potassium	2300
Strontium	6800
Barium	15000
Sodium	38000
All salts are added as chloride salts	

Figure 5.4. An overview of the 200 liter pilot plant. The insulated crystallizer is shown at the left.

Results and Discussion

The cooling behavior.

A temperature profile is obtained by cooling the solution down to the eutectic temperature. From this test the pseudo-eutectic temperature is obtained. The graph in figure 5.5 shows the temperature profile, after the pseudo-eutectic point is reached the temperature of the solution remains almost constant at -23.4°C. The temperature is decreasing only slowly after this point due to the large amount of crystallization heat that is released by the ice and, to a lesser extent, salt formation. Because of the low levels of undercooling attained in this system before crystallization started the temperature jumps (as described in figure 3) are not clearly visible in this graph.

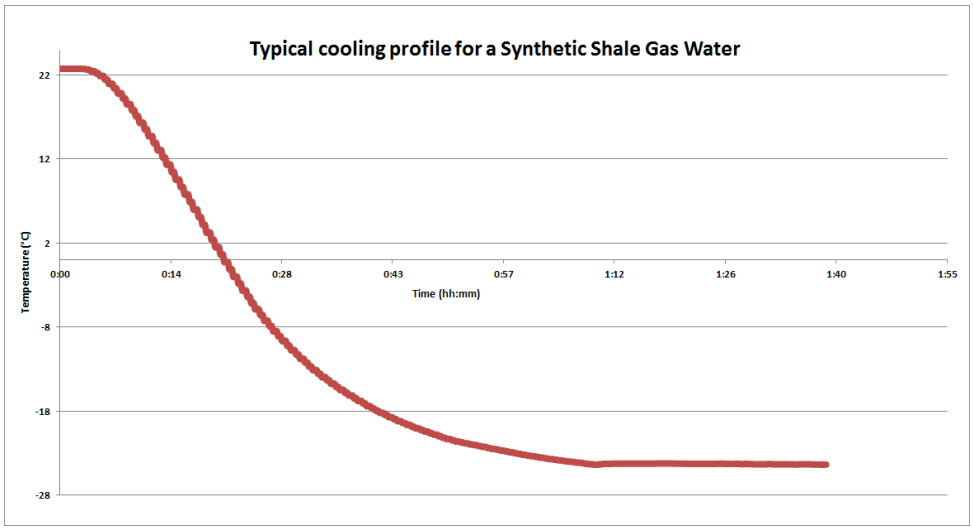

Figure 5.5. Graph showing a typical temperature profile for the cooling of a synthetic shale gas water solution. (Results obtained in the 10L crystallizer, set at -28 °C)

Salt and Ice product purities

To study the purity of the ice and salt products that are formed during the EFC process several experiments were performed in which salt and ice samples were extracted at a temperature of -23.4 °C. These samples were washed and analyzed by ICP-AES analysis. Figure 5.6 shows the results for an experiment in which the ice product was washed five times with ultra-pure water. In figure 5.7 the total amount of ions is shown as a function of washing steps. From this graph it becomes very clear that a high degree of purification(>0.99) is reached after five times washing. The degree of purification is defined as $1\text{-}C_{total,Ice}/C_{total,feed}$ and varies between 0 and 1 for complete removal of all contaminants.
In this experiment also additional elements were added in the form of trace elements (between 10 and 20 ppm). These trace elements were also successfully removed from the ice sample by the washing steps (see table 5.4). From these results it can be concluded that no significant impurity incorporation is taking place during ice formation. So the water product quality is determined by the efficiency of the ice washing operation only. The experimentally obtained degrees of purification as a function of wash steps for each ion is provided in Appendix C1.

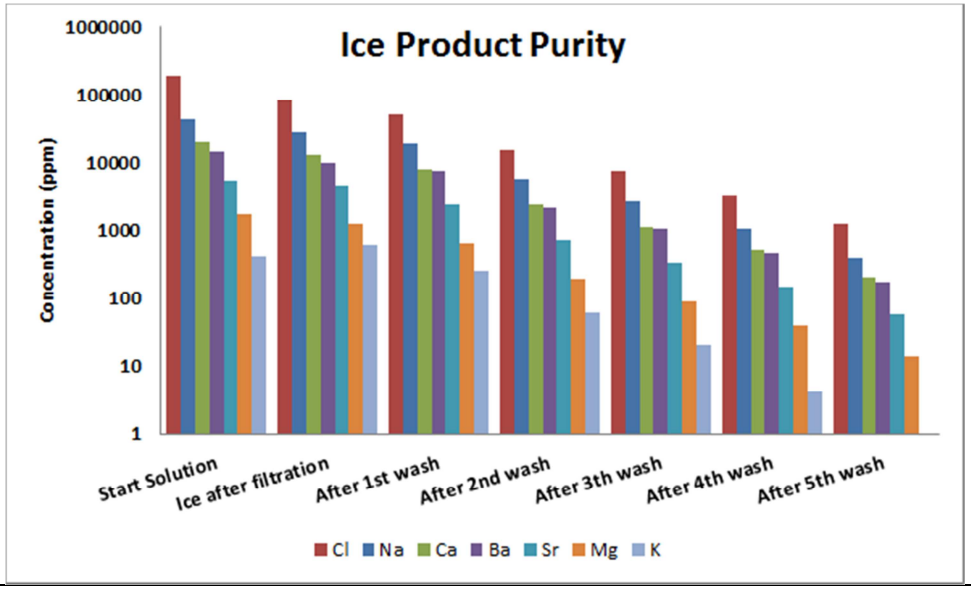

Figure 5.6. Ion concentrations in the ice product samples obtained at -23.4 °C. All concentrations in ppm (by mass). Scale is logarithmic.

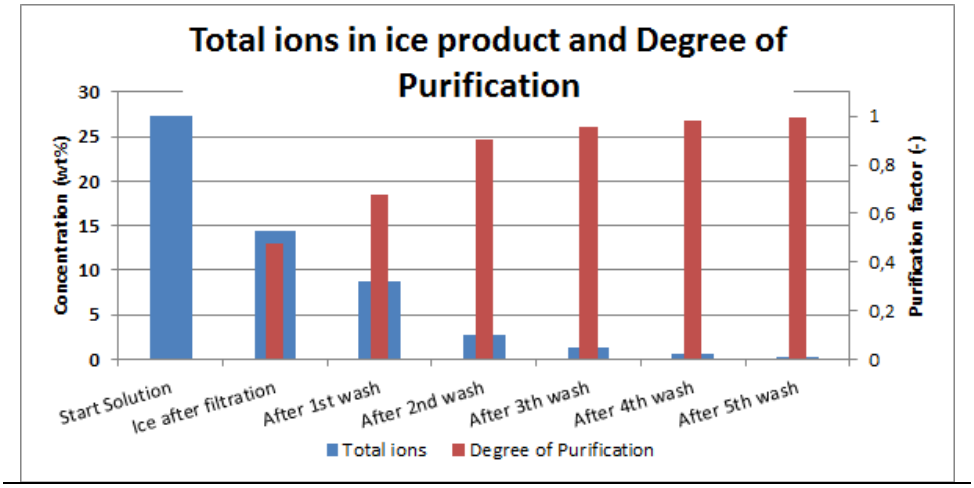

Figure 5.7. Total ion concentrations and the degree of purification as a function of the number of washings.

Table 5.4. Concentrations of trace impurities in the ice samples at -23.4 °C.

	Concentrations in ppm																
Sample	Ag	Al	B	Bi	Cd	Co	Cr	Cu	Fe	Ga	In	Li	Mn	Ni	Pb	Tl	Zn
Start solution	7,8	16,7	16,1	14,5	13,7	14,5	13,8	14,4	13,9	14,2	18,1	13,0	23,3	13,2	15,8	14,8	15,1
Ice after filtration	9,1	10,4	10,8	10,2	8,6	8,8	8,6	9,7	8,4	8,9	13,3	9,1	14,6	7,9	9,0	10,3	8,4
After 1st wash	3,5	6,1	6,0	5,3	5,0	5,3	4,9	5,2	5,0	5,0	6,8	4,8	8,3	4,7	8,0	5,6	5,2
After 2nd wash	0,8	2,4	2,0	0,4	1,7	1,8	1,7	1,6	1,8	1,6	2,0	1,5	2,8	4,3	2,3	1,6	2,4
After 3th wash	0,5	1,5	1,0	0,0	0,8	0,8	0,8	0,8	0,9	0,8	0,9	0,7	1,3	0,8	1,1	0,7	1,4
After 4th wash	0,2	1,0	0,5	0,0	0,4	0,4	0,4	0,3	0,4	0,4	0,4	0,3	0,6	0,4	0,5	0,3	0,9
After 5th wash	0,1	0,8	0,3	0,0	0,1	0,2	0,1	0,1	0,1	0,1	0,2	0,1	0,2	0,1	0,1	0,1	0,8

It must be noted that the washing steps as they are performed experimentally are not related in any way to potential industrial unit operations for ice washing (e.g. wash column).

In a separate experiment salt samples are taken at -23.4 °C. The produced salt product is a mixture of salts consisting mainly of barium and sodium chloride. Extraction of the salt and washing these samples with a saturated NaCl solution gives the results presented in figure 5.8. In this graph only the concentrations of impurities in the salt samples are given, the rest of the salt product consists of Ba, Na, Cl and crystal water. The presence of the impurities can be caused either by impurities inclusions into the $BaCl_2$ and NaCl crystals or by adhering mother liquor. Washing the salt product with a saturated salt solution will remove the adhering mother liquor and thus decrease the amount of impurities. If impurities are included into the crystals itself (either in the form of mother liquor inclusions or within the crystal lattice) they will not be removed in the washing process. Recrystallization of the hydrated crystals into anhydrate crystals can be a way to remove these impurities.

The temperature at which the salt samples are extracted influences the salt product purity in two ways. First, more sodium and barium chloride will crystalize at lower temperatures, thereby diluting the impurities in the final salt mixture. Secondly, other ions will start to crystallize at lower temperatures and thus add to the salt product. More data on the temperature effect on the salt production is given in the next section.

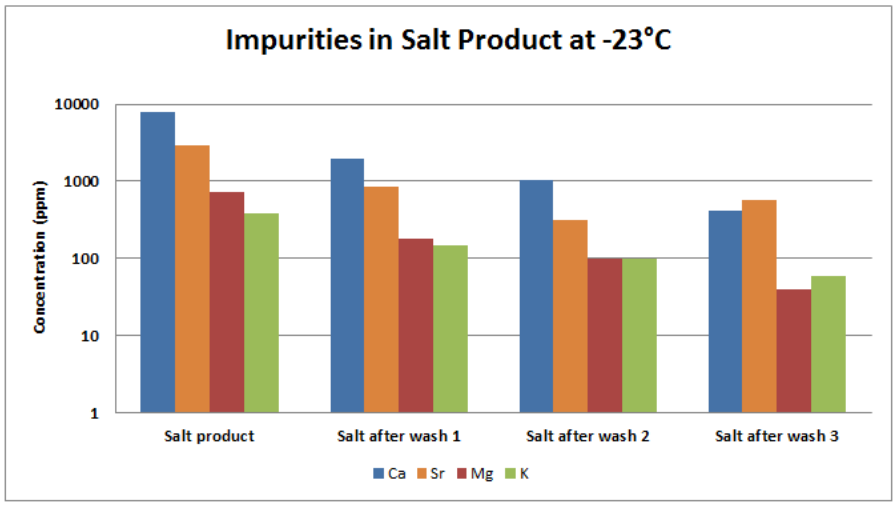

Figure 5.8. Concentrations of impurities in the salt product at -23.4 °C. Main constituents of the salt product are Ba, Na and Cl.

Crystallization behaviour

Currently information on the solubility and crystal forms can only be obtained by experimental work, since all thermodynamic models (e.g. the Pitzer model) need parameters to predict crystallization. These parameters are however very scarce for systems at low temperatures and high ion concentrations

The crystallization behavior (i.e. salt and ice formation as a function of the temperature) was studied in the 10 L crystallizer set-up. Due to the large amount of ice formation it was not possible to continue the experiment below -25.9 °C. In at least one experiment a new starting solution was prepared with concentrations equal to the concentrations measured at -25 °C. However, also this solution showed extensive ice formation preventing the temperature to drop below -30 °C. The results of this last experiment are incorporated in the table 5.6 and figure 5.9 only. All results presented in this section are based on measurements of the concentrations in the mother liquor which are provided in Appendix C3.
From the measured concentrations it is possible to calculate the ice production when a non-crystallizing compound is identified. In this experiment calcium and magnesium show an equal and large increase in concentration due to the removal of water from the solution by ice formation (both 64%). Also, from literature it is known that both $CaCl_2$ and $MgCl_2$ crystallizes at much lower temperatures and higher concentrations than encountered in this experiment [Pronk, 2006 and Ham, 1999]. Although this latter argument alone does not necessary means that no crystallization takes place, because in general solubility is influenced by additional components, e.g. the common ion effect probably decreases the solubility of all salts present in this solution due to the high chloride concentration. However, by combining both arguments it is very likely that both calcium and magnesium values are a correct measure from which to calculate the amount of solution left (and from this also the production and recovery of water and ions). Appendix C4 shows the relative increases in concentration for each ion between feed and brine.
The following three relations are used to obtain the results presented in table 5.5 and 5.6 and figure 5.9.

$$M(T) = \frac{C(0)}{C(T)} \cdot M(0)$$

$$P(X,T) = C(X,0) \cdot M(0) - C(X,T) \cdot M(T)$$

$$R(X,T) = \frac{P(X,T)}{C(X,0) \cdot M(0)} \cdot 100$$

Where;

	M(T)	is the mass of solution left at temperature T. [kg]
	C(0)	is concentration of non-crystallizing ion in start solution. [ppm]
	C(T)	is concentration of non-crystallizing ion at temperature T. [ppm]
	M(0)	is the mass of the starting solution.[kg]
	P(X,T)	is the amount of X formed between start and T. [kg]
	C(X,0)	is the concentration of X in start solution. [kg/kg(sol)]
	C(X,T)	is the concentration of X in solution at T. [kg/kg(sol)]
	R(X,T)	is the percentage of X recovered as a solid at T. [%]

Because these calculations do not account for the water molecules that are incorporated in hydrated salt crystals as crystal water the calculated ice production rates and water recovery are higher than in reality. On the contrary the calculated salt production rates are lower than in reality. The calculation of the total salt and ion recoveries is not influenced by this effect.

Table 5.5. Production and recovery of ice and salt at different operating temperatures.

Temperature	Salt production	Ice production	Salt recovery	Water recovery	Amount of liquid
[°C]	[kg(salt)/kg(start solution)]	[kg(ice)/kg(start solution)]	[% salt recovered from the start solution]	[% pure water recovered from the start solution]	[kg(solution)/kg(start solution)]
Start	0	0	0	0	1
-9,9	-	0,01	-	0,7	1,00
-14,5	0,00	0,02	1,8	2,4	0,98
-22,4	-	0,06	-	7,9	0,94
-24,4	0,01	0,12	5,2	15,7	0,87
-24,5	0,03	0,17	14,2	21,9	0,80
-24,9	0,05	0,23	19,9	30,0	0,72
-25,4	0,07	0,30	28,6	39,0	0,63
-25,6	0,07	0,26	28,8	34,0	0,67
-25,9	0,08	0,31	32,1	41,3	0,61

Due to an error in the analysis two values for salt production are unknown and are represented in this table by a - sign.

It is possible to account for the water leaving as crystal water in the salt product when the exact salt crystal species are known. However, this effect is expected to be small since much more water is crystallizing as ice than as crystal water during this experiment.

As can be seen from table 5.5 ice is starting to crystallize around –9.9 °C. Salt formation starts between -14.5 and -24.4 °C. It is shown by the calculated values for the water recovery that for an operating temperature of -25.9 °C about 41% of the water present in the starting solution is recovered as clean water and 32% of the dissolved components is obtained as solid salt product. The amount of concentrated brine left at this temperature is 61 wt% of the mass of incoming solution.
In table 6 the recoveries of the major crystallizing ions are given. As already described above, calcium and magnesium recoveries are 0 at all temperatures achieved during the experiments. At -25.9 °C 81% of the Ba and 47% of the Na present in the starting solution are removed from the solution and obtained in the solid salt product.

Table 5.6. Recovery of ions from the start solution as a function of temperature.

	Ion recovery (%)			
Temperature	Ba	Cl	Na	K
Start	0	0	0	0
-9,9	0	0	0	0
-14,5	1	2	1	3
-22,4	5	-	1	4
-24,4	51	2	4	5
-24,5	63	13	14	6
-24,9	70	17	27	10
-25,4	77	28	37	11
-25,6	79	26	41	12
-25,9	81	30	47	14
-28,3	89		65	
-29,3	92		69	
-30,1	94		73	

These values were obtained during a follow-up experiment. Unfortunetly only Na and Ba were measured.

Only the crystallizing ions are shown in this table.

The graph in figure 5.9 graphically summarizes the data presented in table 5.5 and 5.6.

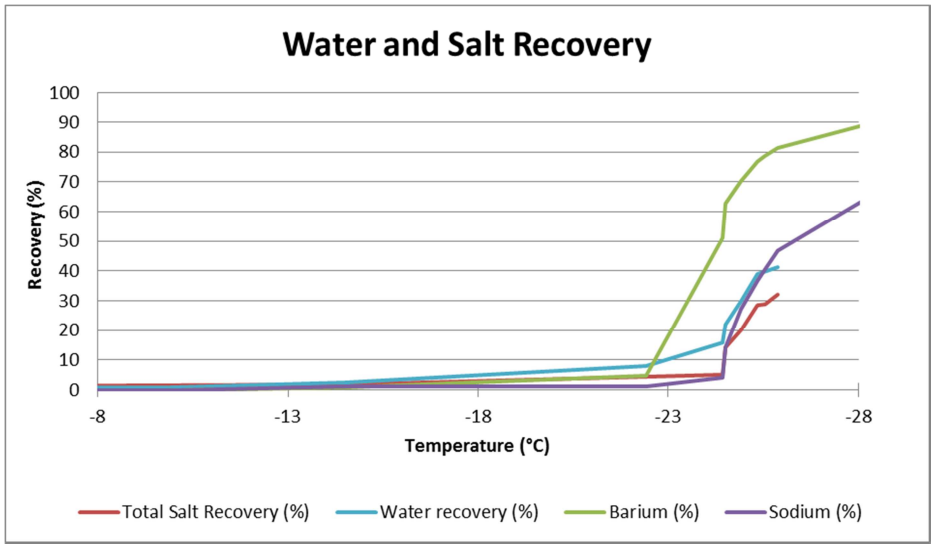

Figure 5.9. Graph showing the percentage recoveries as a function of temperature.

In figure 5.10 the concentrations of salts in the liquid streams entering and leaving this process are shown. The concentrations in the concentrated brine stream are determined by the operational temperature. The values in figure 5.10 are valid for an operational temperature of -25 °C. At this temperature 61 wt% of the feed is leaving as a concentrated brine, this amount can be decreased (to zero) when lower operating temperatures are chosen.

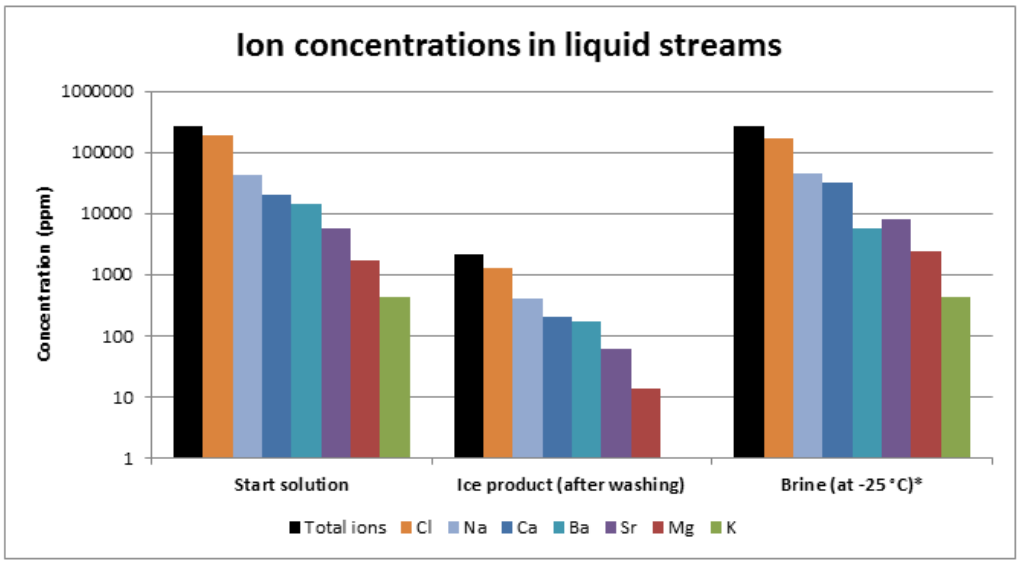

* The concentrations in the ice and brine are obtained in separate experiments with slightly different starting concentrations.

Figure 5.10. Salt concentrations in the liquid streams for a process operated at -25 °C.

Pilot scale batch experiments

To investigate the different aspects of the EFC process at larger scale a 200 liter batch test was done. The main aim of this experiment was to find out whether there are any scaling issues encountered and to obtain a preliminary value for heat transfer in an industrial crystallizer. During the 200 L batch test ice and salt were produced successfully. There was no excessive scaling of the heat exchangers. A photo of the produced salt crystals is shown in figure 5.11. Clearly, various different crystal structures can be seen in this photo. No further work was done to identify the different crystal forms.

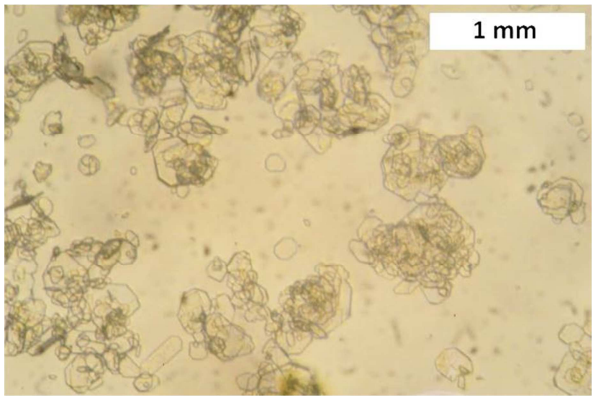

Figure 5.11. Photo of salt crystals produced in the 200 L set-up.

In figure 5.12 the temperature for the batch experiment is shown. Indicated in this graph are also the points at which ice and salt crystals were observed by visual inspection of samples drawn from the crystallizer.

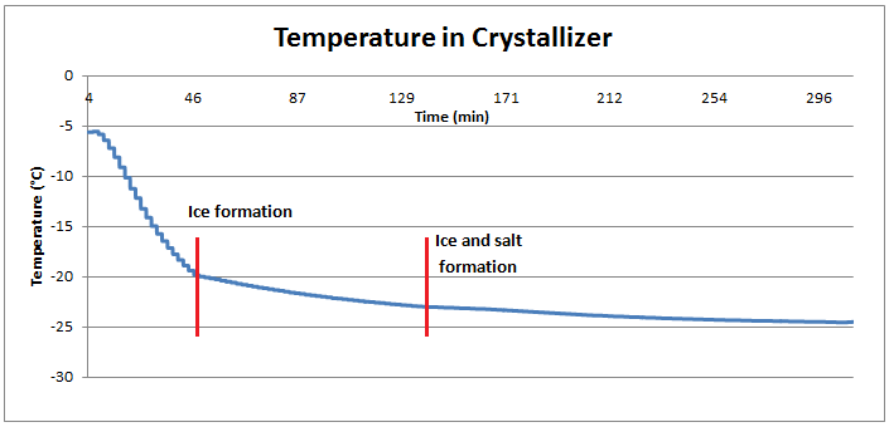

Figure 5.12. Temperature profile for the 200L batch experiment. (Cooling machine setpoint -31 °C).

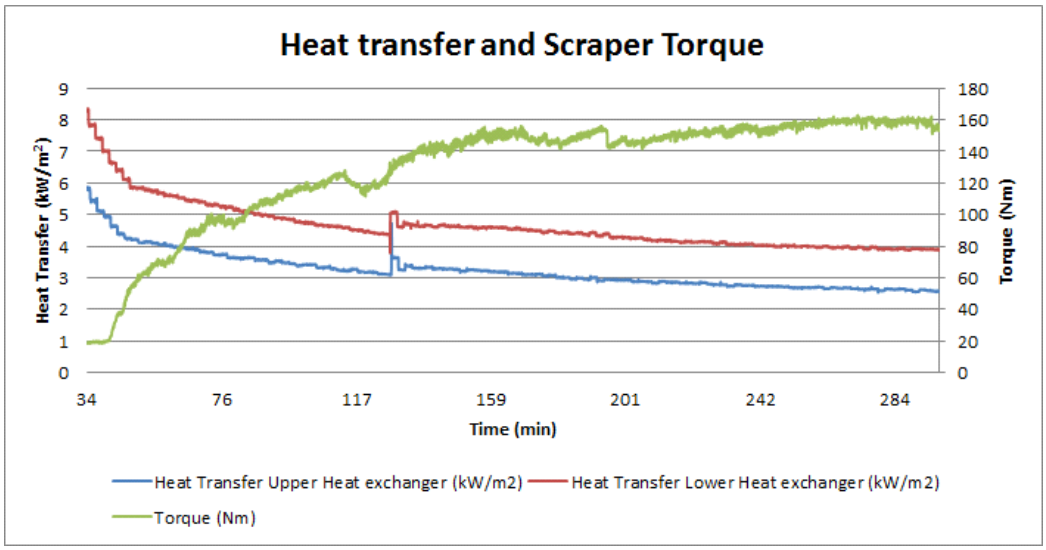

Figure 5.13. Graphs showing the heat transfer rates for the upper and lower heat exchangers in the 200L. The green line represents the scraping torque. The jump in the graphs around t=130 min is caused by a temporarily defect in the cooling machine setting.

The graph in figure 5.13 show the values for heat transfer and scraping torque. It is clear that scaling is occurring after ice formation has started. A heat transfer of 4 kW/m^2 is realized over the range of temperatures where ice and salt are crystallizing (with a temperature difference of ± 7 °C between coolant and solution). This is in good agreement with earlier experimental results for NaCl solutions. The torque required for scraping remains constant around 160 Nm, this is well within the technical capacities of the pilot plant set-up.

Possible Options for treating Shale Gas Water with the Eutectic Freeze Crystallization Process.

This section is intended to give a first impression of how an EFC process might be applied to treat a Shale Gas Water waste stream.
In general three different process schemes can be adapted to treat a waste stream with EFC. In words these are:

- Single stage EFC: Crystallization of ice and salt(s) occur in one crystallizer operated at a constant temperature. For multicomponent mixtures this scheme might lead to incomplete removal of dissolved salts when the operating temperature is too high for all species to crystallize and a relative large amount of concentrated brine is produced in this case. (This is described as option 1 below). When operating at the real eutectic point of a multi-component system all ions and water will be removed as salt and ice. In that case no bleed stream is required (only pure water and solid salt is produced).

- Multi-stage EFC: Combining several EFC crystallizers each operating at a different temperature. So a brine that is leaving from a previous EFC crystallizer is treated further at a lower temperature in a next crystallizer. This will increase salt product purities (by operating at a temperature at which just one salt crystallizes) and clean water production.

- EFC combined with pre- and/or after-treatment: For some waste streams it might be advantageous to use a pre- or after-treatment step in order to improve the EFC performance. Numerous pre- or after-treatments can be considered and their use is very dependent on the waste stream properties and product specifications. Examples are, reverse osmosis, chemical treatment (see option 2 in this chapter), ion exchange and evaporation.

Two different process options will be described; the first is a single stage EFC process and the second option uses a chemical treatment to remove calcium, strontium and barium before the EFC step. The processes described here are not optimized or extensively studied, they serve here as examples only.

Option 1. Single stage Eutectic Freeze Crystallization at -26 °C.

The first option uses the system that was investigated experimentally and for which the results are presented in the previous chapters. It is given here as an example of how the experimental results can be used in a basic process design. A schematic process block scheme is shown in figure 5.14.

As noted before, it is also possible to operate an EFC crystallizer at much lower temperatures where all salts are being removed and thus no concentrated brine is produced (i.e. no bleed stream). For this latter process option no experimental data is obtained and therefore a temperature of -26 °C was chosen here to serve as an example.

It was found that cooling the solution down to temperatures down to -26 °C sodium, barium, potassium and ice are crystallizing from the solution. Calcium, strontium and magnesium however are not removed at all.

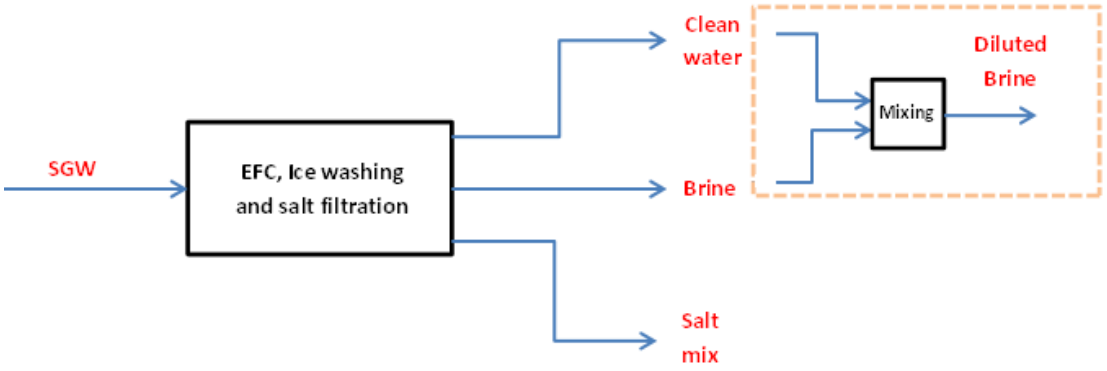

Figure 5.14. Process option 1. A single stage EFC process at -26 °C.

Simple mass balance calculations are performed to determine the product flows and purities. The following assumptions and experimental results are used:

- The operating temperature in the crystallizer is kept constant at -26 °C.
- As basis of calculation a feed flow of 0.16 m^3/hr is taken.
- Potassium is ignored in the calculations.
- The degree of purification of the ice product compared to the feed concentration is 0.99.
- The amount of brine is 61 wt% of the incoming stream.
- Ba and Na concentrations in the brine are calculated with the experimentally obtained values for the relative increase in concentration. (See Appendix C4).
- The formed salt product is a mix of $NaCl.2H_2O$ and $BaCl_2.2H_2O$. Recrystallization is not taken into account in these calculations.
- The salt mix is leaving the process as a dry solid product.

The results for the mass balance calculations are summarized in the stream tables in figure 5.15. From the tables in figure 5.15 it can be seen that for every barrel (0.16 m^3) feed almost 50 L of clean water is produced and 98 L of brine remains as an aqueous waste stream.

A second (and maybe third) EFC crystallizer might produce more ice and salts from this stream at a lower operating temperature. This possibility is not described further in this thesis.

Eventual mixing of the pure water with the remaining brine flow will form a diluted brine flow with at total solid content of 17.5% (compared to 23.2 % in the feed).

In addition some simple energy calculations are done for the process of option 1. In order to make accurate calculations for the energy requirements a more detailed process scheme must be prepared. This was however not in the scope of this project. Only the energy requirement for the crystallizer is calculated. (It should be noted that this will be just a minor part of the overall energy requirements.) The calculated energy consumption can be used in a general comparison with the main alternative for the EFC process, namely Evaporative Crystallization. The salt product that is formed during Evaporative Crystallization will differ from the EFC salts by being anhydrate salts instead of hydrated salt.

Stream name:	SGW	
Flowrate	184,0	kg/h
Solid fraction	0	-
Liquid fraction	1	-
Concentrations		
Ca	2,3	wt%
Na	5,0	wt%
Sr	0,7	wt%
Ba	1,5	wt%
Mg	0,2	wt%
Cl	13,5	wt%
H2O	76,8	wt%
TDS	23,2	wt%

Stream name:	Salt Mix	
Flowrate	21,5	kg/h
Solid fraction	1	-
Liquid fraction	0	-
Concentrations		
BaCl2.2H2O	18,5	wt%
NaCl.2H2O	81,5	wt%
TDS	-	wt%

Stream name:	Brine	
Flowrate	113,0	kg/h
Solid fraction	0	-
Liquid fraction	1	-
Concentrations		
Ca	3,7	wt%
Na	4,4	wt%
Sr	1,1	wt%
Ba	0,5	wt%
Mg	0,3	wt%
Cl	15,1	wt%
H2O	74,9	wt%
TDS	25,1	wt%

Stream name:	Clean water	
Flowrate	49,4	kg/h
Solid fraction	0	-
Liquid fraction	1	-
Concentrations		
Ca	0,02	wt%
Na	0,05	wt%
Sr	0,01	wt%
Ba	0,02	wt%
Mg	0,00	wt%
Cl	0,13	wt%
H2O	99,77	wt%
TDS	0,23	wt%

Stream name:	Diluted Brine	
Flowrate	162,4	kg/h
Solid fraction	0	-
Liquid fraction	1	-
Concentrations		
Ca	2,6	wt%
Na	3,0	wt%
Sr	0,8	wt%
Ba	0,3	wt%
Mg	0,2	wt%
Cl	10,6	wt%
H2O	82,5	wt%
TDS	17,5	wt%

Overview of In and Out going streams

	In		Out	
Flow	kg/h	L/h	kg/h	L/h
SGW	184,0	160,0		
Salt Mix			21,5	8,6
Brine			113,0	98,3
Clean Water			49,4	49,4

Figure 5.15. The stream tables for an hypothetical EFC process operating at -26 °C. Feed flowrate is 1 US barrel/hr.

To calculate the energy requirements for the crystallization process the following assumption where made:

- Both salts have the same crystallization energy, -18.8 kJ/mol (ΔH_{cryst} of $BaCl_2.2H_2O$)
- A constant heat capacity of 4 kJ/(kg.K) for the feed and the brine is assumed.
- A coefficient of performance of 2.45 is used to correlate the cooling duty to electrical power consumption.
- No heat integration is considered (e.g. pre-cooling of the feed with product ice, etc.)
- The comparison in energy requirement between EFC and Evaporative Crystallization is based on the production of equal amounts of clean water from the same amount of feed.
- The energy requirement for Evaporative Crystallization (EC) is based on a single stage evaporation process. (i.e. no Multi Stage Flash).
- The crystallization energy of salt is neglected for the energy calculation of EC. These are small compared to the evaporation energy of water.
- To compare the electrical energy requirement of EFC with the thermal energy required for EC a conversion factor for thermal to electrical energy of 50% is assumed.

The results of the energy calculations are shown in figure 5.16.

Energy requirement for the EFC process (Option 1)		
Cooling the Feed		
Feed flow	0,051	kg/s
Feed Temperature	298	K
Crystallizer Temperature	247	K
Q (Feed)	**-10,4**	**kW**
Crystallization		
Ice Production	0,014	kg/s
BaCl2.2H2O	0,005	mol/s
NaCl2.2H2O	0,052	mol/s
Q (Ice)	-4,6	kW
Q (Salt)	-1,1	kW
Q (Crystallization)	**-5,6**	**kW**
Total Cooling Duty		
Q (Total)	**16,1**	**kW**
Coefficient of Performance	2,45	
Electrical Energy Consumption	**6,6**	**kW**
Efficiency of conversion	50	%
Thermal Energy Consumption	**13,1**	**kW**
Requirements in Electrical Energy Units	**41,0**	**kWh/m3 feed**
	6,6	**kWh/bbl feed***
Requirements in Thermal Energy Units	**82,0**	**kWh/m3 feed**
For Comparison with EC	**13,1**	**kWh/bbl feed***

Energy requirement for the Evaporative Crystallization making an equal amunt of clean water.		
Heating the Feed		
Feed flow	0,051	kg/s
Feed Temperature	298	K
Crystallizer Temperature	373	K
Q (Feed)	**15,3**	**kW**
Evaporation		
Steam Production	0,014	kg/s
Q (steam)	**31,0**	**kW**
Total Heating Duty		
Q Total	**46,3**	**kW**
Requirements in Thermal Energy Units	**289,3**	**kWh/m3 feed**
	46,3	**kWh/bbl feed***

** 1 bbl = 160 L*

Figure 5.16. Comparison between the energy consumption of EFC and EC when making an equal amount of clean water from an equal amount of feed. Only the energy for the crystallization/evaporation process is taken into account.

Option 2. Chemical treatment followed by Eutectic Freeze Crystallization.

As an alternative it is possible to remove a large part of the barium, calcium and strontium with a chemical treatment and process the remaining brine further with EFC. For example the addition of sulfate ions will lead to the precipitation of $CaSO_4$, $BaSO_4$ and $SrSO_4$. Other options for chemical precipitation process are known and generally practiced in waste water treatment, in this report a treatment with Na_2SO_4 is used as an example. Figure 5.17 shows a block scheme for a process in which shale gas water is converted into solid salt, pure water and a bleed stream. Again mixing of the brine and the clean water is shown as an additional step.
This process is not studied before (neither experimentally nor theoretically) so only rough approximations based on earlier experiences are used here to perform simple mass balance calculations.

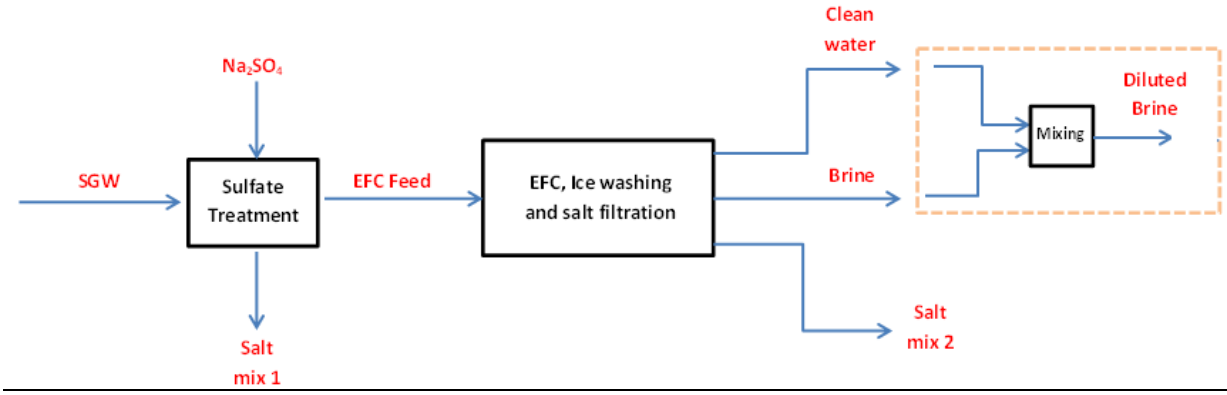

Figure 5.17. Process option 2. Sulfate treatment followed by an EFC process.

The following assumptions are made for this process:

- $BaSO_4$, $SrSO_4$ and $CaSO_4$ solubility after the sulfate treatment are assumed to be in in the order of 10, 500 and 5000 ppm, respectively. [Marshall, 1966. Davis, 1971]
- The formed crystals are $BaSO_4$, $SrSO_4$ and $CaSO_4.2H_2O$ in the sulfate treatment.
- Magnesium crystallization is ignored (in both sulfate treatment and EFC).
- During the EFC process ice and $NaCl.2H_2O$ will crystallize as well as all 90% of the remaining Ba, Sr and Ca will precipitate as sulfates.
- The EFC process is operated at -21 °C, the eutectic point of a pure NaCl-H_2O system.
- 90% of the feed to the EFC process is converted into ice or salt. (The rest leaves as a brine).
- The produced ice is 100% pure.

As can be seen in the tables in figure 5.19 an EFC process that is processing a pre-treated waste stream seems to be an attractive alternative for the single stage EFC process of option 1. The process in option 2 transforms every barrel of feed into 0.65 barrel of clean water. A solid salt product is produced by the sulfate treatment consisting of a mix of $BaSO_4$ (19.1 wt%), $CaSO_4.2H_2O$ (70.3 wt%) and $SrSO_4$ (10.6 wt%). In the EFC process a high purity (>99%) $NaCl.2H_2O$ product is formed. The concentrated brine (i.e. the bleed-stream) can be mixed with the clean water to produce a diluted waste stream (TDS <5%) which might be reused in the shale gas water cycle (i.e. to prepare new fracturing-fluid).

The increase in clean water production is mainly caused by the fact that in option 2 an almost pure NaCl solution is fed to the EFC crystallizer, therefore more ice and salt are produced simultaneously at a constant temperature.

Energy requirement for the EFC process (Option 2)		
Cooling the Feed		
Feed flow	0,050	kg/s
Feed Temperature	298	K
Crystallizer Temperature	247	K
Q (Feed)	**-10,2**	**kW**
Crystallization		
Ice Production	0,029	kg/s
NaCl2.2H2O	0,169	mol/s
Q (Ice)	-9,6	kW
Q (Salt)	-3,2	kW
Q (Crystallization)	**-12,8**	**kW**
Total Cooling Duty		
Q (Total)	**23,0**	**kW**
Coefficient of Performance	2,45	
Electrical Energy Consumption	**9,4**	**kW**
Efficiency of conversion	50	%
Thermal Energy Consumption	**18,7**	**kW**
Requirements in Electrical Energy Units	**58,6**	**kWh/m3 feed**
	9,4	**kWh/bbl feed***
Requirements in Thermal Energy Units	**117,2**	**kWh/m3 feed**
For Comparison with EC	**18,7**	**kWh/bbl feed***

Energy requirement for the Evaporative Crystallization making		
Heating the Feed		
Feed flow	0,050	kg/s
Feed Temperature	298	K
Crystallizer Temperature	373	K
Q (Feed)	**14,9**	**kW**
Evaporation		
Steam Production	0,029	kg/s
Q (steam)	**64,9**	**kW**
Total Heating Duty		
Q Total	**79,9**	**kW**
Requirements in Thermal Energy Units	**499,3**	**kWh/m3 feed**
	79,9	**kWh/bbl feed***

** 1 bbl = 160 L*

Figure 5.18. Comparison between the energy consumption of EFC and EC when making an equal amount of clean water from an equal amount of feed. Only the energy for the crystallization/evaporation process is taken into account.

Stream Tables: Option 2 - EFC at -23 ° with Sulfate Treatment

Stream name:	SGW	
Flowrate	184,0	kg/h
Solid fraction	0	-
Liquid fraction	1	-
Concentrations		
Ca	2,3	wt%
Na	5,0	wt%
Sr	0,7	wt%
Ba	1,5	wt%
Mg	0,2	wt%
Cl	13,5	wt%
SO4	0,0	wt%
H2O	76,8	wt%
TDS	23,2	wt%

Stream name:	Salt Mix 1	
Flowrate	24,6	kg/h
Solid fraction	1	-
Liquid fraction	0	-
Concentrations		
BaSO4	19,1	wt%
CaSO4.2H2O	70,3	wt%
SrSO4	10,6	
TDS	-	wt%

Stream name:	EFC Feed	
Flowrate	179,4	kg/h
Solid fraction	0	-
Liquid fraction	1	-
Concentrations		
Ca	0,1	wt%
Na	8,7	wt%
Sr	0,0	wt%
Ba	0,0	wt%
Mg	0,2	wt%
Cl	13,8	wt%
SO4	0,3	wt%
H2O	76,8	wt%
TDS	23,2	wt%

Stream name:	Clean water	
Flowrate	103,6	kg/h
Solid fraction	0	-
Liquid fraction	1	-
Concentrations		
Ca	0,0	wt%
Na	0,0	wt%
Sr	0,0	wt%
Ba	0,0	wt%
Mg	0,0	wt%
Cl	0,0	wt%
SO4	0,0	wt%
H2O	100,0	wt%
TDS	0,0	wt%

Stream name:	Brine	
Flowrate	17,9	kg/h
Solid fraction	0	-
Liquid fraction	1	-
Concentrations		
Ca	0,6	wt%
Na	9,1	wt%
Sr	0,1	wt%
Ba	0,0	wt%
Mg	1,8	wt%
Cl	19,3	wt%
SO4	1,5	wt%
H2O	67,5	wt%
TDS	32,5	wt%

Stream name:	Salt Mix 2	
Flowrate	57,8	kg/h
Solid fraction	1	-
Liquid fraction	0	-
Concentrations		
NaCl.2H2O	99,1	wt%
BaSO4	0,0	wt%
CaSO4.2H2O	0,8	wt%
SrSO4	0,1	wt%
		wt%
		wt%
		wt%
TDS	-	wt%

Stream name:	Diluted Brine	
Flowrate	121,5	kg/h
Solid fraction	0	-
Liquid fraction	1	-
Concentrations		
Ca	0,09	wt%
Na	1,35	wt%
Sr	0,02	wt%
Ba	0,00	wt%
Mg	0,27	wt%
Cl	2,84	wt%
SO4	0,23	wt%
H2O	95,21	wt%
TDS	4,79	wt%

Stream name:	Na2SO4	
Flowrate	20,0	kg/h
Solid fraction	1	-
Liquid fraction	0	-
Concentrations		
Na2SO4	100,0	wt%
TDS	-	wt%

Overview of In and Out going streams

	In		Out	
Flow	kg/h	L/h	kg/h	L/h
SGW	184	160		
Na2SO4	20	8		
Salt Mix 1			25	10
Brine			18	16
Salt Mix 2			58	23
Clean Water			104	104

Figure 5.19. Stream tables for the process with a sulfate treatment before the EFC process (depicted in figure 5.17).

The tables in figure 5.18 are showing a comparison in energy requirements between EFC and Evaporative Crystallization. The same assumptions are used as for the energy calculations of the option 1 process. Again the calculated energy is limited to the crystallization/evaporation process.

Conclusions

Based on the performed experiments the following conclusions regarding the treatment of shale gas water with EFC can be made:

- Ice is formed from the shale gas water around -10 °C.
- Minor amounts of potassium chloride starts to form -14.5 °C. Barium chloride crystallization starts at -22.4 °C and the first sodium chloride is formed between -22.4 and -24.5 °C.
- A sample of the salt product obtained at -23.4 °C and consists mainly of Ba and Na chloride with minor amounts of Sr (570 ppm), Ca (410 ppm), K (60 ppm) and Mg (40 ppm).
- Due to the crystallization process the temperature is decreasing very slowly below -23.4 °C.
- Water that is produced (in the form of ice) shows a >99% decrease in salt content, compared to the original solution.
- Operating the EFC process at -25.9 °C will recover 31 % of all salt present in the feed solution as a solid salt mixture and 41% of the water is obtained as ice. The total waste stream will be reduced in weight by 49%.
- Batch tests in the 200 L pilot set-up showed no unexpected behavior caused by the up scaling.
- Heat transfer rates of 4 kW/m^2 are achieved with a ΔT of 7 °C.

Some general conclusions based on the described process options can be made.

- Based on the experimental work done it can be concluded that EFC is a technology that is able to treat the shale gas water waste stream and convert it into clean water and solid salt products. Several different process options are possible and based on the requirements set by the client a most optimal process design can be explored in more detail.
- A single stage EFC process operated at -26 °C will transform 27 wt% of the feed into clean water. A concentrated brine is produced (61 wt% of the feed) with a TDS of 25 wt%.
- Combining the clean water with the brine produces a diluted brine with TDS of 17.5 wt%.
- An EFC process operated at lower temperatures will have higher values for the total salt and water recovery. Theoretically a 100 % conversion into salts and clean water can be achieved (probably around an operating temperature of -55 °C for shale gas water).
- Adding sodium sulfate to remove a large fraction of the calcium, strontium and barium from the feed before the EFC crystallizer is considered an attractive process option
- A process with a sulfate treatment step transforms 56 wt% of the feed into clean water and only 10 % leaves the process as a concentrated brine.
- Combining the concentrated brine with the produced pure water produces a diluted brine with TDS of 4.8 wt%. With very low concentrations (< 5 ppm) of the toxic barium.

Chapter 6
Conclusions and Recommendations

In the chapters 3, 4 and 5 detailed conclusions are made based on the results presented and discussed in these chapters. In this chapter some of the more general conclusions from these earlier chapters are given and they are translated into recommendations. The recommendations are divided into recommendations to improve the currently used experimental EFC equipment and in suggestions for further research topics.

General conclusions

- Scaling of the heat exchangers is not observed before ice crystallization starts. In other words, salt crystallization alone does not increase the scraping torque nor decrease the heat transfer coefficient.
- Analysis of the scale layer shows a salt content of 3.4 wt% for a scale formed from a solution with a starting concentration of 8 wt% Na_2SO_4.
- In a system in which first ice is formed there is no significant effect on the scraping torque and heat transfer when also salt starts to crystallize at the eutectic point.
- Addition of $MgCl_2$ and NaCl leads to a significant decrease in scaling and higher heat transfer coefficients compared to the EFC of a pure Na_2SO_4 solution.
- Adding 3 wt% NaCl or $MgCl_2$ to a 8 wt% Na_2SO_4 solution roughly doubles the heat transfer coefficient under eutectic conditions.
- During the EFC of a Na_2SO_4 solution with low levels of impurities (< 600 ppm) the current scrapers construction is not able to sustain total heat transfer rates higher than 1.7 kW.
- Addition of 2.4 wt% NaCl to a Na_2SO_4 solution has a significant and positive effect on the heat transfer rates that could be achieved, >3.1 kW.
- Addition of NaCl does not influence the product purities, it is therefore considered as an attractive measure to increase heat transfer in an industrial EFC process without decreasing the value of the products. *It should be noted however that adding Cl does increase the corrosion tendency of the solution.*
- The observed separation of ice and salt being produced in the crystallizer is not efficient for a Na_2SO_4 solution in the currently used crystallizer design. Large amounts of solids are trapped around the top heat exchanger causing salt contamination of the ice slurry product and a decrease of the heat transfer performance of the upper heat exchanger.
- The method of ice extraction by overflowing is limiting the ice production rate in the crystallizer during continuous operation. Also the performance of the upper heat exchanger is decreased by a large ice solid fraction in the top section of the crystallizer.

- For a typical waste water stream originating from the production of shale gas ice starts to crystallize around -10 °C. Subsequently minor amounts of potassium chloride starts to form around -14.5 °C. Barium chloride crystallization starts at -22.4 °C and the first sodium chloride is formed between -22.4 and -24.5 °C.
- Water that is produced (in the form of ice) shows a >99% decrease in salt content, compared to the original solution. Operating the EFC process at -25.9 °C will recover 31 % of all salt present in the feed solution as a solid salt mixture and 41% of the water is obtained as ice. The total waste stream will be reduced in weight by 49%.
- Based on the experimental work done it can be concluded that EFC is a technology that is able to treat the shale gas water waste stream and convert it into clean water and solid salt

products. Several different process options are possible and based on the requirements set by the client a most optimal process design can be explored in more detail.
- A single stage EFC process operated at -26 °C will transform 27 wt% of the feed into clean water. A concentrated brine is produced (61 wt% of the feed) with a TDS of 25 wt%.
- An EFC process operated at lower temperatures will have higher values for the total salt and water recovery. Theoretically a 100 % conversion into salts and clean water can be achieved (probably around an operating temperature of -55 °C for shale gas water).
- Adding sodium sulfate to remove a large fraction of the calcium, strontium and barium from the feed before the EFC crystallizer is considered to be an attractive process option.

Recommendations on the improvement of the experimental set-ups

- The currently used set-up used for scaling and heat transfer studies is a so called scraped plate crystallizer, this is a dated concept of EFC crystallizer design. Based on several years of research and experiments the scraped wall crystallizer design was identified as the most suited design. It would therefore be logical and useful to replace the current scraped plate 10L set-up with a 10 L scraped wall crystallizer to do representative studies on heat transfer and scaling during the EFC process. At the moment of writing this new 10L set-up is being constructed.
- During experiments in the 200L set-up it was found that the separation of ice, salt and solution is not optimal. This causes relative large amounts of salt crystals being entrained in the ice slurry product. Also the heat transfer of the upper heat exchangers is negatively influenced by the accumulation of solids around the heat exchangers (mainly at the upper heat exchanger). A possible way to improve on this issue is to increase the space between the inner and outer heat exchangers and to increase the space between the crystallizer wall and the heat exchanger.
- Another measure that could possibly improve the heat transfer performance of the upper heat exchanger is to increase the space above this heat exchanger. In this space ice can accumulate without negatively influencing the heat exchange.
- A device should be installed to ensure forced removal of ice from the crystallizer. The current way of removal by overflowing is not working efficiently and is even limiting the ice production rates that can be achieved. A helical screw connected to a variable speed drive could be suited for this purpose.
- It would be a good idea to design a 15-20 L scale crystallizer in which simultaneously scraping, heat transfer and crystallization studies can be done under both batch and continuous conditions. Such an experimental set-up should have the following features:
    - A scraped wall heat exchanger with temperature and flow sensor to obtain the data required for heat transfer calculations.
    - Scrapers that can be easily changed to study the effect of different scraper designs.
    - An instrument to easily vary the rotational speed of the scrapers.
    - A device to extract liquid samples from the crystallizer content for concentration studies without the need to stop the scrapers. A sampling device similar to the sampling device currently used in the ECN crystallizer is suited for this purpose.
    - The possibility to connect an external loop with a so-called flowcell to take inline photos of the produced crystals.
    - Possibility for continuous feeding the crystallizer with fresh solution by means of peristaltic pump. The feed should be introduced into the middle of the crystallizer to prevent contamination of the ice product.
    - A conical shaped bottom to collect the produced salt crystals with an exit connected to a peristaltic pump to remove salt slurry from the crystallizer at a variable rate.

- A helical screw inserted into the top section of the crystallizer to extract ice slurry from the crystallizer at a variable rate.
- A crystallizer wall of transparent material (e.g. PMMA or glass) to be able to see salt/ice separation in the crystallizer. A double wall will avoid ice formation at the outside of the crystallizer and improves thermal insulation.
- It can be operated over a large range of temperatures, i.e. from +30 °C to -60 °C.

Recommendations on further studies

In the introduction of this thesis (Chapter 1) a list of subjects is given which could/should be investigated in order to develop the EFC process further. What follows here are recommendations on future studies related to the work presented in the chapters 3 to 5.

The following studies can be performed to further investigate the scaling behavior under EFC conditions.

- Study a broader range of pure binary systems and look for relation between eutectic concentration and scaling properties.
- Investigate the scale formation process at a microscopic scale in order develop a physical model to describe the processes occurring near the surface. A basis for such a model might be found in the models provided by Pronk [Pronk, 2006] and Qin [Qin, 2009].
- Study the effect of scraper geometry and rotational speed of the scrapers on the heat transfer performance of scraped wall heat exchangers and scale formation. Optimize for optimal energy efficiency.

The following studies can be performed to further investigate the possibilities for the treatment of an industrial sodium sulfate waste stream with the EFC process and the EFC process in general.

- Investigate the recrystallization of $Na_2SO_4.10H_2O$ crystals to anhydrate crystals and the effect of this step on the purity of the final salt product.
- Study the required equipment for the isolation and washing of the ice and salt products.
- Investigate methods to remove ice from the crystallizer to avoid excessive ice accumulation in the crystallizer.
- Investigate the optimal design of the crystallizer vessel and its internals (e.g. the space between the heat exchangers, feed entrance point). The ideal is to achieve complete separation between ice and salt in the crystallizer at high salt and ice production rates.
- Explore the measures that can be taken to prevent sulfide corrosion in the crystallizer and auxiliary equipment during the treatment of an acidic sodium sulfate waste stream.

The following studies can be performed for further investigation of the application of the EFC process in the treatment of a shale gas water stream.

- Investigate the crystallization behavior below -30 °C. This will provide more information on the recovery of all ions and water as a function of operating temperature. The ultimate goal is to locate the eutectic point at which all salts are crystallizing. Operation at this point will result in a zero liquid discharge process.
- Establish the parameters required in a thermodynamic model (e.g. Pitzer's model) to be able to predict crystallization at low temperatures and high concentrations.
- Experiments with real shale gas water samples could be done to validate the results obtained from the synthetic solutions used in the experiments so far.

- Experimentation at a large set-up (100-1000 L) and continuous conditions will be a logical step to further explore different aspects (e.g. isolation and washing of ice and salts, efficiency of the ice/salt/liquid separation, etc.) of the EFC process at a more realistic industrial scale.
- Prepare detailed process schemes and identify the required unit operations for the complete process. Study the heat integration possibilities of the complete EFC-treatment process. This will result in more accurate information on capital and operational costs associated with the complete process.

Acknowledgements

As most people probably already knew and what I found out during many parts of my study is that it is impossible to obtain good results, either for exams or for projects, completely on your own. My master thesis project was by no means an exception on this and therefore I would like to thank anyone who helped me, both intended as well as unintended, with completing this task. I will not even attempt to thank anyone here, however I wish to give some special attention to three persons who were of particular help to me during this final part of my master studies.
Prof. Geert-Jan Witkamp, who gave me the opportunity and freedom to work as an independent master student on such a challenging subject as EFC. I learned a lot during the discussions we had on many subjects.
Next I want to thank Jaap van Spronsen for all his help on the various experimental issues and for learning me a lot about the EFC process and its development. Not many people (if any) have more experience with all the ins and outs of the EFC process as he has.
Finally, the very reason that it was possible to do any EFC experiments at all is because of the skilled hands and knowledge of Hans Evers of EFC Separations BV. He was always willing and able to help me with any practical problems/challenges encountered during my project.

References

[Ham, 1999] **Ham, F. v/d.,** Eutectic Freeze Crystallization**,** *PhD thesis***,** TU Delft, 1999.

[Pronk, 2006] **Pronk, P**., Fluidized bed heat exchangers to prevent fouling in ice slurry systems and industrial crystallizers, *PhD thesis*, TU Delft, 2006.

[Davis, 1971] **Davis, J.W., et al**, Solubility of barium and strontium sulfates in strong electrolyte solutions, *Environmental Science and Technology*, 1971 (5), pp. 1039-1043.

[Marshall, 1968] **Marshall, W.L., et al,** Aqueous systems at high temperature. Solubility to 200 °C of calcium sulfate and its hydrates in sea water and saline water concentrates, and temperature-concentration limits, *Journal of Chemical Engineering data,* 1968, 13, pp. 83-93.

[Veassen, 2003] **Veassen, R.J.C.,** Development of Scraped Eutectic Crystallizers, *PhD thesis*, TU Delft, 2003**.**

[Stepakof, 1974] **Stepakof, G.L., et al,** Development of a eutectic freezing process for brine disposal, *Desalination*, 1974 (14), pp. 25-38

[Schroeder, 1977] **Schroeder, P.J., et al,** Freezing processes: The standard of the future, *Desalination*, 1977 (21), pp. 125-136

[Seader, 2006] **Seader, J.D., Henley, E.J.,** Separation Process Principles, *Wiley*, 2nd ed., 2006.

[Kramer] **Kramer, H.J.M., et al,** Basic process design for crystallization processes, *Reader*, TU Delft.

[Myerson, 2002] **Myerson A.S.**, Handbook of Industrial crystallization, *Butterworth-Heinemann*, 2nd ed., 2002

[Himawan, 2002 **Himawan, C.,** Characterization and population balance modeling of eutectic freeze crystallization, *PhD thesis*, TU Delft, 2002.

[Qin, 2009] **Qin, F.G.F.,** Freezing on subcooled surfaces, phenomena, modeling and applications, *International Journal of heat and mass transfer*, 2009 (52), pp. 1245-1253.

[Reddy, 2010] **Reddy, S.T., et al,** Recovery of $Na_2SO_4.10H_2O$ from an reverse osmosis retentate by eutectic freeze crystallization technology, *Chemical engineering research and design*, 2010 (88), pp. 1153-1157.

[Ullmann's, 2000] **Plessen, H. von,** Sodium Sulfates, *Ullmann's Encyclopedia of Industrial Chemistry*, Wiley-VCH, 2000.

[Webmineral] **Website,** http: //webmineral.com/data/Thenardite.shtml, last visited on 2/2/2012.

[Hamilton, 2008] **Hamilton, A., et al,** Sodium sulfate heptahydrate: direct observation of crystallization in a porous material*, Journal of physics D: Applied physics*, 2008 (41).

[Garett, 2001] **Garett, D.E.,** Sodium Sulfate: Handbook of deposits, processing, properties and use, *Academic Press*, 2001.

[Verbeek, 2011] **Verbeek, B.J.J.,** Eutectic freeze crystallization on sodium chloride, *Master thesis*, TU Delft, 2011.

[Smith, 2011] **Smith, P.,** A model for the corrosion of steel subjected to synthetic produced water containing sulfate, chloride and hydrogen sulfide, *Chemical engineering science*, 2011 (66), pp. 5775-5790.

[Tewari, 1976] **Tewari, P.H., et al,** Dissolution of iron sulfide in aqueous sulfuric acid, *The journal of physical chemistry*, 1976 (80), pp. 1844-1848.

Appendix A. PFD of 200L pilot set-up

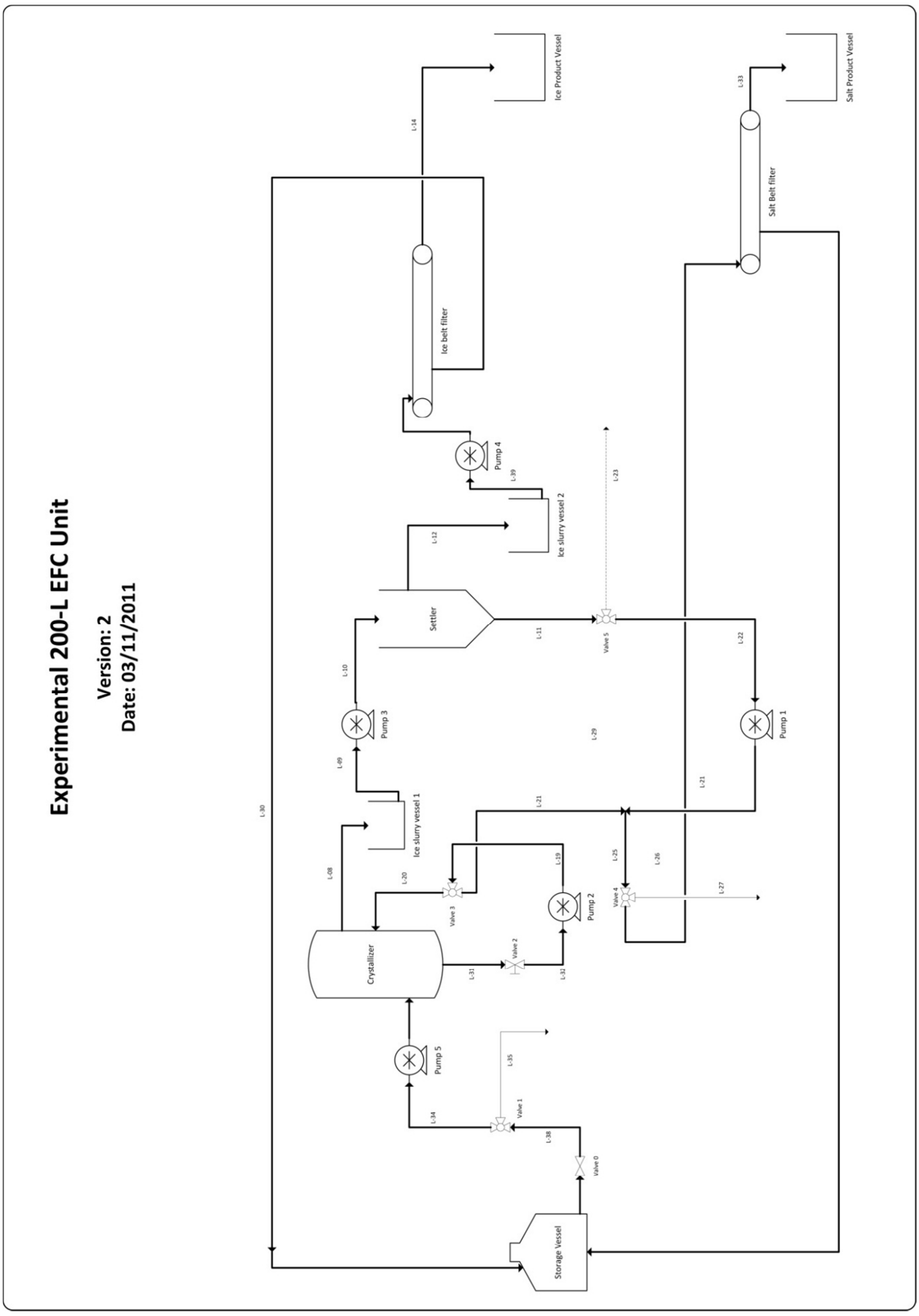

Appendix B Manual for the 200L Set-Up.

Operation Manual for the EFC 200 L Set-up

December 19, 2011

Author: Bart de Graaff

Preparing the solution

Solutions of desired concentration can be prepared in the a large vessel with a stirrer attached (see figure M.1). A balance is present to weigh the salt and water.
After preparation the solution can be pumped into the storage vessel using the utility pump (pump 6).
Several batches of solution are required to fill the storage tank. Approximately 250 (for batch operation) to 500 (for continuous operation) liters of solution are needed for the experiments.

Figure M.1: Vessel to prepare the starting solution.

Starting the crystallizer

The start-up procedure for the skid involves different steps and the order of the steps is important to a certain extent. It is therefore advised to follow the here listed sequence.

Note: This section is especially valid when the skid is located and installed at its usual location in the hall of the P&E department. For field-tests several deviations from the here described procedure may occur.

1. Switch on the computer and open the Labview program to operate the pumps and monitor the flows, temperatures and torque. (See Figure M.2).
   Always use the latest version, this is 'GUI EFC v2.51' (November 7, 2011). Additional information on the computer program can be found in the manual present on the computer.

2. Fill the crystallizer with starting solution.
   a. Open Valve 0 and Valve 1.
   b. Use Pump 5 to pump solution from the storage vessel into the crystallizer.

3. Open the cooling water supply, both in- and outlet. (See figure M.3).
   The cooling water is required for the compressor.

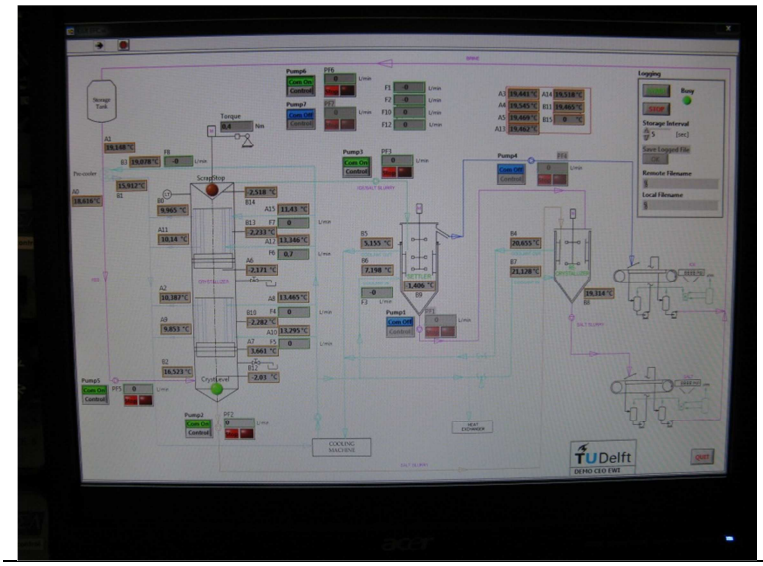

Figure M.2: Computer screen showing the Labview program needed to operate the pumps and log the data.

Figure M.3: Cooling water valves (in open position)

4. Start the cooling water circulation pump. Switch is present at the front-panel labeled: 'Pump cooling water'. (See figure M.4)
   Now the light in the button will turn green and cooling water is circulated to the compressor.

Figure M.4. The Front Panel.

5. Press 'on' on the scraper controller on the front panel under the label 'CDCC scraper motor'. *A safety measure is in place to prevent the scraper is activated when liquid level is too low. Make sure that the level sensor is in place and connected.*

6. Open the Bypass-valve of the cooling circuit at the backside of the skid. (See figure M.5)

7. Switch on the mains on the cooling machine. (See figure M.6)

Figure M.5. Cooling liquid by-pass valve.

Figure M.6. Cooling machine mains.

8. Switch on the cooling liquid circulation pump on the cooling machine. (See figure M.7)

Figure M.7. The cooling machine. The most left button turns on the cooling liquid pump and the one next to it the compressor.

Figure M.8. Cooling liquid valves. Adjust the cooling liquid flows here and read the values at the Siemens controllers or the computer screen.

9. Adjust the flow to the heat exchangers at will by turning the valves at the back of the skid. (See figure M.8)
   When there is sufficient flow through the elements the bypass valve can be closed.
   By closing or opening the bypass valve cooling liquid flow rates can be increased or decreased while keeping the ratios of the different flows constant.

10. Turn on the compressor on the cooling machines front panel (See figure M.7).

11. Set the temperature set point at the display on the cooling machine's front panel.

Starting-up of the small belt filter.

1. Switch on the belt filter with the button ‘ bandfilter’ on the frontpanel.

2. Open the water supply for the belt filter. (See figure M.9)
   Water is used for the cloth washing and for the liquid ring vacuum pump.

3. Open the air valve. (See figure M.10)
   Air is used to operate the belt filter. Press the ‘reset’- button on the ‘Pannevis switch-box’ to see whether the belt is working.

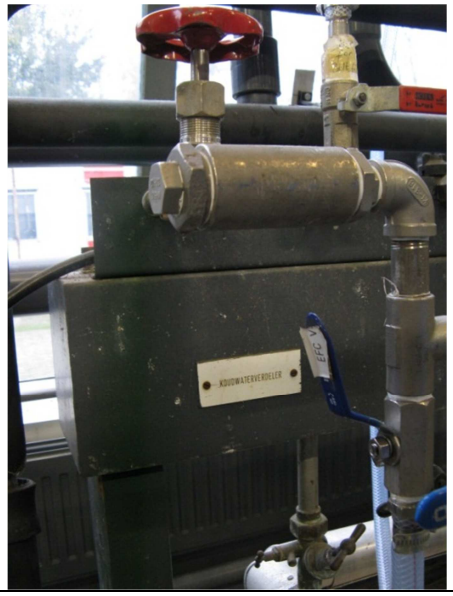

Figure M.9: Water supply for the small belt filter.

Figure M.10. Air valve for the small belt filter.

4. Switch on the mains on the ‘Pannevis box’. See figure M.11.

5. Open and adjust the water flow with the large regulator see figure M.12. Set the flow at around 30.
   This is the water for the filter washing and for the liquid-ring pump.

Figure M.11. The ‘Pannevis switch box’. The green button is the reset. The red switches are from left to right; Filtrate Pumps 1 till 3, Vacuum Pump, Belt Filter Mains.

Figure M.12. Large water flow regulator.

6. Fill the liquid-ring vacuum pump (See figure M.13):
    a. Close the red tap
    b. Open the black tap
    c. Use the small flow regulator (see figure M.14) to fill the pump till water comes out of the black tap.
    d. Stop the water flow and wait till no water leaves the pump.
    Now the water level is just above the pumps axis.
    e. Close the black tap.

Figure M.13. Rearside of the vacuum pump, showing the black and the red valves.

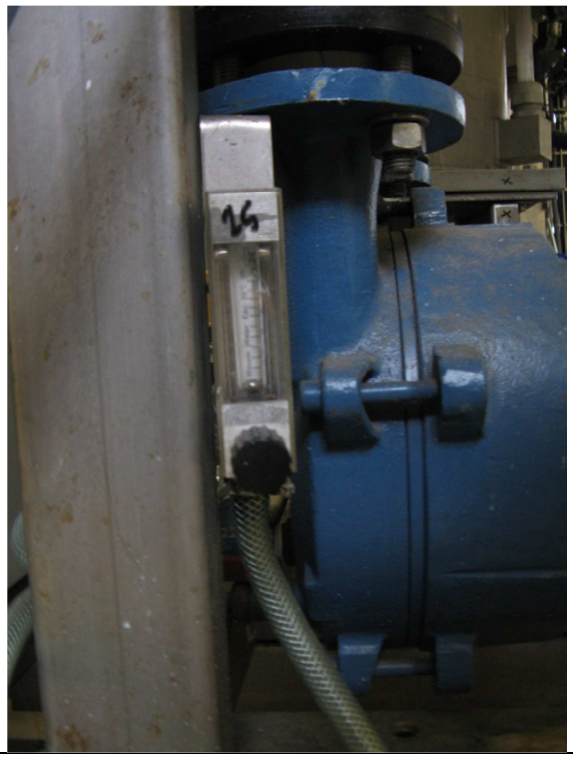

Figure M.14. Flow regulator for the vacuum pump.

7. Start the vacuum pump with the switch on the 'Pannevis switch box'.

8. Re-open the water flow to the vacuum pump with the small flow regulator, set this flow to around 10.
    This is make-up water needed to replenish the water from liquid ring that is entrained in the gas flow. After some time a small flow will come from the liquid separator, this is an extra check to now that enough water is present to sustain the liquid-ring.

9. Start the filtrate pumps (1 to 3) with the switches on the 'Pannevis box'.

10. The belt filter is now ready to receive the slurry.

Stopping the small belt filter

1. Stop the slurry flow to the belt filter and wait till last solids come from the filter.

2. Remove the filtrate return line from the storage vessel.
   To prevent that wash water comes into the storage solution.

3. Start pumping clean water to the belt filter.
   This can be done by placing the suction end of Pump 4 in a bucket filled with clean water.

4. When the filter is cleaned and no water comes from the filtrate return line turn off the filtrate and vacuum pumps on the 'Pannevis Box'.

5. Close the water flow to the spray washer by closing the large water flow regulator.

6. Close the water flow to the vacuum pump by closing the small flow regulator.

7. Open the black and red valve on the vacuum pump to empty it. Leave both valves open.

8. Swtich off the mains on the 'Pannevis box'.

9. Close the general water supply to the belt filter.

10. Close the air supply.

Starting the large belt filter

1. Open the air valve to the large belt filter. (See figure M.15)

Figure M.15. Air valve for the large belt filter

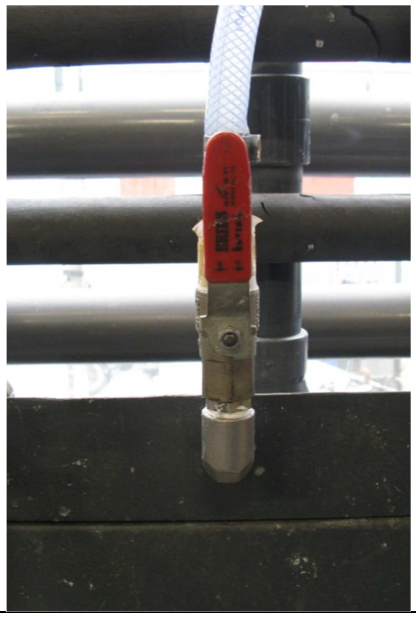

Figure M.16. Water supply to the large belt filter.

2. Open water supply to the belt filter with the red tap. (See figure M.16)

3. Open the water to the filter cloth washing section. This is the tap indicated in figure M.17.

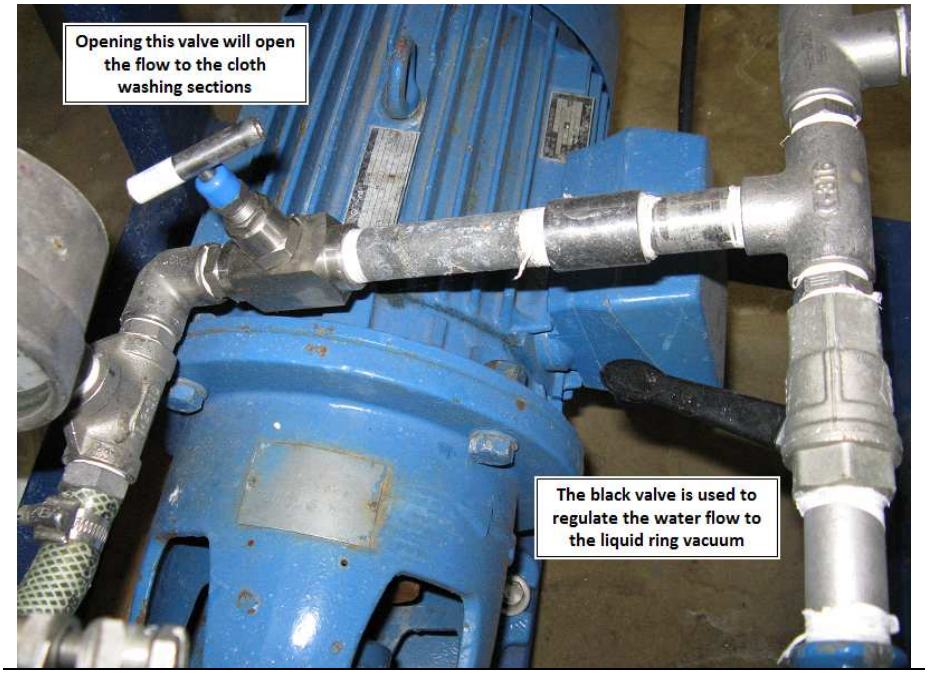

Figure M.17. Water valves to regulate the water flow to the cloth washing and the vacuum pump.

4. Start the belt filter with the black switch (“Aandrijving”) at the backside of the filter. See figure M.18.

Figure M.18. The black switches at the back of the belt filter. The switches in the photo are used for Filtrate pump 4, the vacuum pump and the belt filter (“Aandrijving”)

5. The speed of the filter can be adjusted by turning the button shown in figure M.19.

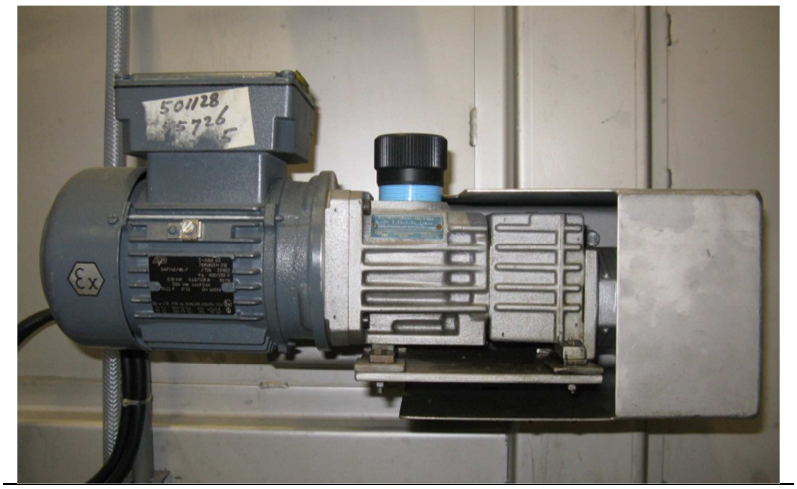

Figure M.19. Regulator to adjust the speed of the belt filter.

6. Fill the liquid ring vacuum pump;
    a. Close the yellow tap at the bottom of the pump. (See figure M.20).
    b. Open water to the pump with the black handle. (See figure M.17)
    c. Wait until water flows from the blue tap halfway the pump. (See figure M.21)
    d. Close the water to the pump and the blue tap.

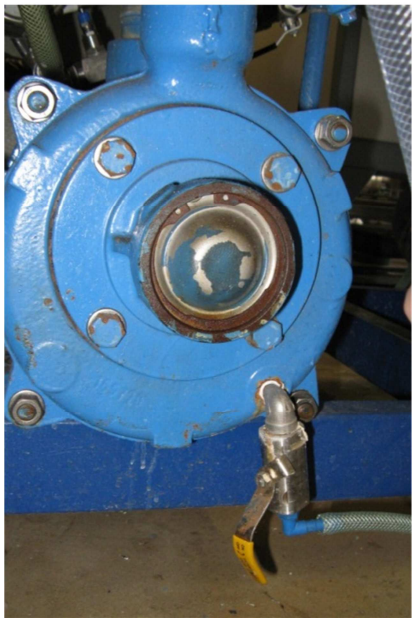

Figure M.20. Yellow tap at the bottom of the pump to empty the vacuum pump.

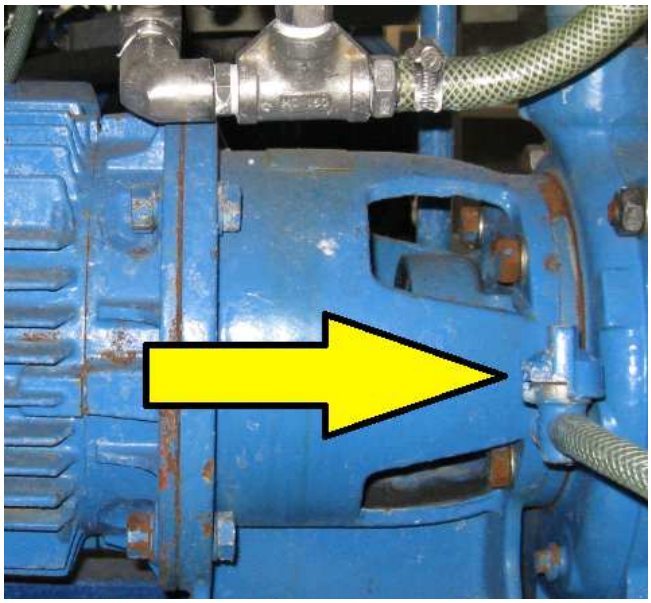

Figure M.21. The yellow arrow indicates the blue tap.

7. Start the vacuum pump with the black switch at the backside of the filter. (See figure M.18).

8. Re-open the water supply to the vacuum pump and adjust the flow such that a small water stream leaves the separator vessel of the pump. (See figure M.17 and M.22).

Figure M.22. The separator vessel of the vacuum pump.

9. Start the filtrate pumps with the black switches (“Filtraatpomp 1 to 4”) located at the back of the beltfilter above the pumps.

10. Start feeding the slurry to the filter.

Stopping the large belt filter

1. Stop the slurry flow to the belt filter and wait till last solids come from the filter.

2. Remove the filtrate return line from the storage vessel.
   To prevent that wash water comes into the storage solution.

3. Start pumping clean water to the belt filter.

4. When the filter is cleaned and no water comes from the filtrate return line turn off the filtrate and vacuum pumps with the switches at the back of the belt filter.

5. Close the water supply for the large belt filter (See figure X)

6. Empty the vacuum ring pump by opening the yellow tap at the bottom

7. Close the air supply to the large belt filter.

Appendix C. Additional results for the Shale gas water study

C1. Calculated values for the degree of purification (compared to the starting solution) for the ice product at -23.4 °C.

$$Degree\ of\ Purification = 1 - \frac{C(sample)}{C(Starting\ solution)}$$

Purification factors for the ice product.

	Ca	Mg	K	Sr	Ba	Cl	Na	Total
Start Solution	0,00	0,00	0,00	0,00	0,00	0,00	0,00	0,00
Ice after filtration	0,38	0,28	-0,42	0,15	0,33	0,54	0,35	0,48
After 1st wash	0,61	0,63	0,40	0,58	0,47	0,73	0,57	0,68
After 2nd wash	0,88	0,89	0,86	0,87	0,85	0,92	0,87	0,90
After 3th wash	0,94	0,95	0,95	0,94	0,93	0,96	0,94	0,95
After 4th wash	0,98	0,98	0,99	0,97	0,97	0,98	0,98	0,98
After 5th wash	0,99	0,99	1,00	0,99	0,99	0,99	0,99	0,99

Example: When ice is washed five times the ice product will contain only 1% of the start solution concentration of each ion.

C2. ICP results of an ice and salt product purity study.

Experiment 29/09/2011 (All concentrations in ppm)									
	Ca	**Mg**	**Fe**	**Mn**	**K**	**Sr**	**Ba**	**Cl**	**Na**
Start Solution	25000	2100	18	5	675	8300	15000	150000	57000
Salt									
	Ca	**Mg**	**Fe**	**Mn**	**K**	**Sr**	**Ba**	**Cl**	**Na**
Salt	7980	710	10	0	390	2880	156350	215160	77120
Salt after wash 1	1950	180	10	0	150	860	150810	231550	91110
Salt after wash 2	1030	100	0	0	100	570	158740	256260	96780
Salt after wash 3	410	40	0	0	60	310	150400	236710	94080
Salt Filtrate	22160	1920	20	10	640	7360	5770	135840	54060
Filtrate after wash 1	4280	380	0	0	240	1570	3060	147570	84610
Filtrate after wash 2	790	70	0	0	90	370	3860	158310	93770
Filtrate after wash 3	290	30	0	0	60	180	4740	162080	96630
Ice									
	Ca	**Mg**	**Fe**	**Mn**	**K**	**Sr**	**Ba**	**Cl**	**Na**
Ice	11390	990	0	0	0	3740	8220	88020	21580
Ice after wash 1	460	40	0	0	20	160	1120	7830	2560
Ice after wash 2	110	10	0	0	10	50	240	1690	560
Ice Filtrate	27450	2410	20	10	720	9010	5870	149210	47650
Filtrate after wash 1	19780	1730	20	0	650	6520	8340	130310	45340
Filtrate after wash 2	1320	120	0	0	60	500	7260	24720	9800

Results of the experiment of 29/9/2011. All concentrations are in ppm (10 000 ppm = 1wt%)

C3. ICP results of an experiment in which the concentration in the mother liquor is followed upon cooling.

Solute concentrations as a function of temperature during a batch EFC.

	Concentrations (ppm)							
Temperature (°C)	Calcium	Magnesium	Potassium	Strontium	Barium	Chloride	Sodium	Manganese
Starting liquid	22600	1700	380	6000	13700	149000	45900	7
-9,92	22700	1700	410	6100	13800	151000	46700	7
-14,51	23100	1700	340	6200	13900	149000	46400	8
-18,54	22400	1700	390	5900	13700	152000	45200	7
-22,41	24000	1800	350	6200	13900	161000	48200	8
-24,44 A*	26200	1900	470	7000	7300	165000	51900	8
-24,44 B*	26000	2000	420	6900	7700	167000	50700	8
-24,5	28300	2100	550	7500	6400	162000	49200	9
-24,9	31200	2400	430	8100	5600	170000	46100	10
-25,35	35600	2700	540	9600	5000	170000	45800	12
-25,56	33600	2500	480	8700	4400	163000	40600	11
-25,87	37100	2800	490	9500	4200	172000	40000	12

** A is a sample taken just before the eutectic point was reached and B was taken just after the temperature jump that indicates the eutectic point.*

C4. Relative increases in ion concentration between feed solution and the produced brine at -25.9 °C.

$$Relative\ increase = \frac{C(Brine) - C(Start\ solution)}{C(Start\ Solution)} \cdot 100$$

Relative increase (%)							
Ca	Mg	K	Sr	Ba	Cl	Na	Mn
64,2	64,6	31,3	58,6	-69,5	15,7	-12,9	61,0